ACOUSTIC RADIATION FROM BAFFLED PLANAR SOURCES: A SERIES APPROACH

by

NADIR AKKAYA, B.S.

A THESIS

IN

MECHANICAL ENGINEERING

Submitted to the Graduate Faculty
of Texas Tech University in
Partial Fulfillment of
the Requirements for
the Degree of

MASTER OF SCIENCE

IN

MECHANICAL ENGINEERING

Approved

August, 1999

ACKNOWLEDGMENTS

My sincerest gratitude and thanks go to Dr. Atila Ertas for giving me such a fascinating research topic and for his continuous encouragement. Without his insightful guidance, this work would not have been possible. I would also like to thank the other members of my thesis committee, Dr. Timothy T. Maxwell and Dr. William P. Vann for their helpful criticism and advice.

I am very grateful to Dr. Thomas D. Burton for the financial support granted to me by the Department of Mechanical Engineering during my graduate study.

A word of thanks is extended to Dr. Olkan Cuvalci and the researchers of the Dynamic Systems and Vibrations Laboratory.

I would also like to thank my parents, brother, and sister for their unrelenting support and encouragement through the years.

TABLE OF CONTENTS

ABSTRACT

The acoustic radiation from harmonically vibrating planar sources (pistons and thin plates) is investigated. Triangular, rectangular, circular, and elliptical sources are studied. Clamped and simply supported boundary conditions are considered for plates. The far-field acoustic pressure, the acoustic intensity, and the acoustic power expressions are obtained analytically. Two different approaches are used to find the acoustic power for some cases, and the results are compared. The intensity and power expressions are the time-averaged ones, and the latter is applicable only to sufficiently low frequency of vibrations. Finally, the dependence of the results on various design parameters, such as frequency of vibration and source geometry, is investigated.

FIGURES

SYMBOLS

A	Displacement coefficient for circular and clamped elliptical plates
A_0	Displacement coefficient for clamped elliptical plates
A_1	Displacement coefficient for clamped elliptical plates
A_2	Displacement coefficient for clamped elliptical plates
A_p	Area of the source
a	Length of the rectangular geometry
a_0	Length of the horizontal edge for the triangular geometry
a_1	Semi-major axis of the elliptical geometry
α	Polar coordinate
B	Displacement coefficient for circular plates
b	Width of the rectangular geometry
b_0	Length of the second edge for the triangular geometry
b_1	Semi-minor axis of the elliptical geometry
β	Angle between the two edges of the triangular geometry
C	Displacement function parameter associated with ε for rectangular plates; also displacement coefficient for circular plates
C'	Displacement function parameter associated with ε' for rectangular plates
c	Speed of sound in air
D	Flexural rigidity of the plate material; also displacement coefficient for circular plates
d	Distance between source infinitesimal element and far-field point
δ	Variable in displacement functions of clamped elliptical plates
E	Modulus of elasticity of the plate material
ε	Displacement function parameter in the y-direction for the clamped-clamped boundary condition of rectangular plates for even n

ε'	Displacement function parameter in the y-direction for the clamped-clamped boundary condition of rectangular plates for odd n; also for the clamped-simply supported boundary condition for any n
F	Forcing function
F_0	Uniform forcing function
f	Time-dependent forcing function; also frequency (Hz) for the free vibration of rectangular plates
G_x	Frequency parameter for rectangular plates
G_y	Frequency parameter for rectangular plates
γ	Displacement function parameter in the x-direction for the clamped-clamped boundary condition of rectangular plates for even m
γ'	Displacement function parameter in the x-direction for the clamped-clamped boundary condition of rectangular plates for odd m; also for the clamped-simply supported boundary condition for any m
H_x	Frequency parameter for rectangular plates
H_y	Frequency parameter for rectangular plates
h	Thickness of the plate
I	Acoustic intensity
i	Complex number
K	Displacement function parameter associated with γ for rectangular plates
K'	Displacement function parameter associated with γ' for rectangular plates
k	Acoustic wave number
L	Representative length of the source
λ	Frequency parameter for the free vibration of rectangular and circular plates
$\overline{\lambda}$	Roots of the characteristic equations for circular plates
M	Bending moment
m	Number of nodal lines in the x-direction for rectangular plates
μ	Frequency parameter for the forced vibration of circular plates

N	Non-dimensional quantity for triangular piston sources
n	Number of nodal lines in the y-direction for rectangular plates
p	Far-field acoustic pressure
$\|p\|$	Magnitude of the far-field acoustic pressure
p_s	Acoustic pressure on the surface of the sources
ϕ	Spherical coordinate
Π	Total approximate acoustic power
Π_2	First term of the acoustic power
Π_1	Second term of the acoustic power
$\Pi_{1.1}$	First term of the secondary acoustic power expression
$\Pi_{1.2}$	Second term of the secondary acoustic power expression
$\Pi_{1.3}$	Third term of the secondary acoustic power expression
$\Pi_{1.4}$	Fourth term of the secondary acoustic power expression
$\Pi_{1.5}$	Fifth term of the secondary acoustic power expression
$\Pi_{1.6}$	Sixth term of the secondary acoustic power expression
Π_3	Third term of the acoustic power
ψ_1	Parameter used in far-field acoustic pressure and acoustic intensity expressions
ψ_2	Parameter used in far-field acoustic pressure and acoustic intensity expressions
R	Spherical coordinate; also radius of the far-field hemisphere
R_a	Aspect ratio for rectangular and elliptical sources
R_t	Ratio of the lengths of the two edges of the triangular geometry
r	Polar coordinate
r_0	Radius of the circular geometry
ρ	Density of air
ρ_m	Density of the plate material
ρ_p	Mass of the plate per unit area
S	Surface of the sources

t	Time
θ	Spherical coordinate
u	Transverse velocity distribution over the sources
u^*	Complex conjugate of u
υ	Poisson's ratio of the plate material
W	Displacement function
W_0	Amplitude of vibration for piston sources; also displacement coefficient for plates
W_1	First part of the general solution W for the free vibration of circular plates
W_2	Second part of the general solution W for the free vibration of circular plates
w	Time-dependent displacement function
Ω	Forcing frequency
ω	Frequency of vibration for piston sources; also natural frequency for plates
X	Waveform in the x-direction for rectangular plates
x	Cartesian coordinate
x'	Initial cartesian coordinate for the triangular geometry; also the x component of the radiating infinitesimal element
x_1	Equation of one of the edges of the triangular geometry with respect to the x - y system
x_1'	Equation of the same edge with respect to the x' - y' system
x_2	Equation of the other edge of the triangular geometry with respect to the x - y system
x_2'	Equation of the same edge with respect to the x' - y' system
Y	Waveform in the y-direction for rectangular plates
y	Cartesian coordinate
y'	Initial cartesian coordinate for the triangular geometry; also the y component of the radiating infinitesimal element
z	Cartesian coordinate

CHAPTER I
INTRODUCTION

1.1 Introductory Remarks

Acoustics is the science that studies the emission, transmission, and reception of sound waves. It touches on disciplines as different as psychology and meteorology, and includes many subdisciplines such as architectural acoustics, structural acoustics, bio-acoustics, environmental acoustics, and musical acoustics (Temkin, 1981).

"If a tree falls in the forest, and no one is there to hear it, will there be sound?" This was one of the popular questions discussed and debated by scientists in the eighteenth century. This question can be answered with a yes or a no, because "sound" is an interesting word that has acquired two meanings. The answer depends upon whether it is regarded as a physical phenomenon (a mechanical radiant energy that is transmitted through the air) or as a sensation inside the mind of a listener; the first is an objective definition while the second being a subjective one. But whether regarded objectively or subjectively, it is a fact that in physical terms, sound has power (Chedd, 1970).

The physical manifestation of sound is a time-dependent pressure variation around a static pressure in a compressible fluid, such as air or water. These variations can be generated by vibrations or motions of structures (Junger and Feit, 1972).

Noise or acoustic noise, on the other hand, is defined as unwanted sound and therefore it is a sound that annoys, disturbs, bothers, irritates, perturbs, agitates, interferes with, distracts, or harms (Ghering, 1978).

Naturally, when talking about sound, especially noise, the audible frequency range – that is, the range between about 16 Hz and 16 kHz – is of primary interest. Vibrations and waves at lower frequencies (infrasound) generally belong to the fields of mechanical vibrations or seismics, whereas those at higher frequencies belong to the field of ultrasonics (Cremer et al., 1987).

Since noise is an unwanted sound, there may be cases in which it should be eliminated or at least minimized. Therefore the quantification of sound radiated from structures is an important issue from a noise control point of view.

It is also important for the engineer to have general expressions for acoustic properties of structural elements. In acoustics, generally speaking, finding closed form or even approximate expressions for these properties may be difficult unless some practical restrictions on the physical shapes of the structures are included. The most important structural elements are, in the applied mechanics sense, beams, plates, or shells. Therefore, there seems to be adequate motivation for developing analytical tools for the sound radiated from structural elements to take effective noise control measures.

1.2 Scope of the Study

The main objective of this study is to develop general analytical expressions for far-field acoustic pressure distribution, acoustic intensity, and acoustic power radiation due to harmonically vibrating planar sources, namely pistons and thin plates.

Triangular, rectangular, circular, and elliptical sources are studied. Clamped and simply supported boundary conditions are considered for plates.

The acoustic intensity and the acoustic power radiation expressions are the time-averaged ones, and the latter apply only to low kL values (a non-dimensional quantity in which k is the acoustic wave number, and L is a representative length of the source of interest).

For some cases, two different approaches are used to obtain the acoustic power expressions and the results are compared.

Finally, the dependence of the results obtained on various design parameters, such as frequency of vibration and source geometry, is investigated.

1.3 Literature Survey

Since the first step in an acoustics problem is a vibration analysis, it is better to start with vibration of plates. This field has been studied extensively by many researchers. In the present study, the analysis is limited to thin plates having three different geometric shapes; namely, rectangular, circular, and elliptical plates. Therefore, the literature survey is also limited with these cases.

Leissa (1969) investigated the vibrations of plates in detail. In this comprehensive study, he compiled the available knowledge for the frequencies and mode shapes of circular, elliptical, triangular, rectangular, parallelogram, and several other quadrilateral plates. He also analyzed anisotropic plates, plates with inplane forces, and plates with variable thickness. The chapters on fundamental equations of classical plate theory, circular, and elliptical plates were especially useful for this study.

Warburton (1954) studied the free transverse vibrations of rectangular plates. He considered all possible combinations of the three different boundary conditions (free, clamped, and simply supported) and used assumed deflection functions satisfying the plate equation and the boundary conditions to find the frequencies. The free vibration analysis and the assumed deflection functions presented in this paper constitute the basis for the analysis of thin rectangular plates in this study. This paper will be discussed in detail in Chapter IV.

Bhat (1985) obtained natural frequencies of rectangular plates by utilizing a set of beam characteristic orthogonal polynomials in the Rayleigh-Ritz method, and he compared them with the frequencies obtained with other methods. His results are superior to the ones in the literature for lower modes, especially for plates with any free edges.

Bhat et al. (1990) investigated the natural frequencies of rectangular plates of non-uniform thickness with different boundary conditions by using four different methodologies; namely, the Rayleigh-Ritz method with characteristic orthogonal polynomial shape functions, the Rayleigh-Ritz method with a shape function including two exponents to be determined by minimizing the fundamental frequency coefficient, the optimized Kantorovich method, and the finite element method. They compared and discussed the results.

Dickinson and Di Blasio (1986) used series composed of orthogonal polynomial functions in the Rayleigh-Ritz method to analyze the flexural vibration of isotropic and orthotropic rectangular plates. They also considered the vibration of plates subject to in-plane direct and shear loading, together with the associated elastic buckling problem. Finally, they used these functions to determine the natural frequencies and mode shapes.

Nayfeh et al. (1976) presented a general procedure to determine the natural frequencies and mode shapes of nearly annular and circular plates. They used the method of strained parameters together with a transfer of the boundary conditions. They also presented some numerical results for clamped elliptical and square plates. The method yielded qualitatively and quantitatively accurate results.

Chonan (1978) studied the random vibration of an elastically supported circular plate with an elastically restrained edge and an initial radial tension. He derived analytical expressions for the mean square displacement and moment by using the orthogonality property of the mode functions. He also presented numerical results for a range of parameters, and analyzed the effects of the elastic edge constraint, the radial tension, and the stiffness of the foundation on the statistical responses of the plate.

Kim and Dickinson (1989) used series composed of orthogonally generated polynomial functions in the Rayleigh-Ritz method to analyze the flexural vibration of thin, flat annular and circular plates. Their approach is applicable to plates having some complicating effects, such as anisotropy, varying thickness, or intermediate concentric ring supports.

Lam et al. (1992) developed a general numerical method to predict the natural frequencies and the mode shapes for transverse vibration of circular and elliptical plates. They used a set of orthogonal plate functions in the Rayleigh-Ritz method to approximate the eigenvalues and eigenvectors. For all cases, their results were in good agreement with the literature.

Singh and Chakraverty (1992) computed the first four frequencies and mode shapes for simply supported elliptical and circular plates of uniform thickness by utilizing orthogonal polynomials in the Rayleigh-Ritz method. For numerical convergence, they worked out successive approximations. They also considered different aspect ratios for elliptical plates, and compared the results with the literature for some cases.

Shibaoka (1956) solved the transverse vibration of a clamped elliptical plate in an exact manner by using Mathieu and modified Mathieu functions, and he showed the relationship between the frequency of the fundamental mode of vibration and the

eccentricity of the plate graphically. He also obtained an approximate formula for the mentioned relationship, which can be used for small eccentricities.

Leissa (1967) used a three-term deflection function in the Rayleigh-Ritz method to obtain the fundamental frequencies of a simply supported elliptical plate. Sato (1972) used Mathieu and modified Mathieu functions to analyze the free flexural vibrations of the same plate. Simply supported elliptical plates are out of scope of the present study, but an analysis similar to the approximate acoustic analysis presented in Chapter VI can be used to obtain a simple acoustic power expression for this plate.

Laura et al. (1976) studied the forced vibrations of a circular plate elastically restrained against rotation and subjected to two types of loading. They used simple polynomial expressions and a variational approach to analyze the behavior of the plate.

Leissa (1978) extended the Rayleigh-Ritz-Galerkin methods used widely for free vibration problems to problems of forced vibrations of continuous bodies with damping. He applied the method to two classical examples, namely, a string and a clamped circular plate.

The acoustic radiation from structures is also an extensively studied field. Since the analysis is only limited to the acoustic radiation from planar sources, the literature will also be limited with this topic.

Williams (1983) developed a power series expansion of the acoustic power radiated from baffled or unbaffled planar sources in terms of the various moments of the given velocity distribution in the source plane. He also derived an alternate form of the power series expansion in terms of the Fourier transformed velocity and its derivatives in k space. Finally, he used the formulation to find the first several terms of the acoustic power radiated from a simply supported, a clamped, and a free rectangular plate.

Snyder and Tanaka (1995) calculated the total acoustic power output of an infinitely baffled, simply supported rectangular panel at low frequencies by using its modal radiation efficiencies.

Berry et al. (1990) analyzed the sound radiation from a baffled, rectangular plate with edges elastically restrained against deflection and rotation. They investigated the effects of boundary conditions on the sound radiation when the frequency is below the

critical frequency of the plate. Laura and Ercoli (1992) commented on this paper regarding the free and forced vibrations of plates. Berry et al. (1992) replied their comment.

Wallace (1972) determined the radiation resistance corresponding to the natural modes of a finite rectangular panel theoretically by using the total energy radiated to the far-field. He obtained asymptotic solutions for the low frequency region and curves covering the entire frequency range through numerical integration.

Currey and Cunefare (1995) provided a theoretical analysis for the acoustic radiation of a vibrating rectangular plate through the eigenvalue problem. They analyzed the characteristics of the radiation modes of rectangular plates under long-wavelength conditions. They also investigated the bounding and convergence behavior of the radiation efficiencies under these conditions.

Rahman and Ertas (1994) calculated the total acoustic power radiated from one side of a baffled rectangular plate vibrating at one of its natural modes numerically. They considered different boundary conditions, aspect ratios, thickness ratios, and mode orders for the plates.

Alper and Magrab (1970) studied the radiation from the forced harmonic vibrations of a clamped circular plate. The motion in the plate was described by the Mindlin-Timoshenko theory, which includes the effects of transverse shear and rotary inertia. They obtained the solutions with the use of orthogonal functions, and their solution removed all previous restrictions regarding the boundary conditions of the plate, symmetry of the forcing and applicable frequency range.

Nakayama et al. (1980) calculated the transient acoustic pressure field due to an elastic circular plate excited by a normal incident plane sound pulse. They also obtained the impulse response of this pressure field by assuming a simple expression for the radiation impedance of the vibrating plate.

Williams and Maynard (1982) evaluated the Rayleigh's integral formula numerically for planar radiators of any shape, with any specified velocity distribution in the source plane by using a fast Fourier transform algorithm. Their algorithm increased the speed of computations drastically.

Cunefare (1991) developed a technique for deriving the optimal surface velocity distribution on the surface of a finite baffled beam. The importance of this is that the optimal velocity distribution minimizes the radiation efficiency of the beam for a specified maximum permissible mode and frequency. He then considered simply supported and clamped-clamped boundary conditions for the beam as examples.

Levine (1984) established an exact representation for the time-averaged power output generated by individual modes of a normal surface velocity distribution on a simply supported, baffled rectangular plate. His analysis enabled analytical estimates to be found in the short wavelength range and provided details unresolved by numerical analysis.

Deffayet and Nelson (1988) applied the quadratic optimization theory to determine the minimum sound power output of a baffled simply supported panel when the radiation is controlled with additional monopole sources. They assumed the point monopole sources to be coincident with the panel surface and used the interference of sound fields to minimize the power output.

Kompella (1994) studied the effects of geometry and boundary conditions on the radiated acoustic power. He considered rectangular and circular plates with several different boundary conditions, and investigated the variation of the acoustic power with different design parameters.

Other than these references, some books can also be mentioned shortly. Beyer (1999) gave an excellent account of the last two hundred years of acoustics. Chedd (1970) emphasized important areas of applications of acoustics. Ghering (1978) and Rettinger (1973) provided general information about acoustic noise control. The books by Kinsler and Frey (1950), Hunter (1957), and Temkin (1981) were helpful for the fundamentals of acoustics. For the structural acoustics the books by Junger and Feit (1972) and by Cremer et al. (1987) were useful. Finally, the book by McLachlan (1955) was needed for calculations including Bessel functions.

CHAPTER II
ACOUSTIC RADIATION FROM PLANAR SOURCES

2.1 Assumptions

To define the range of validity of the results obtained, the underlying assumptions will be stated. Since in an acoustics problem there are different media involved, the air being the acoustic medium and the planar sources being the solid medium in the present study, they generally have their own assumptions.

For the acoustic medium, the first assumption is that pressure deviations from the hydrostatic pressure (what is called far-field acoustic pressure in this study) are a linear function of the fractional density change (the condensation) and of the fractional volume change (the dilatation). Therefore, the perturbations to the equations of motions of the acoustic medium are assumed to be small; in other words, time-dependent functions represent slight deviations from the time-independent equilibrium conditions. The medium is also assumed to be homogeneous and inviscid. Normally, in an acoustics problem, there is dynamic interaction between the acoustic medium and the structure. When the ratio of the density of the medium to the density of the structure material is considerably low, then the forces applied by the medium on the structure can be neglected. Therefore, the dynamics of the structure can be analyzed as if it is in vacuum. Otherwise, coupled differential equations would have to be solved which would make the problem much more complex.

This study covers pistons and plates as structural elements, and there are assumptions which are applicable to both of them. The first of these assumptions is that the structures are assumed to be baffled; that is to say, in the plane, only the source vibrates, and the remaining part of the plane is rigid and stationary. Otherwise, there will be a velocity field around the source, which has to be known to analyze the problem. Secondly, the bottom side of the source is vacuumed. This means that there is no acoustic medium beneath it and the acoustic radiation is only to the half-space above the source.

For plates, there are some other assumptions. First of all, the plate is isotropic, elastic, and homogeneous. Secondly, only the transverse vibrations and deflections are

considered, and these deflections are small when compared to the plate dimensions. The thickness of the plate is uniform, and it is small when compared to other plate dimensions. Therefore, thin plate assumption can be used. Lastly, the influence of shear and rotary inertia is negligible in the vibration analysis.

2.2 Methodology

The following steps are used to obtain the necessary acoustic quantities:

i. Assumption of a displacement function for the piston, or solution of the plate equation with the boundary conditions to obtain a displacement function for the plate;

ii. Derivation of the surface velocity distribution of the source from the displacement function.

After the previous step, two directions are followed to obtain acoustic power expressions.

For the far-field integration approach:

iii. Derivation of the far-field pressure distribution from the velocity distribution;

iv. Derivation of the acoustic intensity from the far-field pressure;

v. Derivation of the acoustic power from the acoustic intensity;

For the surface integration approach:

iii. Derivation of the acoustic power from the velocity distribution directly.

2.3 Far-field Acoustic Pressure Distribution

The acoustic pressure produced at any far-field point by the vibration of a planar source is the sum of the pressures that would be produced by an equivalent assembly of simple sources; in other words, infinitesimal elements on the surface of the source. Each infinitesimal element of area dS of a harmonically vibrating source mounted in an infinite baffle, as shown in Fig. 2.1, contributes an element of pressure dp given by

$$dp = -i\frac{\rho ck}{2\pi d}udS\exp\left[i\left(-\omega t + kd\right)\right] \tag{2.1}$$

at a far-field point P. In Eq. (2.1), ρ is the equilibrium density of the acoustic medium; c is the speed of sound in the same medium; d is the distance between the far-field point

and the infinitesimal element; u is the transverse velocity distribution on the surface of the source; and ω is the frequency of vibration.

An equation for the acoustic pressure at this far-field point can be obtained by integrating dp given by Eq. (2.1) over the surface of the vibrating source. Then, the pressure produced by the planar source at that specific far-field point is expressed as

$$p = -i\frac{\rho c k \exp(-i\omega t)}{2\pi d}\int_S u \exp(ikd)dS\,, \tag{2.2}$$

where s denotes the surface of the source. Eq. (2.2) is called Rayleigh's formula or Rayleigh integral.

The acoustic wave number, k, is given by

$$k = \frac{\omega}{c}. \tag{2.3}$$

By using the geometry of Fig. 2.1 and the trigonometric relations, it can be shown that the distance, d, between the far-field point P and the center of the infinitesimal element, point A, is

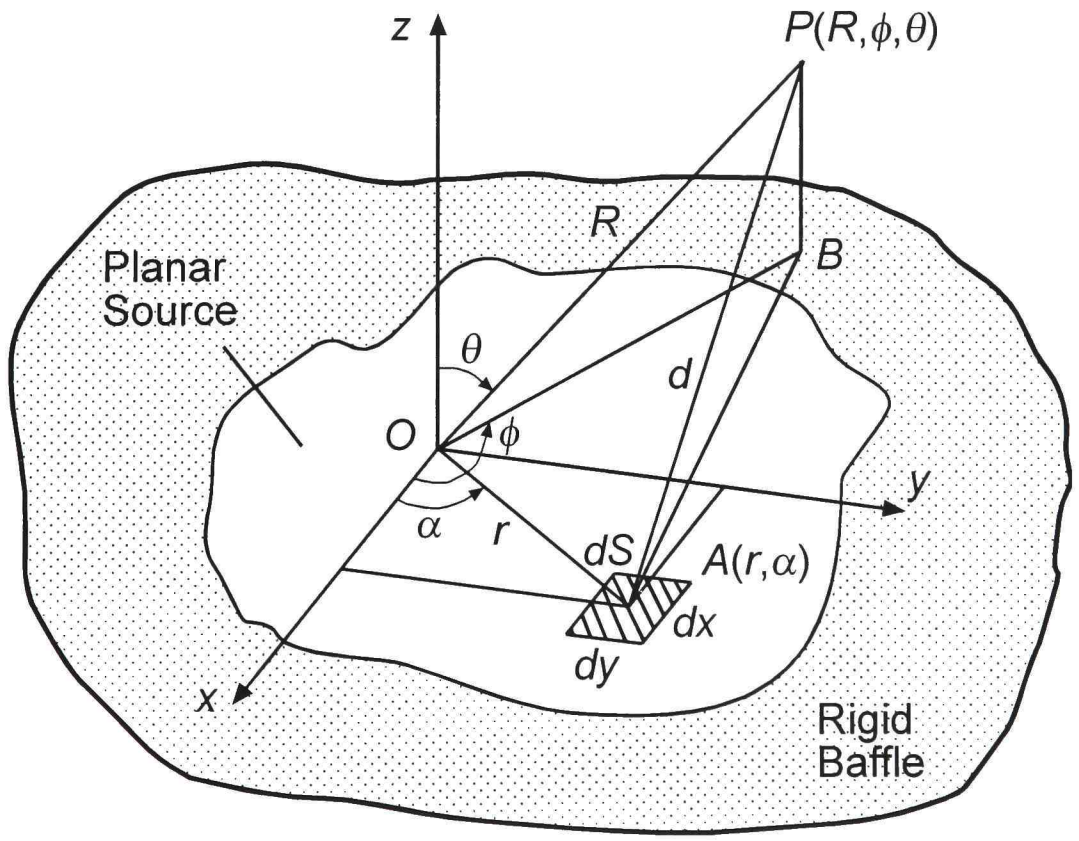

Figure 2.1. A Planar Source and the Coordinate System.

$$d = \left[R^2 + r^2 - 2Rr\sin(\theta)\cos(\phi - \alpha)\right]^{1/2}, \tag{2.4}$$

where d, r, α, R, ϕ, and θ are as shown in the figure.

If d, given by Eq. (2.4), is substituted into Rayleigh's formula, the surface integral in Eq. (2.2) becomes too complex. Therefore, its binomial expansion should be used to have a simplified but still accurate expression. After the expansion, it becomes

$$d = R - r\sin(\theta)\cos(\phi - \alpha) + O\left(\frac{r^2}{R}\right). \tag{2.5}$$

The assumption of P being a far-field point requires R being very much greater than r ($R \rangle\rangle r$). This means that d in the denominator of Eq. (2.2) can be approximated by R, but d in the exponential term of the same equation should also include the second term in Eq. (2.5) since it refers to a phase difference between different infinitesimal elements.

After all these simplifications, Eq. (2.2) can be written as

$$p(R,\phi,\theta,t) = -i\frac{\rho ck\exp\left[i(-\omega t + kR)\right]}{2\pi R}\int_S u\exp\left[-ikr\sin(\theta)\cos(\phi - \alpha)\right]dS, \tag{2.7}$$

where R, ϕ, and θ are the spherical coordinates locating the far-field point P and they should not be confused with the coordinates of the surface integral. In other words, they should be treated as constants inside the surface integral because the aim is to find the pressure created by the whole source at a fixed far-field point.

Sometimes using different coordinate systems for different source shapes may be more convenient. Therefore, it is a good idea to express the surface integral in Eq. (2.7) in both polar and rectangular coordinate systems.

To obtain the far-field pressure expression in which the surface integral is written in terms of polar coordinates (r and α), $rdrd\alpha$ is substituted for dS in Eq. (2.7). Thus, the far-field pressure in polar coordinates becomes

$$p(R,\phi,\theta,t) = -i\frac{\rho ck\exp\left[i(-\omega t + kR)\right]}{2\pi R}\int_S u(r,\alpha)\exp\left[-ikr\sin(\theta)\cos(\phi - \alpha)\right]rdrd\alpha\,. \tag{2.8}$$

To express the surface integral in rectangular coordinates (x and y), dS should be replaced by $dxdy$. The $\cos(\phi-\alpha)$ term should be expanded, and, upon this expansion, it should be realized that $r\cos(\alpha)$ is equal to x, and $r\sin(\alpha)$ is equal to y. After these changes, the far-field pressure in rectangular coordinates can be written as

$$p(R,\phi,\theta,t) = -i\frac{\rho ck\exp[i(-\omega t+kR)]}{2\pi R} \times \int_S u(x,y)\exp\{-ik\sin(\theta)[\cos(\phi)x+\sin(\phi)y]\}dxdy. \tag{2.9}$$

2.4 Acoustic Intensity

Acoustic disturbances for which the pressure is uniform on planes normal to the direction of propagation are known as plane waves. As the plane waves propagate through the acoustic medium, energy is transmitted from one part of the medium to another. The time-averaged rate at which the energy is transferred per unit area is the acoustic intensity; in other words, it is the acoustic power flow per unit area (Fahy and Walker, 1998).

For plane progressive waves and in the case of a harmonically vibrating source, the average of the intensity over all time is (Junger and Feit, 1972)

$$I(R,\phi,\theta) = \frac{|p(R,\phi,\theta)|^2}{2\rho c}, \tag{2.10}$$

where $|p(R,\phi,\theta)|$ is the amplitude of $p(R,\phi,\theta,t)$ given by Eqs. (2.7) to (2.9) (whichever is used) without the time-dependent term $\exp(-i\omega t)$. A derivation of Eq. (2.10) is presented in Appendix A.

2.5 Acoustic Power Radiation

Acoustic power radiation can be defined as the rate of acoustic energy delivered by a source. Since the acoustic intensity is the acoustic power flow per unit area, the total acoustic power radiated by any source can be obtained by integrating the acoustic intensity over a surface of convenience.

In the present study, two approaches are used to obtain the total acoustic power radiated from planar sources; namely, far-field and surface integration approaches and their advantages and disadvantages are discussed.

In the far-field integration approach, the radial component of the acoustic intensity is integrated over an imaginary far-field hemisphere enclosing the source (Junger and Feit, 1972), and this explains the reason for writing the far-field pressure expressions in terms of spherical coordinates in previous sections. For analytical studies, a hemisphere over the source is the most suitable choice as the enclosing surface since it allows one to use spherical coordinates. For experimental studies, on the other hand, the choice of planar surfaces forming a cube or a parallelepiped over the source would be much better because acoustic intensity measurements can be made more easily on planar surfaces than on curved ones.

The total acoustic power radiation can be written as

$$\Pi = \int_{\phi=0}^{2\pi} \int_{\theta=0}^{\pi/2} I(R,\phi,\theta)\sin(\theta) R^2 d\theta d\phi \,, \tag{2.11}$$

where $I(R,\phi,\theta)$ is given by Eq. (2.10), $I(R,\phi,\theta)\sin(\theta)$ is the radial component of the acoustic intensity, and $R^2 d\theta d\phi$ is the area of the infinitesimal surface element of the hemisphere.

The other approach is to integrate the (real) acoustic intensity over the surface of the source, and, in this case, the acoustic power can be written as (Snyder and Tanaka, 1995)

$$\Pi = \frac{1}{2}\mathrm{Re}\left(\int_S p_s u^* dS \right), \tag{2.12}$$

where p_s is the surface pressure, and u^* is the complex conjugate of the surface velocity.

As a continuation of the derivation given for Eq. (2.10), a derivation of Eq. (2.12) is also presented in Appendix A.

The surface pressure can still be given by Eq. (2.2), and if this expression is substituted into Eq. (2.12) after suppressing the harmonic time dependent term $\exp(-i\omega t)$, one can get

$$\Pi = \frac{1}{2}\mathrm{Re}\left[\int_S \left(-i\frac{\rho c k}{2\pi d}\int_S u' \exp(ikd) dS' \right) u^* dS \right], \tag{2.13}$$

where primes are used to distinguish between the contents of the two surface integrals.

The suppression of the time dependence is again due to the fact that the time-averaged intensity is integrated over the surface and all of the above acoustic power formulations account for this averaging process in itself. To clarify this point further, the reader is referred to Appendix A.

In Eq. (2.13), taking d in the denominator into the inner integral, grouping all constant terms outside the integrals, using Eq. (2.3) to replace the first k, and rearranging yields

$$\Pi = \frac{1}{2}\mathrm{Re}\left(-i\frac{\rho\omega}{2\pi}\int_S\int_S u' \frac{\exp(ikd)}{d} dS' u^* dS \right). \tag{2.14}$$

Using Euler's formula to expand the $\exp(ikd)$ term in Eq. (2.14) and taking the real part of the whole quantity inside the parenthesis, the total acoustic power becomes

$$\Pi = \frac{\rho\omega}{4\pi}\int_S\int_S u' u^* \frac{\sin(kd)}{d} dS' dS\,. \tag{2.15}$$

If rectangular coordinates are used, Eq. (2.15) can be simplified further. Since $z = 0$ on the surface of the source, d is given by

$$d = \left[(x - x')^2 + (y - y')^2 \right]^{1/2}, \tag{2.16}$$

where (x', y') locates the radiating infinitesimal element, while (x, y) can be thought of as the location of the far-field point, or the receiving point, although this point is also on the surface. This is because the surface over which the acoustic intensity is integrated is the surface of the source itself.

If $\sin(kd)$ in Eq. (2.15) is expanded in its MacLaurin series, all d 's are replaced with the expression given by Eq. (2.16), and, then, simplifying a series expansion for the total acoustic power can be obtained as

$$\Pi = \frac{\rho\omega}{4\pi}\sum_{m=0}^{\infty} \frac{k^{2m+1}}{(2m+1)!}(-1)^m \int_S\int_S u(x', y') u^*(x, y) \left[(x - x')^2 + (y - y')^2 \right]^m dS dS'\,. \tag{2.17}$$

The binomial expansion of the term bracketed in Eq. (2.17) can be written as

$$\begin{aligned}\left[(x-x')^2+(y-y')^2\right]^m &= \sum_{l=0}^{m}\binom{m}{l}(x-x')^{2m-2l}(y-y')^{2l} \\ &= \sum_{l=0}^{m}\sum_{p=0}^{2m-2l}\sum_{q=0}^{2l}\binom{m}{l}\binom{2m-2l}{p}\binom{2l}{q}x^{2m-2l-p}x'^{p}y^{2l-q}y'^{q},\end{aligned} \tag{2.18}$$

where m, l, p, q are indices and $\binom{m}{l}=m!/l!(m-l)!$.

Substituting Eq. (2.18) into Eq. (2.17), replacing one of the k's with ω/c, and writing the elemental areas in terms of rectangular coordinates yields

$$\begin{aligned}\Pi = \frac{\rho\omega^2}{4\pi c}\sum_{m=0}^{\infty}\frac{(-1)^m k^{2m}}{(2m+1)!}\sum_{l=0}^{m}\sum_{p=0}^{2m-2l}\sum_{q=0}^{2l}\binom{m}{l}\binom{2m-2l}{p}\binom{2l}{q} \\ \times\int_S u(x',y')x'^{p}y'^{q}dx'dy'\int_S u^*(x,y)x^{2m-2l-p}y^{2l-q}dxdy.\end{aligned} \tag{2.19}$$

This is a difficult expression to deal with because it is an infinite sum. But for any source geometry, the total acoustic power can be written in terms of even powers of kL. Therefore, by taking only a few terms of this series into account, approximate analytic expressions for acoustic power can be obtained. This may seem a huge limitation; actually, it is in the sense that one cannot "map" acoustic power through the whole "spectrum" of kL values. But, even low kL values refer to fairly high frequency values in practice.

In the present study, in obtaining approximate power expressions, only the first two m values in Eq. (2.19) are considered; in other words, $m=0$ and $m=1$ cases.

For $m=0$, the only combination of indices is

$$(m,l,p,q)=(0,0,0,0).$$

For $m=1$, there are six different combinations, and they are given by

$$(m,l,p,q)=(1,0,0,0),\ (1,0,1,0),\ (1,0,2,0),\ (1,1,0,0),\ (1,1,0,1),\ (1,1,0,2).$$

Let us write down the power expressions for each set of indices, but for convenience let us also denote each of them with different subscripts of Π.

For $m=0$ or $(m,l,p,q)=(0,0,0,0)$:

$$\Pi_0 = \frac{\rho\omega^2}{4\pi c}\int_S u(x',y')dx'dy'\int_S u^*(x,y)dxdy\,. \tag{2.20}$$

For $m=1$, and

for $(m,l,p,q)=(1,0,0,0)$:

$$\Pi_{1.1} = \frac{\rho\omega^2}{4\pi c}\left(-\frac{k^2}{6}\right)\int_S u(x',y')dx'dy'\int_S u^*(x,y)x^2dxdy\,, \tag{2.21}$$

for $(m,l,p,q)=(1,0,1,0)$:

$$\Pi_{1.2} = \frac{\rho\omega^2}{4\pi c}\left(-\frac{k^2}{3}\right)\int_S u(x',y')x'dx'dy'\int_S u^*(x,y)xdxdy\,, \tag{2.22}$$

for $(m,l,p,q)=(1,0,2,0)$:

$$\Pi_{1.3} = \frac{\rho\omega^2}{4\pi c}\left(-\frac{k^2}{6}\right)\int_S u(x',y')x'^2dx'dy'\int_S u^*(x,y)dxdy\,, \tag{2.23}$$

for $(m,l,p,q)=(1,1,0,0)$:

$$\Pi_{1.4} = \frac{\rho\omega^2}{4\pi c}\left(-\frac{k^2}{6}\right)\int_S u(x',y')dx'dy'\int_S u^*(x,y)y^2dxdy\,, \tag{2.24}$$

for $(m,l,p,q)=(1,1,0,1)$:

$$\Pi_{1.5} = \frac{\rho\omega^2}{4\pi c}\left(-\frac{k^2}{3}\right)\int_S u(x',y')y'dx'dy'\int_S u^*(x,y)ydxdy\,, \tag{2.25}$$

and for $(m,l,p,q)=(1,1,0,2)$:

$$\Pi_{1.6} = \frac{\rho\omega^2}{4\pi c}\left(-\frac{k^2}{6}\right)\int_S u(x',y')y'^2dx'dy'\int_S u^*(x,y)dxdy\,. \tag{2.26}$$

Combining all six power terms for $m=1$, the second power term can be written as

$$\Pi_1 = \sum_{i=1}^{6}\Pi_{1.i}\,. \tag{2.27}$$

Finally, the total acoustic power can be approximated as

$$\Pi \cong \Pi_0 + \Pi_1\,. \tag{2.28}$$

If one more power term (Π_2) would be included in Eq. (2.28), this additional term would contain nineteen different power components in itself. It can be realized that

without Π_2, there are already seven power terms (one from Π_0, and six from Π_1) and, therefore, taking only the first two m values into account is a reasonable approximation. In addition, the effect of one more term would be negligible for $kL\langle\langle 1$.

The reader is referred to Williams (1983) for an excellent treatment of this second approach as well as an alternate one.

Converting the above acoustic power formulation into polar coordinates is easy. Substituting $r\cos(\alpha)$, $r\sin(\alpha)$, and $rdrd\alpha$ for x, y, and $dxdy$, respectively, into Eq. (2.19), writing the velocities in terms of polar coordinates, and making the simplifications, Π becomes

$$\Pi = \frac{\rho\omega^2}{4\pi c}\sum_{m=0}^{\infty}\frac{(-1)^m k^{2m}}{(2m+1)!}\sum_{l=0}^{m}\sum_{p=0}^{2m-2l}\sum_{q=0}^{2l}\binom{m}{l}\binom{2m-2l}{p}\binom{2l}{q} \times \int_S u(r',\alpha')r'^{\,p+q+1}\cos^p(\alpha')\sin^q(\alpha')dr'd\alpha' \times \int_S u^*(r,\alpha)r^{2m-p-q+1}\cos^{2m-2l-p}(\alpha)\sin^{2l-q}(\alpha)drd\alpha. \tag{2.29}$$

And, the individual power terms can be written as

$$\Pi_0 = \frac{\rho\omega^2}{4\pi c}\int_S u(r',\alpha')r'dr'd\alpha'\int_S u^*(r,\alpha)rdrd\alpha\,, \tag{2.30}$$

$$\Pi_{1.1} = \frac{\rho\omega^2}{4\pi c}\left(-\frac{k^2}{6}\right)\int_S u(r',\alpha')r'dr'd\alpha'\int_S u^*(r,\alpha)r^3\cos^2(\alpha)drd\alpha\,, \tag{2.31}$$

$$\Pi_{1.2} = \frac{\rho\omega^2}{4\pi c}\left(-\frac{k^2}{3}\right)\int_S u(r',\alpha')r'^2\cos(\alpha')dr'd\alpha'\int_S u^*(r,\alpha)r^2\cos(\alpha)drd\alpha\,, \tag{2.32}$$

$$\Pi_{1.3} = \frac{\rho\omega^2}{4\pi c}\left(-\frac{k^2}{6}\right)\int_S u(r',\alpha')r'^3\cos^2(\alpha')dr'd\alpha'\int_S u^*(r,\alpha)rdrd\alpha\,, \tag{2.33}$$

$$\Pi_{1.4} = \frac{\rho\omega^2}{4\pi c}\left(-\frac{k^2}{6}\right)\int_S u(r',\alpha')r'dr'd\alpha'\int_S u^*(r,\alpha)r^3\sin^2(\alpha)drd\alpha\,, \tag{2.34}$$

$$\Pi_{1.5} = \frac{\rho\omega^2}{4\pi c}\left(-\frac{k^2}{3}\right)\int_S u(r',\alpha')r'^2\sin(\alpha')dr'd\alpha'\int_S u^*(r,\alpha)r^2\sin(\alpha)drd\alpha\,, \tag{2.35}$$

and

$$\Pi_{1.6} = \frac{\rho\omega^2}{4\pi c}\left(-\frac{k^2}{6}\right)\int_S u(r',\alpha')r'^3\sin^2(\alpha')dr'd\alpha'\int_S u^*(r,\alpha)rdrd\alpha\,. \qquad (2.36)$$

Eqs. (2.27) and (2.28) can still be used regardless of the coordinate system.

At this point, the second approach may seem cumbersome when the first approach is considered. In fact, this is not the case. Although the first method could be given by Eq. (2.11) alone, upon substitution of the far-field pressure expressions into this equation, the integrals become impossible to evaluate (even for the simplest pressure expressions). This forces one to try for a numerical solution or expand the contents of these integrals in their series forms and to try to obtain a series expansion for the acoustic power. Even in the latter case, for most of the geometric shapes considered in this study, the integrals become too complex, making the first approach inefficient for an analytic study. Therefore, this approach is used for a few cases only. On the other hand, acoustic power expressions for $kL\langle\langle 1$ could be obtained by using the second approach for all of the source types and shapes considered in this study.

Another important point to add is that, by using the second approach, one can obtain acoustic power expressions directly with the knowledge of surface velocity distribution of the source, whereas, there are some other intermediate steps to obtain them when using the first approach.

CHAPTER III
TRIANGULAR GEOMETRY

The first source geometry considered is the triangular one because it is one of the simplest geometric shapes considered in this study. It is recognized that triangular pistons may not have any practical applications and to the author's knowledge, they were not seen in the literature. But, in any event, it is an interesting problem to start with.

3.1 Triangular Pistons

In this section, the far-field acoustic pressure and the acoustic power expressions will be obtained for the most general case of a triangular piston, as shown in Fig. 3.1. The expressions are derived in such a way that they allow one to find the mentioned quantities just by specifying the lengths of the two edges of the triangle and the angle between them, namely a_0, b_0, and β, respectively. The geometry and the coordinate system used are shown in the same figure.

For a harmonically vibrating piston the displacement function can be given as

$$w(t) = W_0 \exp(-i\omega t), \tag{3.1}$$

where W_0 and ω are the amplitude and the frequency of vibration, respectively. Taking the first time derivative of w and then suppressing the $-i\exp(-i\omega t)$ term, the velocity becomes

$$u = \omega W_0 . \tag{3.2}$$

This velocity distribution will be the same for all piston shapes considered in this study. The complex $-i$ term is suppressed to have a real velocity factor while the suppression of the $\exp(-i\omega t)$ term is due to the fact that the formulation presented in Chapter II accounts for the harmonic time-dependence coming from the velocity. Therefore, throughout this study, the velocities and their complex conjugates are real and equal for all planar sources.

3.1.1 Far-field Acoustic Pressure Distribution

Since the imaginary hemisphere enclosing the source should be concentric with its geometric center, point O shown in Fig. 3.1 is accepted as the center of the source for the derivation of the far-field acoustic pressure expression. This point is the intersection of lines connecting the mid-points of the sides with the opposite corners. Using this geometry, the equations of lines $O'B$ and AB with respect to the x' - y' system are given by

$$x_1' = \frac{\cos(\beta)}{\sin(\beta)} y',$$

and

$$x_2' = \frac{(b_0 \cos(\beta) - a_0)}{b_0 \sin(\beta)} y' + a_0,$$

respectively.

Then, the equations of these lines with respect to the x - y system become

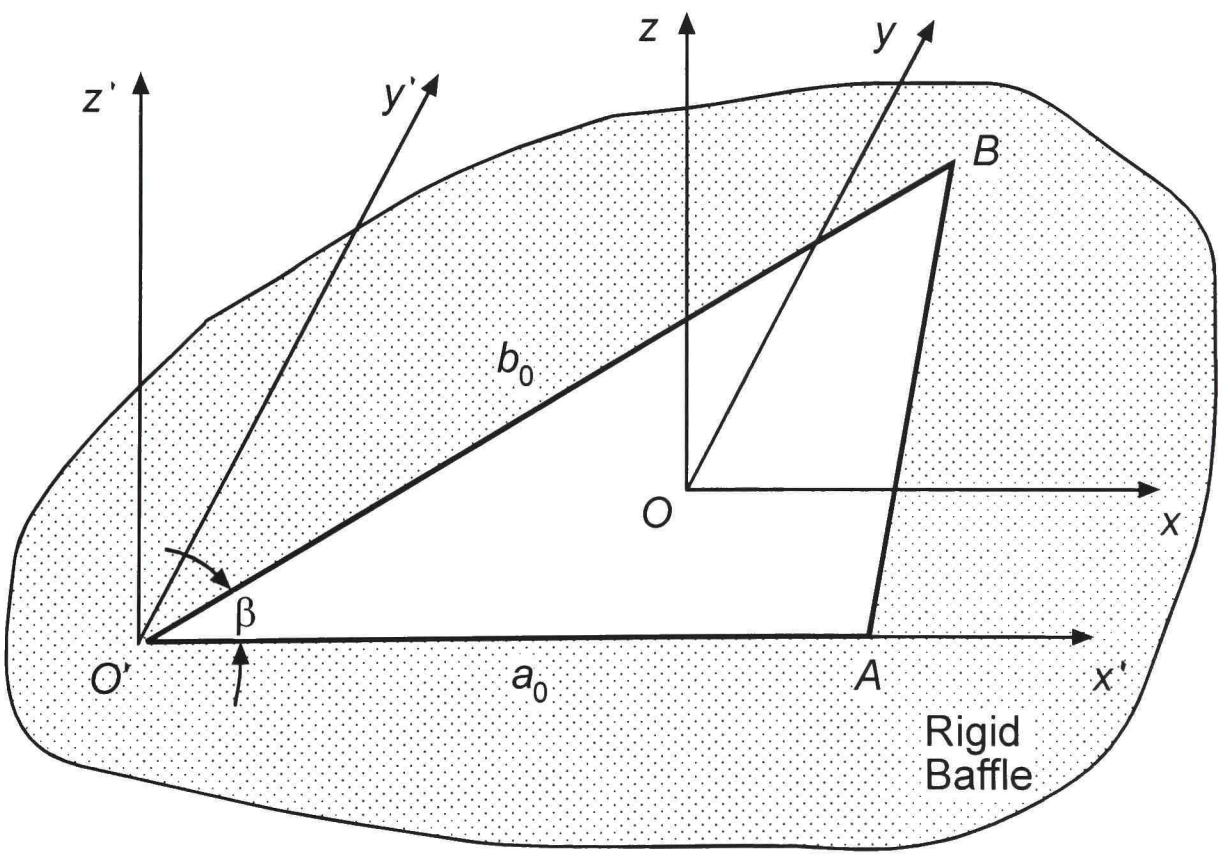

Figure 3.1. A Triangular Piston and the Coordinate System.

$$x_1 = \frac{\cos(\beta)}{\sin(\beta)} y - \frac{a_0}{3}, \tag{3.3}$$

and

$$x_2 = \frac{\left(b_0 \cos(\beta) - a_0\right)}{b_0 \sin(\beta)} y + \frac{a_0}{3}, \tag{3.4}$$

respectively.

Now, Eq. (2.9) is used to obtain the far-field acoustic pressure expression, and the limits for the surface integral are x_1 and x_2 given by Eqs. (3.3) and (3.4) in x-direction, $-b_0 \sin(\beta)/3$ and $2b_0 \sin(\beta)/3$ in y-direction.

Substituting the velocity given by Eq. (3.2) into Eq. (2.9), putting the corresponding integration limits, replacing the first k with ω / c, and rearranging yields

$$\begin{aligned} p(R,\phi,\theta,t) = -i \frac{\rho \omega^2 W_0 \exp\left[i(-\omega t + kR)\right]}{2\pi R} \\ \times \int_{-b_0 \sin(\beta)/3}^{2b_0 \sin(\beta)/3} \left[\int_{x_1}^{x_2} \exp(-i\psi_1 x) dx \right] \exp(-i\psi_2 y) dy, \end{aligned} \tag{3.5}$$

where

$$\psi_1 = k \sin(\theta)\cos(\phi), \tag{3.6}$$

and

$$\psi_2 = k \sin(\theta)\sin(\phi). \tag{3.7}$$

After integrating Eq. (3.5) and simplifying, the far-field pressure expression becomes

$$\begin{aligned} p(R,\phi,\theta,t) = i \frac{\rho \omega^2 W_0 A_p \exp\left[i(-\omega t + kR)\right]}{\pi R} \\ \times \left\{ \frac{\exp(iN)}{(\psi_1 a_0)\left[3N - (\psi_1 a_0)\right]} - \frac{\exp\left\{i\left[N - (\psi_1 a_0)\right]\right\}}{(\psi_1 a_0)\left[3N - 2(\psi_1 a_0)\right]} + \frac{\exp\left\{i\left[-2N + (\psi_1 a_0)\right]\right\}}{\left[3N - (\psi_1 a_0)\right]\left[3N - 2(\psi_1 a_0)\right]} \right\}, \end{aligned} \tag{3.8}$$

where A_p is the piston surface area given by

$$A_p = \frac{1}{2} a_0 b_0 \sin(\beta), \tag{3.9}$$

and N is a non-dimensional quantity expressed as

$$N = \frac{1}{3}\left\{\left\{\left[\psi_1 \cos(\beta) + \psi_2 \sin(\beta)\right] b_0\right\} + \left(\psi_1 a_0\right)\right\}.$$

The magnitude of the far-field acoustic pressure can be obtained from Eq. (3.8) as

$$\left|p(R,\phi,\theta)\right| = \frac{\rho\omega^2 W_0 A_p}{\pi R(\psi_1 a_0)\left[3N-(\psi_1 a_0)\right]\left[3N-2(\psi_1 a_0)\right]} \times \begin{Bmatrix} (\psi_1 a_0)^2 + \left[3N-(\psi_1 a_0)\right]^2 + \left[3N-2(\psi_1 a_0)\right]^2 \\ -2\left[3N-(\psi_1 a_0)\right]\left[3N-2(\psi_1 a_0)\right]\cos(\psi_1 a_0) \\ +2(\psi_1 a_0)\left[3N-2(\psi_1 a_0)\right]\cos(3N-\psi_1 a_0) \\ -2(\psi_1 a_0)\left[3N-(\psi_1 a_0)\right]\cos(3N-2\psi_1 a_0) \end{Bmatrix}^{1/2}. \tag{3.10}$$

Substituting this result into Eq. (2.10), the acoustic intensity becomes

$$I(R,\phi,\theta) = \frac{\rho\omega^4 {W_0}^2 {A_p}^2}{2\pi^2 R^2 c(\psi_1 a_0)^2\left[3N-(\psi_1 a_0)\right]^2\left[3N-2(\psi_1 a_0)\right]^2} \times \begin{Bmatrix} (\psi_1 a_0)^2 + \left[3N-(\psi_1 a_0)\right]^2 + \left[3N-2(\psi_1 a_0)\right]^2 \\ -2\left[3N-(\psi_1 a_0)\right]\left[3N-2(\psi_1 a_0)\right]\cos(\psi_1 a_0) \\ +2(\psi_1 a_0)\left[3N-2(\psi_1 a_0)\right]\cos(3N-\psi_1 a_0) \\ -2(\psi_1 a_0)\left[3N-(\psi_1 a_0)\right]\cos(3N-2\psi_1 a_0) \end{Bmatrix}. \tag{3.11}$$

3.1.2 Acoustic Power Radiation

As stated before, there may be cases where the use of the first approach for acoustic power derivations is not efficient and the present problem is one of them. Therefore, the surface integration approach is preferred.

Substituting the velocity given by Eq. (3.2) into Eq. (2.20) and simplifying, the first power term can be written as

$$\Pi_0 = \frac{\rho\omega^4 {W_0}^2}{4\pi c}\int_S dx'dy' \int_S dxdy. \tag{3.12}$$

Realizing that each of these two integrals is essentially the area of the piston, the dominant power term becomes

$$\Pi_0 = \frac{\rho\omega^4 W_0^{\,2} A_p^{\,2}}{4\pi c}, \tag{3.13}$$

where A_p is given by Eq. (3.9).

Substituting the velocity into Eqs. (2.21) to (2.26), integrating, adding them up by using Eq. (2.27), factoring the square of the piston area out, and simplifying, the second power term reduces to

$$\Pi_1 = \frac{\rho\omega^4 W_0^{\,2} A_p^{\,2}}{4\pi c}\left\{-\frac{\left[1 - R_t\cos(\beta) + R_t^{\,2}\right]}{54}(ka_0)^2\right\}, \tag{3.14}$$

where

$$R_t = \frac{b_0}{a_0}. \tag{3.15}$$

Finally, by using Eq. (2.28), the total approximate acoustic power becomes

$$\Pi \cong \frac{\rho\omega^4 W_0^{\,2} A_p^{\,2}}{4\pi c}\left\{1 - \frac{\left[1 - R_t\cos(\beta) + R_t^{\,2}\right]}{54}(ka_0)^2\right\}. \tag{3.16}$$

CHAPTER IV
RECTANGULAR GEOMETRY

Rectangular pistons and plates are studied in this chapter.

4.1 Rectangular Pistons

The far-field acoustic pressure, the acoustic intensity, and the acoustic power expressions will be obtained for a rectangular piston as shown in Fig. 4.1. The geometry and the coordinate system used are shown in the same figure. To find the acoustic power expressions, both of the approaches described in Chapter II are used because in this case the form of the far-field pressure expression is simple enough, allowing the use of the far-field integration approach.

4.1.1 Far-field Acoustic Pressure Distribution

Substituting the velocity given by Eq. (3.2) into Eq. (2.9), integrating (now the limits are $-a/2$ to $a/2$ in the x-direction and $-b/2$ to $b/2$ in the y-direction), and simplifying, the far-field pressure distribution becomes

$$p(R,\phi,\theta,t) = -i\frac{2\rho\omega^2 W_0 A_p \exp[i(-\omega t + kR)]}{\pi R}\left\{\frac{\sin[(\psi_1 a)/2]\sin[(\psi_2 b)/2]}{(\psi_1 a)(\psi_2 b)}\right\}, \quad (4.1)$$

where A_p is the area of the rectangular piston (or plate) given by

$$A_p = ab, \quad (4.2)$$

and ψ_1, ψ_2 are given by Eqs. (3.6) and (3.7), respectively.

4.1.2 Acoustic Power Radiation

4.1.2.1 Far-field Integration Approach

The magnitude of the far-field pressure, given by Eq. (4.1), can be written as

$$|p(R,\phi,\theta)| = \frac{2\rho\omega^2 W_0 A_p}{\pi R}\left\{\frac{\sin[(\psi_1 a)/2]\sin[(\psi_2 b)/2]}{(\psi_1 a)(\psi_2 b)}\right\}. \quad (4.3)$$

By substituting this pressure magnitude into Eq. (2.10), the acoustic intensity can be obtained as

$$I(R,\phi,\theta)=\frac{2\rho\omega^4 W_0^{\,2} A_p^{\,2}}{\pi^2 R^2 c}\left\{\frac{\sin\left[(\psi_1 a)/2\right]\sin\left[(\psi_2 b)/2\right]}{(\psi_1 a)(\psi_2 b)}\right\}^2. \tag{4.4}$$

Plugging the acoustic intensity into Eq. (2.11) with ψ_1 and ψ_2 in their open forms and rearranging yields

$$\Pi=\frac{\rho\omega^4 W_0^{\,2} A_p^{\,2}}{4\pi c}\left\{\frac{8}{\pi}\int_{\phi=0}^{2\pi}\int_{\theta=0}^{\pi/2}\frac{\sin^2\left[ka\sin(\theta)\cos(\phi)/2\right]\sin^2\left[kb\sin(\theta)\sin(\phi)/2\right]}{(ka)^2(kb)^2\sin^3(\theta)\cos^2(\phi)\sin^2(\phi)}d\theta d\phi\right\}. \tag{4.5}$$

This double integral is difficult to evaluate in closed form; therefore, MacLaurin series expansions of the terms in the numerator are substituted to obtain a series expansion for the acoustic power. The MacLaurin series expansion of $\sin\left[ka\sin(\theta)\cos(\phi)/2\right]$ is

$$\sin\left[ka\sin(\theta)\cos(\phi)/2\right]=\sum_{j=0}^{\infty}\frac{(-1)^j(ka)^{2j+1}\sin^{2j+1}(\theta)\cos^{2j+1}(\phi)}{2^{2j+1}(2j+1)!}.$$

Then, its square becomes

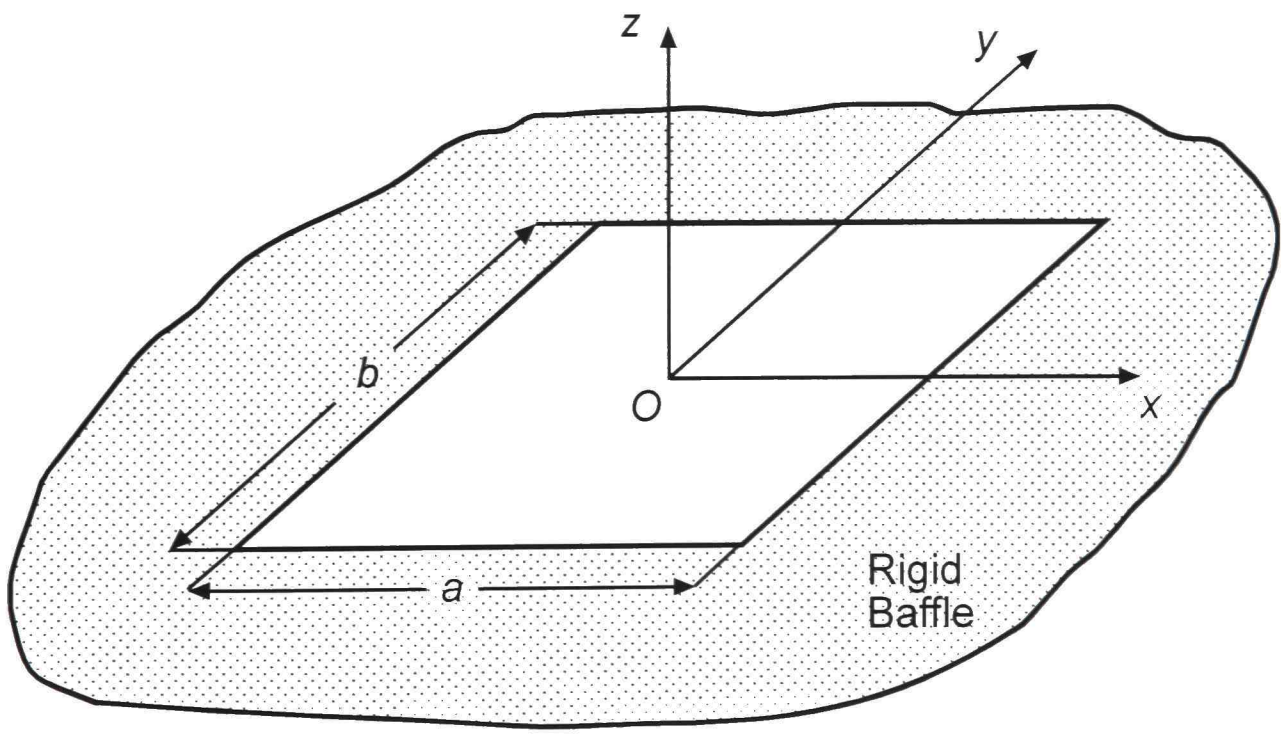

Figure 4.1. A Rectangular Piston and the Coordinate System.

$$\sin^2\left[ka\sin(\theta)\cos(\phi)/2\right]=\sum_{j=0}^{\infty}\sum_{l=0}^{\infty}\frac{(-1)^{j+l}(ka)^{2(j+l+1)}\sin^{2(j+l+1)}(\theta)\cos^{2(j+l+1)}(\phi)}{2^{2(j+l+1)}(2j+1)!(2l+1)!}.$$

In the same way, the second term can be written as

$$\sin^2\left[kb\sin(\theta)\sin(\phi)/2\right]=\sum_{q=0}^{\infty}\sum_{v=0}^{\infty}\frac{(-1)^{q+v}(kb)^{2(q+v+1)}\sin^{2(q+v+1)}(\theta)\sin^{2(q+v+1)}(\phi)}{2^{2(q+v+1)}(2q+1)!(2v+1)!}.$$

Multiplying these two terms, substituting the result into Eq. (4.5), and simplifying, the acoustic power expression reduces to

$$\Pi=\frac{\rho\omega^4 W_0^{\,2}A_p^{\,2}}{4\pi c}\times\left\{\frac{1}{2\pi}\int_{\phi=0}^{2\pi}\int_{\theta=0}^{\pi/2}\sum_{j=0}^{\infty}\sum_{l=0}^{\infty}\sum_{q=0}^{\infty}\sum_{v=0}^{\infty}\left[\begin{array}{l}\dfrac{(-1)^{j+l+q+v}(ka)^{2(j+l+q+v)}R_a^{\,2(q+v)}}{2^{2(j+l+q+v)}(2j+1)!(2l+1)!(2q+1)!(2v+1)!}\\ \times\sin^{2(j+l+q+v)+1}(\theta)\cos^{2(j+l)}(\phi)\sin^{2(q+v)}(\phi)d\theta d\phi\end{array}\right]\right\},\tag{4.6}$$

where R_a is the aspect ratio of the rectangle defined as

$$R_a=\frac{b}{a}.\tag{4.7}$$

The first approximation to the acoustic power can be obtained by considering only the first values of the indices given by $(j,l,q,v)=(0,0,0,0)$. Substituting this combination into Eq. (4.6), integrating, and simplifying, one can get

$$\Pi\cong\frac{\rho\omega^4 W_0^{\,2}A_p^{\,2}}{4\pi c}$$

which is familiar from Chapter III. For a triangular piston, the same result (Eq. (3.11)) was obtained for the dominant power term by using the surface integration approach. In fact, this result can be generalized to all pistons regardless of their shapes, but higher order acoustic power terms will not necessarily have the same forms.

A better approximation for the power can be obtained by considering the first two values of the indices in Eq. (4.6). This time, there are sixteen different combinations of them and they are: $(j,l,q,v)=(0,0,0,0)$, $(0,0,0,1)$, $(0,0,1,0)$, $(0,0,1,1)$, $(0,1,0,0)$, $(0,1,0,1)$,

$(0,1,1,0)$, $(0,1,1,1)$, $(1,0,0,0)$, $(1,0,0,1)$, $(1,0,1,0)$, $(1,0,1,1)$, $(1,1,0,0)$, $(1,1,0,1)$, $(1,1,1,0)$, and $(1,1,1,1)$. Substituting these cases into Eq. (4.6) separately, integrating, adding them up, and rearranging, the acoustic power becomes

$$\Pi \cong \frac{\rho\omega^4 W_0^2 A_p^2}{4\pi c}\left[\begin{array}{l} 1-\dfrac{\left(1+R_a^2\right)}{36}(ka)^2+\dfrac{\left(3+4R_a^2+3R_a^4\right)}{8640}(ka)^4 \\ -\dfrac{R_a^2\left(1+R_a^2\right)}{241920}(ka)^6+\dfrac{R_a^4}{34836480}(ka)^8 \end{array}\right]. \tag{4.8}$$

This is a surprising result because by using the surface integration approach, only the first two terms of the acoustic power were obtained in Chapter III, but now with the far-field integration approach five terms were obtained. The surface integration approach has the capability of yielding a specific number of terms of the acoustic power; in other words, one can decide on the number of power terms desired beforehand, although in the present approach this is not the case. Since in this approach mathematical difficulties forced us to expand difficult terms in their series form, generally, it cannot be said that including the first n terms in all expansions results in n terms of the acoustic power. This is because there may be interrelations between the expanded functions which results in higher powers of kL; for example, the multiplication of the two series as in this case.

Another important point to add is that if the number of terms in all expanded functions is increased by one, most of the previously found power terms will be affected. Therefore, in this sense, the surface integration approach is better.

No attempt has been made to obtain the total approximate acoustic power when the first three values of the indices are considered, and this analysis is enough for the scope of this study.

4.1.2.2 Surface Integration Approach

Substituting the velocity given by Eq. (3.2) into Eq. (2.20), integrating, and simplifying, the dominant power term becomes

$$\Pi_0 = \frac{\rho\omega^4 W_0^2 A_p^2}{4\pi c},$$

where A_p is given by Eq. (4.2) and as stated before this result is the same for all pistons.

To obtain the second term of the acoustic power, substituting the velocity into Eqs. (2.21) to (2.26), integrating, adding them together, and simplifying yields

$$\Pi_1 = \frac{\rho\omega^4 W_0^{\,2} A_p^{\,2}}{4\pi c}\left[-\frac{\left(1+R_a^{\,2}\right)}{36}(ka)^2\right], \tag{4.9}$$

where R_a is given by Eq. (4.7).

Finally, the total approximate acoustic power can be written as

$$\Pi \cong \frac{\rho\omega^4 W_0^{\,2} A_p^{\,2}}{4\pi c}\left[1-\frac{\left(1+R_a^{\,2}\right)}{36}(ka)^2\right]. \tag{4.10}$$

As can be seen, the first two terms of Eqs. (4.8) and (4.10) (the power results obtained by using different approaches) are the same.

4.2 Rectangular Plates

The far-field acoustic pressure, the acoustic intensity (whenever possible), and the acoustic power expressions will be obtained for rectangular plates with several different boundary conditions. To find the acoustic power expressions, only the surface integration approach will be used because the far-field pressure expressions are much more complex when compared to piston radiators.

To start with the acoustic problem, a velocity distribution over the plate is necessary; therefore, vibrations of the plates should be analyzed. In this study only the free harmonic vibrations of rectangular plates are considered.

4.2.1 Free Vibration Analysis

A rectangular plate, such as the one shown in Fig. 4.2, must satisfy the boundary conditions and the plate equation given by

$$D\nabla^4 w + \rho_p \frac{\partial^2 w}{\partial t^2} = 0 \tag{4.11}$$

where w is the transverse displacement, ρ_p is the mass per unit area of the plate and D is the flexural rigidity defined as

$$D = \frac{Eh^3}{12\left(1-\upsilon^2\right)}. \tag{4.12}$$

Here, E and υ is the modulus of elasticity and the Poisson's ratio of the plate material, respectively, and h is the thickness of the plate. In Eq. (4.11), $\nabla^4 = \nabla^2 \cdot \nabla^2$ where ∇^2 is the Laplacian operator. Then, writing ∇^4 in rectangular coordinates, substituting, and rearranging, Eq. (4.11) becomes

$$\frac{\partial^4 w}{\partial x^4} + 2\frac{\partial^4 w}{\partial x^2 \partial y^2} + \frac{\partial^4 w}{\partial y^4} + \frac{12\rho_p\left(1-\upsilon^2\right)}{Eh^3}\frac{\partial^2 w}{\partial t^2} = 0. \tag{4.13}$$

In general, it is impossible to find a form for w to satisfy Eq. (4.13) together with the boundary conditions. Warburton (1954) used the Rayleigh method assuming waveforms similar to those of beams to derive a simple approximate frequency expression for all modes of vibration. He considered three different boundary conditions; namely, clamped, simply supported, and free edges. There are fifteen different combinations of these boundary conditions for a rectangular plate and he tabulated the terms in the mentioned frequency expression for each of these combinations. He also stated that his assumed waveforms satisfy all of the boundary conditions for clamped and

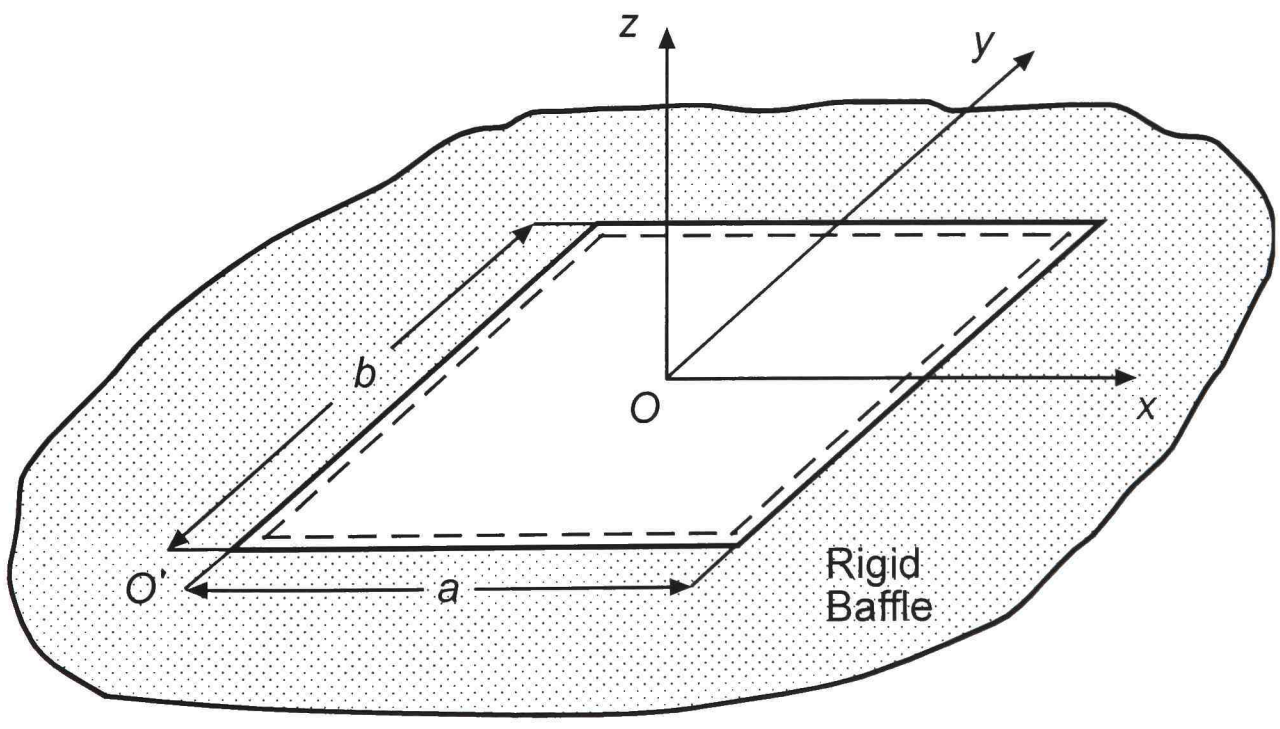

Figure 4.2. A Simply Supported Rectangular Plate.

simply supported edges, but they are only approximate for free edges. Therefore, in this study, only the first two types of boundary conditions (including all six possibilities) are considered. If this approach is used, the displacement function at any point (x,y) on the plate at time t can be given as

$$w(x,y,t) = W_0 X(x) Y(y) \exp(-i\omega t), \tag{4.14}$$

where $X(x)$ and $Y(y)$ are the so-called waveforms in both directions.

For any mode of vibration, the nodal pattern is defined by m and n, the number of nodal lines in the x and y directions, respectively. For clamped and simply supported boundary conditions, these numbers include the edges. Denoting the mode by nodal lines is suitable if the nodal lines are approximately parallel to the edges of the plate. When the plate is square and similarly supported in both directions, the nodal lines may not be parallel to the edges. The only exception to this is a plate with all four edges simply supported; in this case the nodal lines are always parallel to the edges.

Out of the six considered cases, two may exhibit this behavior, namely, a plate with all four edges clamped and a plate with two neighboring edges clamped and the other two simply supported. If the plate is square and all edges are clamped, and additionally, if $m-n = \pm 2,\ \pm 4,\ \pm 6, \ldots$, then the normal modes are of the types $m/n + n/m$ and $m/n - n/m$ (or $m/n \pm n/m$) and these patterns do not consist of lines parallel to the edges. Also, if the plate is a square one with two neighboring edges clamped and the other two simply supported, and additionally, if $m \neq n$, again the same modes exist. For these two cases one cannot simply use the displacement function given by Eq. (4.14) and the form of displacement functions will be analyzed in their corresponding sections.

Now, let us write down the waveforms for different combinations of boundary conditions in the x-direction. Warburton gave those waveforms with respect to point O' in Fig. 4.2 and the following waveforms are the transformed ones taking point O in the same figure as the center:

i. simply supported at $x = -a/2$ and $x = a/2$

$$X(x) = \sin\left[\frac{(m-1)\pi(x+a/2)}{a}\right] \text{ for } m = 2,\ 3,\ 4,\ldots; \tag{4.15}$$

ii. clamped at $x = -a/2$ and $x = a/2$

$$X(x) = \cos\left(\frac{\gamma x}{a}\right) + K\cosh\left(\frac{\gamma x}{a}\right) \text{ for } m = 2,\ 4,\ 6,\ldots, \tag{4.16a}$$

where $K = \dfrac{\sin(\gamma/2)}{\sinh(\gamma/2)}$ and $\tan(\gamma/2) + \tanh(\gamma/2) = 0$;

$$X(x) = \sin\left(\frac{\gamma' x}{a}\right) + K'\sinh\left(\frac{\gamma' x}{a}\right) \text{ for } m = 3,\ 5,\ 7,\ldots, \tag{4.16b}$$

where $K' = -\dfrac{\sin(\gamma'/2)}{\sinh(\gamma'/2)}$ and $\tan(\gamma'/2) - \tanh(\gamma'/2) = 0$;

iii. clamped at $x = -a/2$ and simply supported at $x = a/2$

$$X(x) = \sin\left[\gamma'\left(\frac{x}{2a} - \frac{1}{4}\right)\right] + K'\sinh\left[\gamma'\left(\frac{x}{2a} - \frac{1}{4}\right)\right] \text{ for } m = 2,\ 3,\ 4,\ldots, \tag{4.17}$$

where K' and γ' are the same as in Eq. (4.16b).

The corresponding expressions for $Y(y)$ can be obtained by replacing m, x, a, γ, γ', K, and K' with n, y, b, ε, ε', C, and C' in Eqs. (4.15) to (4.17).

For any boundary condition, a non-dimensional frequency factor, proportional to frequency, can be given as

$$\lambda^2 = \frac{\rho_p a^4 (2\pi f)^2}{\pi^4 D}, \tag{4.18}$$

where $2\pi f$ is the circular frequency ω.

For all of the six possibilities, this frequency factor can be determined from

$$\lambda^2 = G_x{}^4 + \left(G_y / R_a\right)^4 + 2H_x H_y / R_a{}^2, \tag{4.19}$$

where R_a is the aspect ratio of the rectangular plate given by Eq. (4.7) and the coefficients G_x, G_y, H_x, and H_y depend on the nodal pattern and the boundary conditions. The values of these coefficients are given in Table 4.1 for all six cases. Eq. (4.19) is not applicable to rectangular plates with any free edges.

Table 4.1: Coefficients in Frequency Equation (Eq. (4.19))

S: *Simply Supported* , *C*: *Clamped*

Boundary Condition	m	G_x	H_x
$S-S-S-S$	2, 3, 4,...	$m-1$	$(m-1)^2$
$C-S-S-S$	2, 3, 4,...	$m-\frac{3}{4}$	$\left(m-\frac{3}{4}\right)^2\left[1-\frac{1}{\left(m-\frac{3}{4}\right)\pi}\right]$
$C-S-C-S$	2	1.506	1.248
	3, 4, 5,...	$m-\frac{1}{2}$	$\left(m-\frac{1}{2}\right)^2\left[1-\frac{2}{\left(m-\frac{1}{2}\right)\pi}\right]$
$C-C-S-S$	2, 3, 4,...	$m-\frac{3}{4}$	$\left(m-\frac{3}{4}\right)^2\left[1-\frac{1}{\left(m-\frac{3}{4}\right)\pi}\right]$
$C-C-S-C$	2, 3, 4,...	$m-\frac{3}{4}$	$\left(m-\frac{3}{4}\right)^2\left[1-\frac{1}{\left(m-\frac{3}{4}\right)\pi}\right]$
$C-C-C-C$	2	1.506	1.248
	3, 4, 5,...	$m-\frac{1}{2}$	$\left(m-\frac{1}{2}\right)^2\left[1-\frac{2}{\left(m-\frac{1}{2}\right)\pi}\right]$

Table 4.1: Continued

Boundary Condition	n	G_y	H_y
$S-S-S-S$	2, 3, 4,...	$n-1$	$(n-1)^2$
$C-S-S-S$	2, 3, 4,...	$n-1$	$(n-1)^2$
$C-S-C-S$	2, 3, 4,...	$n-1$	$(n-1)^2$
$C-C-S-S$	2, 3, 4,...	$n-\frac{3}{4}$	$\left(n-\frac{3}{4}\right)^2\left[1-\frac{1}{\left(n-\frac{3}{4}\right)\pi}\right]$
$C-C-S-C$	2	1.506	1.248
	3, 4, 5,...	$n-\frac{1}{2}$	$\left(n-\frac{1}{2}\right)^2\left[1-\frac{2}{\left(n-\frac{1}{2}\right)\pi}\right]$
$C-C-C-C$	2	1.506	1.248
	3, 4, 5,...	$n-\frac{1}{2}$	$\left(n-\frac{1}{2}\right)^2\left[1-\frac{2}{\left(n-\frac{1}{2}\right)\pi}\right]$

Source: Warburton (1954)

Since Warburton's frequency results for these cases compared well with the literature, it is a good approximation to use the mentioned waveforms in writing the displacement functions for the free vibration of rectangular plates.
Now, some specific cases are considered.

4.2.2 Simply Supported Rectangular Plates

A simply supported rectangular plate, as shown in Fig. 4.2, is studied.

4.2.2.1 Displacement Function and Velocity Distribution

The waveform in the x-direction is given by Eq. (4.15) and in the y-direction it can be written as

$$Y(y) = \sin\left[\frac{(n-1)\pi(y+b/2)}{b}\right] \text{ for } n = 2,\ 3,\ 4,\ldots. \tag{4.20}$$

Substituting these waveforms into Eq. (4.14), the displacement function can be expressed as

$$w(x,y,t) = W_0 \sin\left[\frac{(m-1)\pi(x+a/2)}{a}\right]\sin\left[\frac{(n-1)\pi(y+b/2)}{b}\right]\exp(-i\omega t). \tag{4.21}$$

Taking the first time derivative and suppressing the $-i\exp(-i\omega t)$ term, the velocity distribution over the simply supported rectangular plate becomes

$$u(x,y) = \omega W_0 \sin\left[\frac{(m-1)\pi(x+a/2)}{a}\right]\sin\left[\frac{(n-1)\pi(y+b/2)}{b}\right]. \tag{4.22}$$

4.2.2.2 Far-field Acoustic Pressure Distribution

Substituting the given velocity distribution into Eq. (2.9), integrating, and factoring the area given by Eq. (4.2) out, the far-field pressure expression can be obtained as

$$p(R,\phi,\theta,t) = -i\frac{\rho\omega^2 W_0 A_p \exp\left[i(-\omega t + kR)\right]\pi(m-1)(n-1)}{2R\left\{(\psi_1 a)^2 - \left[\pi(m-1)\right]^2\right\}\left\{(\psi_2 b)^2 - \left[\pi(n-1)\right]^2\right\}}$$
$$\times\left\{\left[1+(-1)^m\right]\cos(\psi_1 a/2) + i\left[1-(-1)^m\right]\sin(\psi_1 a/2)\right\} \qquad (4.23)$$
$$\times\left\{\left[1+(-1)^n\right]\cos(\psi_2 b/2) + i\left[1-(-1)^n\right]\sin(\psi_2 b/2)\right\},$$

where ψ_1 and ψ_2 are given by Eqs. (3.6) and (3.7), respectively.

It can be noticed that for different combinations of even and odd values of m and n, the far-field pressure expression simplifies further. These simplified forms and the far-field acoustic intensity expressions for each case are presented in Appendix B.

4.2.2.3 Acoustic Power Radiation

Substituting the velocity given by Eq. (4.22) into Eq. (2.20), integrating, factoring the area square out, and simplifying, the dominant acoustic power expression becomes

$$\Pi_0 = \frac{\rho\omega^4 W_0^2 A_p^2}{4\pi c}\left\{\frac{4\left[1+(-1)^m\right]\left[1+(-1)^n\right]}{\pi^4(m-1)^2(n-1)^2}\right\}. \qquad (4.24)$$

To obtain the second term of the acoustic power, substituting the velocity into Eqs. (2.21) to (2.26), integrating, adding them together, and simplifying yields

$$\Pi_1 = \frac{\rho\omega^4 W_0^2 A_p^2}{4\pi c}\left[-\frac{2}{3\pi^4(m-1)^2(n-1)^2}\right]$$
$$\times\left\{\left[1+(-1)^n\right]\left\{1-\frac{4\left[1+(-1)^m\right]}{\pi^2(m-1)^2}\right\}+\left[1+(-1)^m\right]R_a^2\left\{1-\frac{4\left[1+(-1)^n\right]}{\pi^2(n-1)^2}\right\}\right\}(ka)^2, \qquad (4.25)$$

where R_a is the aspect ratio given by Eq. (4.7).

The total approximate acoustic power can be obtained by adding these two expressions.

As in the far-field pressure analysis, for even and odd values of m and n, these expressions simplify further and these simplified acoustic power terms are given in Appendix C.

4.2.3 Rectangular Plates with One Clamped and Three Simply Supported Edges

A rectangular plate with one clamped and three simply supported edges, as shown in Fig. 4.3, is studied.

4.2.3.1 Displacement Function and Velocity Distribution

The waveforms in x and y directions are given by Eqs. (4.17) and (4.20), respectively. Substituting them into Eq. (4.14), the displacement function becomes

$$w(x,y,t) = W_0\left\{\sin\left[\gamma'\left(\frac{x}{2a}-\frac{1}{4}\right)\right]+K'\sinh\left[\gamma'\left(\frac{x}{2a}-\frac{1}{4}\right)\right]\right\} \times \sin\left[\frac{(n-1)\pi(y+b/2)}{b}\right]\exp(-i\omega t). \tag{4.26}$$

Then, the velocity distribution can be found as

$$u(x,y) = \omega W_0\left\{\sin\left[\gamma'\left(\frac{x}{2a}-\frac{1}{4}\right)\right]+K'\sinh\left[\gamma'\left(\frac{x}{2a}-\frac{1}{4}\right)\right]\right\}\sin\left[\frac{(n-1)\pi(y+b/2)}{b}\right]. \tag{4.27}$$

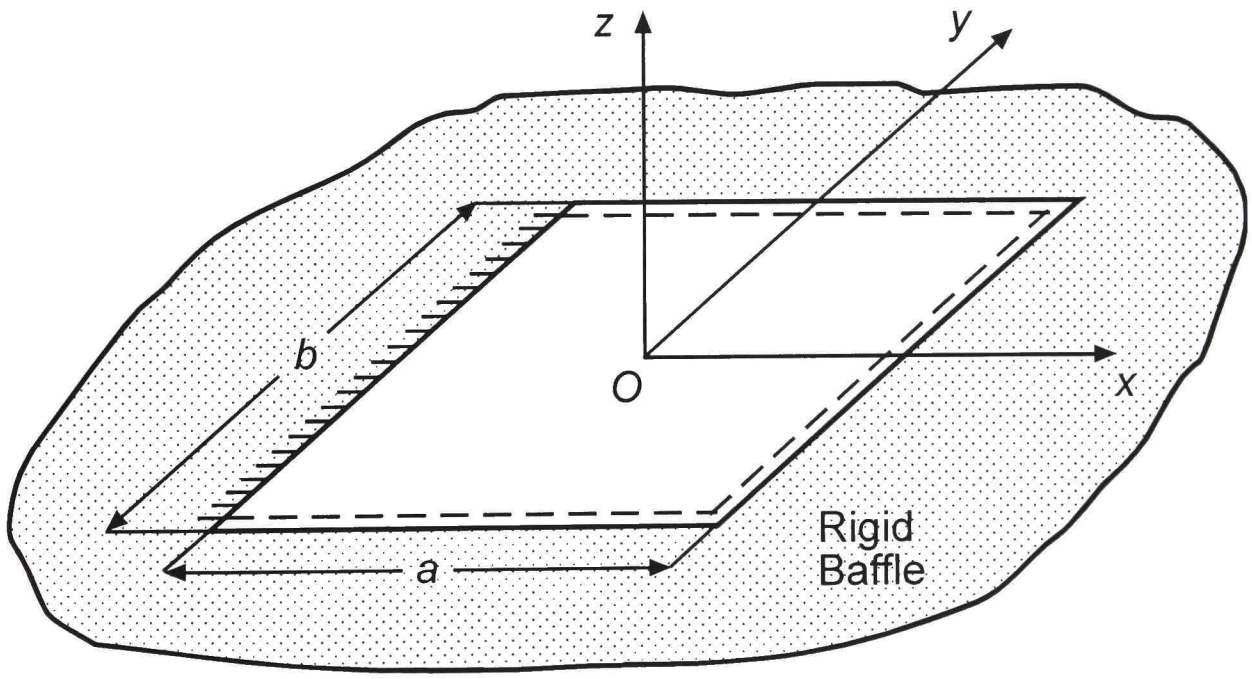

Figure 4.3. A Rectangular Plate with One Clamped and Three Simply Supported Edges.

4.2.3.2 Far-field Acoustic Pressure Distribution

Substituting the given velocity distribution into Eq. (2.9), integrating, and simplifying, the far-field acoustic pressure distribution can be obtained as

$$p(R,\phi,\theta,t) = i\frac{\rho\omega^2 W_0 A_p \exp\left[i(-\omega t + kR)\right]}{R} \times \frac{(n-1)\left\{(-1)^n \exp\left[i(\psi_1 a - \psi_2 b)/2\right] + \exp\left[i(\psi_1 a + \psi_2 b)/2\right]\right\}}{\left\{(\psi_2 b)^2 - \left[\pi(n-1)\right]^2\right\}\left[(2\psi_1 a)^4 - \gamma'^4\right]} \times \begin{Bmatrix} \gamma' \exp(-i\psi_1 a)\left[\gamma'^2(1-K') + (2\psi_1 a)^2(1+K')\right] \\ -K'\left[(2\psi_1 a)^2 - \gamma'^2\right]\left[\gamma' \cosh(\gamma'/2) - i(2\psi_1 a)\sinh(\gamma'/2)\right] \\ -\left[(2\psi_1 a)^2 + \gamma'^2\right]\left[\gamma' \cos(\gamma'/2) - i(2\psi_1 a)\sin(\gamma'/2)\right] \end{Bmatrix}, \quad (4.28)$$

where ψ_1 and ψ_2 are given by Eqs. (3.6) and (3.7), respectively.

4.2.3.3 Acoustic Power Radiation

Substituting the velocity given by Eq. (4.27) into Eq. (2.20), integrating, and simplifying, the first acoustic power term initially becomes

$$\Pi_0 = \frac{\rho\omega^4 W_0^2 A_p^2}{4\pi c}\left\{\left[1+(-1)^n\right]\frac{\left\{\left[\cos(\gamma'/2)-1\right] - K'\left[\cosh(\gamma'/2)-1\right]\right\}}{\pi(n-1)(\gamma'/2)}\right\}^2.$$

As can be noticed, this expression simplifies further when K' given by Eq. (4.16b) is substituted. Then, the dominant acoustic power term can be obtained as

$$\Pi_0 = \frac{\rho\omega^4 W_0^2 A_p^2}{4\pi c} \times \left\{\left[1+(-1)^n\right]\frac{\left\{\sinh(\gamma'/2)\left[\cos(\gamma'/2)-1\right] + \sin(\gamma'/2)\left[\cosh(\gamma'/2)-1\right]\right\}}{\pi(n-1)(\gamma'/2)\sinh(\gamma'/2)}\right\}^2. \quad (4.29)$$

Finally, for even and odd values of n, Eq. (4.29) becomes

for even n:

$$\Pi_0 = \frac{\rho\omega^4 W_0^2 A_p^2}{4\pi c}\left\{\frac{2\left\{\sinh(\gamma'/2)\left[\cos(\gamma'/2)-1\right] + \sin(\gamma'/2)\left[\cosh(\gamma'/2)-1\right]\right\}}{\pi(n-1)(\gamma'/2)\sinh(\gamma'/2)}\right\}^2, \quad (4.30a)$$

and for odd n:

$$\Pi_0 = 0. \tag{4.30b}$$

The second term of the acoustic power was also obtained in a similar manner. But, it was too long and the author was unable to simplify it further to a presentable form as the one given for the simply supported rectangular plate; therefore, it is not presented.

4.2.4 Rectangular Plates with Two Opposing Edges Clamped and Other Edges Simply Supported

A rectangular plate with two opposing edges clamped and the other edges simply supported, as shown in Fig. 4.4, is studied.

4.2.4.1 Displacement Function and Velocity Distribution

The waveforms in x and y directions are given by Eqs. (4.16) and (4.20), respectively. Substituting them into Eq. (4.14), the displacement function becomes for even m:

$$w(x,y,t) = W_0\left[\cos\left(\frac{\gamma x}{a}\right) + K\cosh\left(\frac{\gamma x}{a}\right)\right]\sin\left[\frac{(n-1)\pi(y+b/2)}{b}\right]\exp(-i\omega t), \tag{4.31a}$$

and for odd m:

$$w(x,y,t) = W_0\left[\sin\left(\frac{\gamma' x}{a}\right) + K'\sinh\left(\frac{\gamma' x}{a}\right)\right]\sin\left[\frac{(n-1)\pi(y+b/2)}{b}\right]\exp(-i\omega t). \tag{4.31b}$$

Then, as in the previous cases, the velocities can be obtained as

For even m:

$$u(x,y) = \omega W_0\left[\cos\left(\frac{\gamma x}{a}\right) + K\cosh\left(\frac{\gamma x}{a}\right)\right]\sin\left[\frac{(n-1)\pi(y+b/2)}{b}\right], \tag{4.32a}$$

and for odd m:

$$u(x,y) = \omega W_0\left[\sin\left(\frac{\gamma' x}{a}\right) + K'\sinh\left(\frac{\gamma' x}{a}\right)\right]\sin\left[\frac{(n-1)\pi(y+b/2)}{b}\right]. \tag{4.32b}$$

4.2.4.2 Far-field Acoustic Pressure Distribution

Substituting the given velocities into Eq. (2.9), integrating, and simplifying, the far-field acoustic pressure distributions for even and odd values of m and n can be obtained and they are presented in Appendix D.

4.2.4.3 Acoustic Power Radiation

Substituting the velocities given by Eqs. (4.32) into Eq. (2.20), integrating, and simplifying, the dominant acoustic power terms become

for even m:

$$\Pi_0 = \frac{\rho\omega^4 W_0^2 A_p^2}{4\pi c}\left\{\left[1+(-1)^n\right]\frac{2\sin(\gamma/2)}{\pi(n-1)(\gamma/2)}\right\}^2, \tag{4.33a}$$

and for odd m:

$$\Pi_0 = 0. \tag{4.33b}$$

Therefore, only for $(m,n)=(\text{even},\text{even})$, there is a nonzero Π_0 term and it is given by

$$\Pi_0 = \frac{\rho\omega^4 W_0^2 A_p^2}{4\pi c}\left\{\frac{4\sin(\gamma/2)}{\pi(n-1)(\gamma/2)}\right\}^2. \tag{4.34}$$

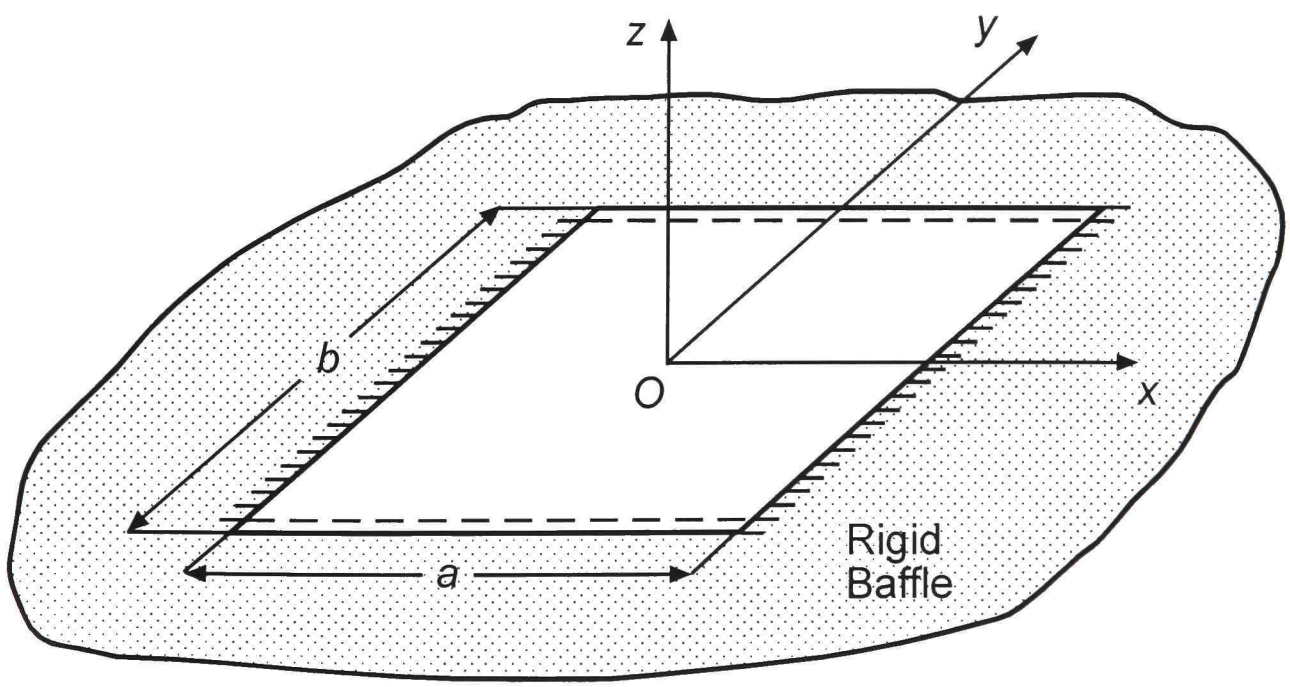

Figure 4.4. A Rectangular Plate with Two Opposing Edges Clamped and Other Edges Simply Supported.

The second terms of the acoustic power were also found as in other cases and again they are not given because of the length of the expressions. But it should be noted that for $(m,n)=(\text{odd},\text{odd})$, Π_1 becomes zero.

4.2.5 Rectangular Plates with Two Neighboring Edges Clamped and Other Edges Simply Supported

A rectangular plate with two neighboring edges clamped and the other edges simply supported, as shown in Fig. 4.5, is studied.

4.2.5.1 Displacement Function and Velocity Distribution

This is the first case in which if the plate is square or almost square (i.e., if $R_a=1$ or $R_a\cong 1$), the modes $m/n\pm n/m$ exist and for these cases the nodal patterns do not consist of lines. For such cases, Warburton used a two-term deflection function in the Rayleigh-Ritz method and investigated the transition of patterns as R_a approaches 1. But, in this study, almost square plates are skipped and the analysis is limited to rectangular and exactly square plates. Now, let us write down the displacement functions for both cases:

i. If the plate is rectangular, or, if it is square and $m=n$, the waveform in x-direction is given by Eq. (4.17) and in y-direction it can be written as

$$Y(y)=\sin\left[\varepsilon'\left(\frac{y}{2b}-\frac{1}{4}\right)\right]+C'\sinh\left[\varepsilon'\left(\frac{y}{2b}-\frac{1}{4}\right)\right] \text{ for } n=2,\ 3,\ 4,\ldots. \tag{4.35}$$

Substituting these waveforms into Eq. (4.14), the displacement function becomes

$$\begin{aligned} w(x,y,t)=W_0&\left\{\sin\left[\gamma'\left(\frac{x}{2a}-\frac{1}{4}\right)\right]+K'\sinh\left[\gamma'\left(\frac{x}{2a}-\frac{1}{4}\right)\right]\right\}\\ &\times\left\{\sin\left[\varepsilon'\left(\frac{y}{2b}-\frac{1}{4}\right)\right]+C'\sinh\left[\varepsilon'\left(\frac{y}{2b}-\frac{1}{4}\right)\right]\right\}\exp(-i\omega t). \end{aligned} \tag{4.36}$$

Then, the velocity distribution can be given as

$$u(x,y)=\omega W_0\left\{\sin\left[\gamma'\left(\frac{x}{2a}-\frac{1}{4}\right)\right]+K'\sinh\left[\gamma'\left(\frac{x}{2a}-\frac{1}{4}\right)\right]\right\}$$
$$\times\left\{\sin\left[\varepsilon'\left(\frac{y}{2b}-\frac{1}{4}\right)\right]+C'\sinh\left[\varepsilon'\left(\frac{y}{2b}-\frac{1}{4}\right)\right]\right\}. \tag{4.37}$$

ii. If the plate is square and $m\neq n$, the displacement function is expressed as

$$w(x,y,t)=W_0\left\{\begin{array}{l}\left\{\sin\left[\gamma'\left(\frac{x}{2a}-\frac{1}{4}\right)\right]+K'\sinh\left[\gamma'\left(\frac{x}{2a}-\frac{1}{4}\right)\right]\right\}\\ \times\left\{\sin\left[\varepsilon'\left(\frac{y}{2a}-\frac{1}{4}\right)\right]+C'\sinh\left[\varepsilon'\left(\frac{y}{2a}-\frac{1}{4}\right)\right]\right\}\\ \pm\left\{\sin\left[\varepsilon'\left(\frac{x}{2a}-\frac{1}{4}\right)\right]+C'\sinh\left[\varepsilon'\left(\frac{x}{2a}-\frac{1}{4}\right)\right]\right\}\\ \times\left\{\sin\left[\gamma'\left(\frac{y}{2a}-\frac{1}{4}\right)\right]+K'\sinh\left[\gamma'\left(\frac{y}{2a}-\frac{1}{4}\right)\right]\right\}\end{array}\right\}\exp(-i\omega t), \tag{4.38}$$

where plus sign refers to the mode $m/n+n/m$ while minus sign refers to the mode $m/n-n/m$ of the plate. As can be noticed, when writing Eq. (4.38), all b's were replaced with a's because they are the same for a square plate.

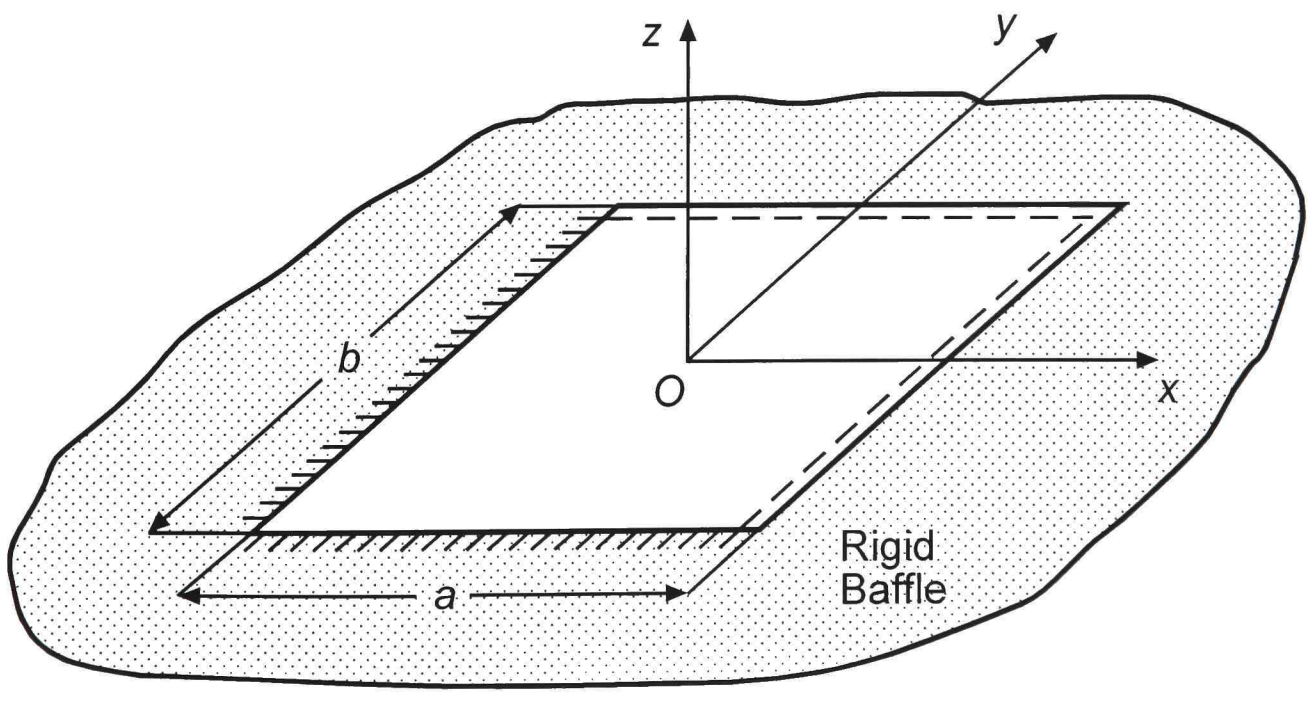

Figure 4.5. A Rectangular Plate with Two Neighboring Edges Clamped and Other Edges Simply Supported.

From Eq. (4.38), the velocity distribution can be obtained as

$$u(x,y)=\omega W_0\begin{Bmatrix}\left\{\sin\left[\gamma'\left(\frac{x}{2a}-\frac{1}{4}\right)\right]+K'\sinh\left[\gamma'\left(\frac{x}{2a}-\frac{1}{4}\right)\right]\right\}\\ \times\left\{\sin\left[\varepsilon'\left(\frac{y}{2a}-\frac{1}{4}\right)\right]+C'\sinh\left[\varepsilon'\left(\frac{y}{2a}-\frac{1}{4}\right)\right]\right\}\\ \pm\left\{\sin\left[\varepsilon'\left(\frac{x}{2a}-\frac{1}{4}\right)\right]+C'\sinh\left[\varepsilon'\left(\frac{x}{2a}-\frac{1}{4}\right)\right]\right\}\\ \times\left\{\sin\left[\gamma'\left(\frac{y}{2a}-\frac{1}{4}\right)\right]+K'\sinh\left[\gamma'\left(\frac{y}{2a}-\frac{1}{4}\right)\right]\right\}\end{Bmatrix}. \tag{4.39}$$

4.2.5.2 Far-field Acoustic Pressure Distribution

Substituting the given velocity distributions into Eq. (2.9), integrating, and simplifying, the far-field pressure expressions for both cases can be obtained and they are given in Appendix E.

4.2.5.3 Acoustic Power Radiation

Plugging the velocity distributions given by Eqs. (4.37) and (4.39) into Eq. (2.20), integrating, and making the usual simplifications, the dominant acoustic power terms become

i. if the plate is rectangular, or, if it is square and $m=n$

$$\Pi_0=\frac{\rho\omega^4 W_0^{\,2} A_p^{\,2}}{4\pi c}\left\{\frac{\sinh(\gamma'/2)\left[1-\cos(\gamma'/2)\right]+\sin(\gamma'/2)\left[1-\cosh(\gamma'/2)\right]}{(\gamma'/2)\sinh(\gamma'/2)}\right\}^2 \times\left\{\frac{\sinh(\varepsilon'/2)\left[1-\cos(\varepsilon'/2)\right]+\sin(\varepsilon'/2)\left[1-\cosh(\varepsilon'/2)\right]}{(\varepsilon'/2)\sinh(\varepsilon'/2)}\right\}^2, \tag{4.40}$$

ii. if it is square and $m\neq n$

for the mode $m/n+n/m$:

$$\Pi_0 = \frac{\rho\omega^4 W_0^2 A_p^2}{2\pi c}\left\{\frac{\sinh(\gamma'/2)\left[1-\cos(\gamma'/2)\right]+\sin(\gamma'/2)\left[1-\cosh(\gamma'/2)\right]}{(\gamma'/2)\sinh(\gamma'/2)}\right\}^2 \times\left\{\frac{\sinh(\varepsilon'/2)\left[1-\cos(\varepsilon'/2)\right]+\sin(\varepsilon'/2)\left[1-\cosh(\varepsilon'/2)\right]}{(\varepsilon'/2)\sinh(\varepsilon'/2)}\right\}^2, \tag{4.41a}$$

for the mode $m/n-n/m$:

$$\Pi_0 = 0. \tag{4.41b}$$

The second terms of the acoustic power were also found as in other cases, but again they are not given because of the length of the expressions.

4.2.6 Rectangular Plates with One Simply Supported and Three Clamped Edges

A rectangular plate with one simply supported and three clamped edges, as shown in Fig. 4.6, is studied.

4.2.6.1 Displacement Function and Velocity Distribution

The waveform in x-direction is given by Eq. (4.17) and in y-direction, it is given by

$$Y(y) = \cos\left(\frac{\varepsilon y}{b}\right) + C\cosh\left(\frac{\varepsilon y}{b}\right) \text{ for } n = 2,\ 4,\ 6,\ldots \tag{4.42a}$$

and

$$Y(y) = \sin\left(\frac{\varepsilon' y}{b}\right) + C'\sinh\left(\frac{\varepsilon' y}{b}\right) \text{ for } n = 3,\ 5,\ 7,\ldots. \tag{4.42b}$$

Substituting these waveforms into Eq. (4.14), the displacement functions become

for even n:

$$w(x,y,t) = W_0\left\{\sin\left[\gamma'\left(\frac{x}{2a}-\frac{1}{4}\right)\right] + K'\sinh\left[\gamma'\left(\frac{x}{2a}-\frac{1}{4}\right)\right]\right\} \times\left[\cos\left(\frac{\varepsilon y}{b}\right) + C\cosh\left(\frac{\varepsilon y}{b}\right)\right]\exp(-i\omega t), \tag{4.43a}$$

for odd n:

$$w(x,y,t) = W_0\left\{\sin\left[\gamma'\left(\frac{x}{2a}-\frac{1}{4}\right)\right]+K'\sinh\left[\gamma'\left(\frac{x}{2a}-\frac{1}{4}\right)\right]\right\} \times\left[\sin\left(\frac{\varepsilon' y}{b}\right)+C'\sinh\left(\frac{\varepsilon' y}{b}\right)\right]\exp(-i\omega t). \quad (4.43b)$$

Therefore, the velocity distributions can be written as

for even n:

$$u(x,y) = \omega W_0\left\{\sin\left[\gamma'\left(\frac{x}{2a}-\frac{1}{4}\right)\right]+K'\sinh\left[\gamma'\left(\frac{x}{2a}-\frac{1}{4}\right)\right]\right\}\left[\cos\left(\frac{\varepsilon y}{b}\right)+C\cosh\left(\frac{\varepsilon y}{b}\right)\right], \quad (4.44a)$$

for odd n:

$$u(x,y) = \omega W_0\left\{\sin\left[\gamma'\left(\frac{x}{2a}-\frac{1}{4}\right)\right]+K'\sinh\left[\gamma'\left(\frac{x}{2a}-\frac{1}{4}\right)\right]\right\}\left[\sin\left(\frac{\varepsilon' y}{b}\right)+C'\sinh\left(\frac{\varepsilon' y}{b}\right)\right]. \quad (4.44b)$$

4.2.6.2 Far-field Acoustic Pressure Distribution

Substituting the velocity distributions given above into Eq. (2.9), integrating, and simplifying, the far-field pressure expressions were obtained and they are presented in Appendix F.

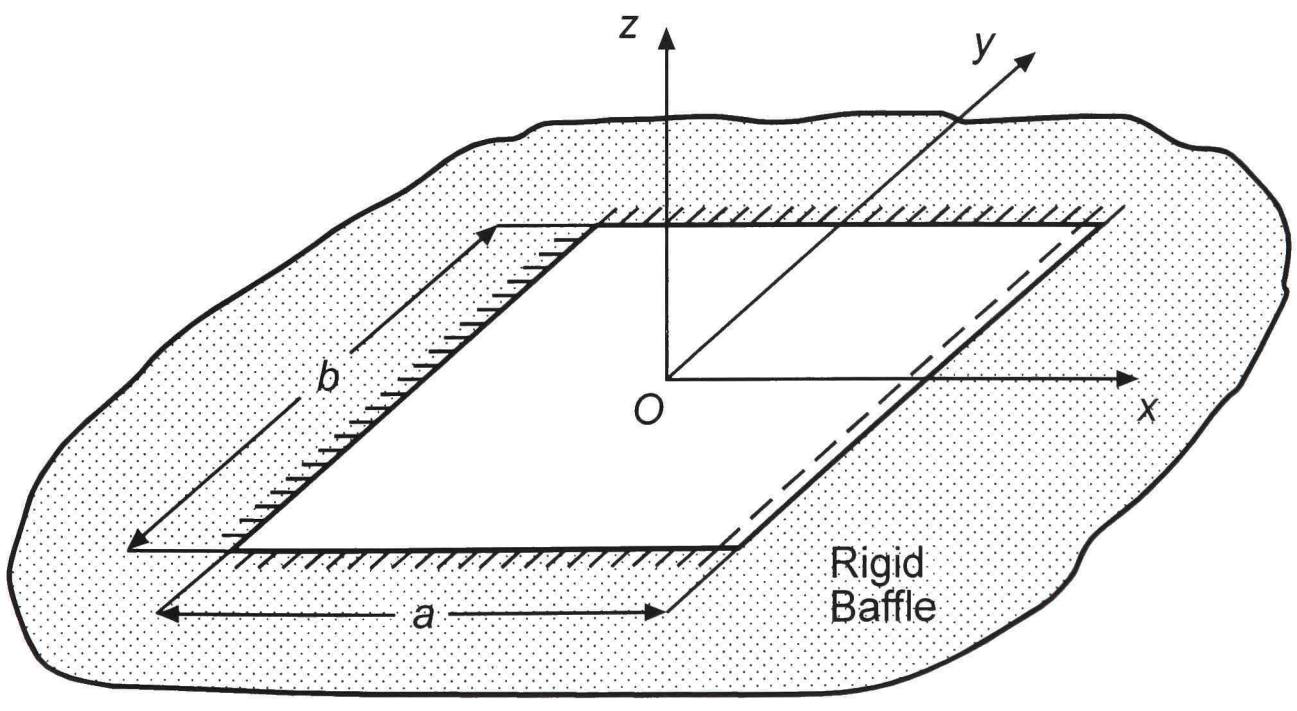

Figure 4.6. A Rectangular Plate with One Simply Supported and Three Clamped Edges.

4.2.6.3 Acoustic Power Radiation

After substituting the velocity distributions given by Eqs. (4.44) into Eq. (2.20), integrating, and simplifying, the dominant acoustic power terms become

for even n:

$$\Pi_0 = \frac{\rho\omega^4 W_0^2 A_p^2}{4\pi c}\left[\frac{2\sin(\varepsilon/2)}{(\varepsilon/2)}\right]^2 \times\left\{\frac{\sinh(\gamma'/2)\left[1-\cos(\gamma'/2)\right]+\sin(\gamma'/2)\left[1-\cosh(\gamma'/2)\right]}{(\gamma'/2)\sinh(\gamma'/2)}\right\}^2, \tag{4.45a}$$

for odd n:

$$\Pi_0 = 0. \tag{4.45b}$$

The second power terms were also found, but they are not given.

4.2.7 Clamped Rectangular Plates

A clamped rectangular plate, as shown in Fig. 4.7, is studied.

4.2.7.1 Displacement Function and Velocity Distribution

This is the second case in which if the plate is square, the modes $m/n \pm n/m$ exist. Therefore, two-term displacement functions should be used for clamped square plates as done for square plates with two neighboring edges clamped and others simply supported.

The waveforms in x and y-directions are given by Eqs. (4.16) and Eqs. (4.42), respectively. Substituting them into Eq. (4.14), the displacement functions become

i. if the plate is rectangular, or, if it is square and $m-n \neq \pm 2,\ \pm 4,\ \pm 6,\ldots$

for $(m,n) = (\text{even},\text{even})$:

$$w(x,y,t) = W_0\left[\cos\left(\frac{\gamma x}{a}\right)+K\cosh\left(\frac{\gamma x}{a}\right)\right]\left[\cos\left(\frac{\varepsilon y}{b}\right)+C\cosh\left(\frac{\varepsilon y}{b}\right)\right]\exp(-i\omega t), \tag{4.46a}$$

for $(m,n) = (\text{even},\text{odd})$:

$$w(x,y,t) = W_0\left[\cos\left(\frac{\gamma x}{a}\right)+K\cosh\left(\frac{\gamma x}{a}\right)\right]\left[\sin\left(\frac{\varepsilon' y}{b}\right)+C'\sinh\left(\frac{\varepsilon' y}{b}\right)\right]\exp(-i\omega t), \tag{4.46b}$$

for $(m,n)=(\text{odd},\text{even})$:

$$w(x,y,t)=W_0\left[\sin\left(\frac{\gamma' x}{a}\right)+K'\sinh\left(\frac{\gamma' x}{a}\right)\right]\left[\cos\left(\frac{\varepsilon y}{b}\right)+C\cosh\left(\frac{\varepsilon y}{b}\right)\right]\exp(-i\omega t), \qquad (4.46c)$$

for $(m,n)=(\text{odd},\text{odd})$:

$$w(x,y,t)=W_0\left[\sin\left(\frac{\gamma' x}{a}\right)+K'\sinh\left(\frac{\gamma' x}{a}\right)\right]\left[\sin\left(\frac{\varepsilon' y}{b}\right)+C'\sinh\left(\frac{\varepsilon' y}{b}\right)\right]\exp(-i\omega t). \qquad (4.46d)$$

For a square plate, b in these equations can be replaced with a and the only condition for cases (4.46a) and (4.46d) to exist is $m=n$.

Then, the velocities can be written as

for $(m,n)=(\text{even},\text{even})$:

$$u(x,y)=\omega W_0\left[\cos\left(\frac{\gamma x}{a}\right)+K\cosh\left(\frac{\gamma x}{a}\right)\right]\left[\cos\left(\frac{\varepsilon y}{b}\right)+C\cosh\left(\frac{\varepsilon y}{b}\right)\right], \qquad (4.47a)$$

for $(m,n)=(\text{even},\text{odd})$:

$$u(x,y)=\omega W_0\left[\cos\left(\frac{\gamma x}{a}\right)+K\cosh\left(\frac{\gamma x}{a}\right)\right]\left[\sin\left(\frac{\varepsilon' y}{b}\right)+C'\sinh\left(\frac{\varepsilon' y}{b}\right)\right], \qquad (4.47b)$$

for $(m,n)=(\text{odd},\text{even})$:

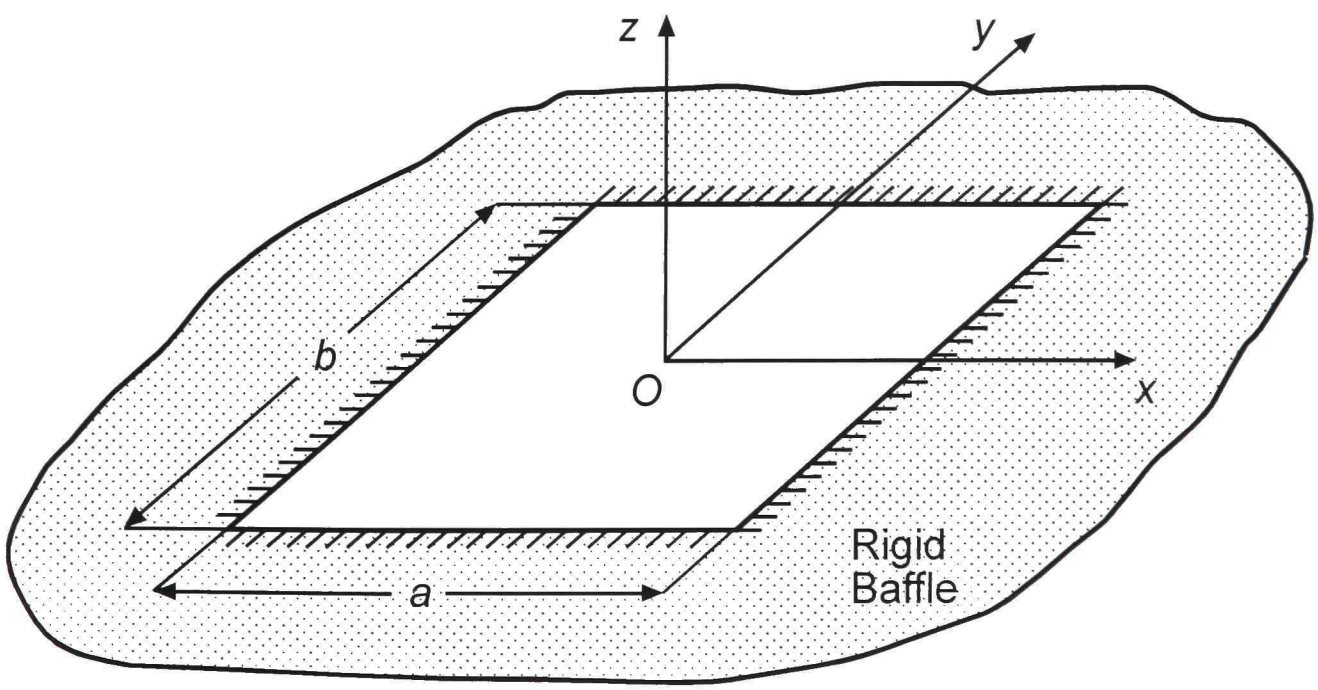

Figure 4.7. A Clamped Rectangular Plate.

$$u(x,y)=\omega W_0\left[\sin\left(\frac{\gamma' x}{a}\right)+K'\sinh\left(\frac{\gamma' x}{a}\right)\right]\left[\cos\left(\frac{\varepsilon y}{b}\right)+C\cosh\left(\frac{\varepsilon y}{b}\right)\right], \qquad (4.47c)$$

for $(m,n)=(\text{odd},\text{odd})$:

$$u(x,y)=\omega W_0\left[\sin\left(\frac{\gamma' x}{a}\right)+K'\sinh\left(\frac{\gamma' x}{a}\right)\right]\left[\sin\left(\frac{\varepsilon' y}{b}\right)+C'\sinh\left(\frac{\varepsilon' y}{b}\right)\right]. \qquad (4.47d)$$

ii. if it is square and $m-n=\pm 2,\ \pm 4,\ \pm 6,\ldots$, the displacement functions become

for $(m,n)=(\text{even},\text{even})$:

$$w(x,y,t)=W_0\left\{\begin{array}{l}\left[\cos\left(\frac{\gamma x}{a}\right)+K\cosh\left(\frac{\gamma x}{a}\right)\right]\left[\cos\left(\frac{\varepsilon y}{a}\right)+C\cosh\left(\frac{\varepsilon y}{a}\right)\right]\\ \pm\left[\cos\left(\frac{\varepsilon x}{a}\right)+C\cosh\left(\frac{\varepsilon x}{a}\right)\right]\left[\cos\left(\frac{\gamma y}{a}\right)+K\cosh\left(\frac{\gamma y}{a}\right)\right]\end{array}\right\}\exp(-i\omega t), \qquad (4.48a)$$

for $(m,n)=(\text{odd},\text{odd})$:

$$w(x,y,t)=W_0\left\{\begin{array}{l}\left[\sin\left(\frac{\gamma' x}{a}\right)+K'\sinh\left(\frac{\gamma' x}{a}\right)\right]\left[\sin\left(\frac{\varepsilon' y}{a}\right)+C'\sinh\left(\frac{\varepsilon' y}{a}\right)\right]\\ \pm\left[\sin\left(\frac{\varepsilon' x}{a}\right)+C'\sinh\left(\frac{\varepsilon' x}{a}\right)\right]\left[\sin\left(\frac{\gamma' y}{a}\right)+K'\sinh\left(\frac{\gamma' y}{a}\right)\right]\end{array}\right\}\exp(-i\omega t). \qquad (4.48b)$$

Accordingly, the velocity distributions are given as

for $(m,n)=(\text{even},\text{even})$:

$$u(x,y)=\omega W_0\left\{\begin{array}{l}\left[\cos\left(\frac{\gamma x}{a}\right)+K\cosh\left(\frac{\gamma x}{a}\right)\right]\left[\cos\left(\frac{\varepsilon y}{a}\right)+C\cosh\left(\frac{\varepsilon y}{a}\right)\right]\\ \pm\left[\cos\left(\frac{\varepsilon x}{a}\right)+C\cosh\left(\frac{\varepsilon x}{a}\right)\right]\left[\cos\left(\frac{\gamma y}{a}\right)+K\cosh\left(\frac{\gamma y}{a}\right)\right]\end{array}\right\}, \qquad (4.49a)$$

for $(m,n)=(\text{odd},\text{odd})$:

$$u(x,y)=\omega W_0\left\{\begin{array}{l}\left[\sin\left(\frac{\gamma' x}{a}\right)+K'\sinh\left(\frac{\gamma' x}{a}\right)\right]\left[\sin\left(\frac{\varepsilon' y}{a}\right)+C'\sinh\left(\frac{\varepsilon' y}{a}\right)\right]\\ \pm\left[\sin\left(\frac{\varepsilon' x}{a}\right)+C'\sinh\left(\frac{\varepsilon' x}{a}\right)\right]\left[\sin\left(\frac{\gamma' y}{a}\right)+K'\sinh\left(\frac{\gamma' y}{a}\right)\right]\end{array}\right\}. \qquad (4.49b)$$

4.2.7.2 Far-field Acoustic Pressure Distribution

Substituting the given velocity distributions into Eq. (2.9), integrating, and simplifying, the far-field acoustic pressure expressions were obtained and they are given in Appendix G.

4.2.7.3 Acoustic Power Radiation

Plugging the velocities given by Eqs. (4.47) and (4.49) into Eq. (2.20), integrating, and simplifying, the dominant acoustic power terms become

i. if the plate is rectangular, or, if it is square and $m-n \neq \pm 2,\ \pm 4,\ \pm 6,\ldots$

for $(m,n)=(\text{even},\text{even})$:

$$\Pi_0 = \frac{\rho\omega^4 W_0^{\,2} A_p}{4\pi c}\left[\frac{4\sin(\gamma/2)\sin(\varepsilon/2)}{(\gamma/2)(\varepsilon/2)}\right]^2, \tag{4.50a}$$

and for $(m,n)=(\text{even},\text{odd})$, (odd,even), and (odd,odd):

$$\Pi_0 = 0; \tag{4.50b}$$

ii. if it is square and $m-n=\pm 2,\ \pm 4,\ \pm 6,\ldots$

for $(m,n)=(\text{even},\text{even})$:

for mode $m/n+n/m$:

$$\Pi_0 = \frac{\rho\omega^4 W_0^{\,2} A_p}{4\pi c}\left[\frac{8\sin(\gamma/2)\sin(\varepsilon/2)}{(\gamma/2)(\varepsilon/2)}\right]^2, \tag{4.51a}$$

for the mode $m/n-n/m$:

$$\Pi_0 = 0, \tag{4.51b}$$

for $(m,n)=(\text{odd},\text{odd})$, for both modes $m/n\pm n/m$:

$$\Pi_0 = 0, \tag{4.51c}$$

The second terms of the acoustic power were also found. Nonzero Π_1 terms are not given. But it is important to note that if the plate is rectangular, or, if it is square and $m-n \neq \pm 2,\ \pm 4,\ \pm 6,\ldots$, Π_1 becomes zero for $(m,n)=(\text{odd},\text{odd})$. Also, if it is square and $m-n=\pm 2,\ \pm 4,\ \pm 6,\ldots$, Π_1 is zero for the mode $m/n+n/m$ for

$(m,n)=(\text{odd},\text{odd})$. More interestingly, for the mode $m/n-n/m$, Π_1 is zero for both $(m,n)=(\text{even},\text{even})$ and (odd,odd).

CHAPTER V
CIRCULAR GEOMETRY

Circular pistons and plates are studied in this chapter.

5.1 Circular Pistons

The far-field acoustic pressure, the acoustic intensity, and the acoustic power expressions are obtained for a circular piston shown in Fig. 5.1. The geometry and the coordinate system used are shown in the same figure. As in the rectangular piston, both the far-field and surface integration approaches are used to find the acoustic power radiation.

5.1.1 Far-field Acoustic Pressure Distribution

Circular geometry is well-suited for polar coordinates. Therefore, substituting the velocity given by Eq. (3.2) into Eq. (2.8), rotating the x-z plane in Fig. 5.1 to the plane including the far-field point P (this makes the angle ϕ zero, simplifying the integration), replacing the first k with ω / c, and rearranging yields

$$p(R,\theta,t) = -i\frac{\rho\omega^2 W_0 \exp\left[i(-\omega t + kR)\right]}{2\pi R}\int_{r=0}^{r_0}\left\{\int_{\alpha=0}^{2\pi}\exp\left[-ik\sin(\theta)r\cos(\alpha)\right]d\alpha\right\}rdr\,. \tag{5.1}$$

To take the inner integral, the general relation

$$J_m(x) = \frac{(-i)^m}{2\pi}\int_0^{2\pi}\exp\left[ix\cos(\psi)\right]\cos(m\psi)d\psi \tag{5.2}$$

can be used (Hunter, 1957). Here, $J_m(x)$ is the Bessel function of the first kind of order m. Substituting $m = 0$ into Eq. (5.2) and simplifying, the integral becomes

$$\int_0^{2\pi}\exp\left[ix\cos(\psi)\right]d\psi = 2\pi J_0(x)\,. \tag{5.3}$$

After comparing the integrals in Eqs. (5.1) and (5.3), the former can be written as

$$\int_0^{2\pi}\exp\left[-ik\sin(\theta)r\cos(\alpha)\right]d\alpha = 2\pi J_0\left[-k\sin(\theta)r\right].$$

Substituting this result into Eq. (5.1) and simplifying gives

$$p(R,\theta,t) = -i\frac{\rho\omega^2 W_0 \exp\left[i(-\omega t + kR)\right]}{R}\int_{r=0}^{r_0} rJ_0\left[-k\sin(\theta)r\right]dr\,.$$

To take this integral, the identity

$$\int xJ_0(x)dx = xJ_1(x)$$

of Bessel functions can be used. Then, the final form of the far-field pressure becomes

$$p(R,\theta,t) = -i\frac{\rho\omega^2 W_0 A_p \exp\left[i(-\omega t + kR)\right]}{\pi R}\left\{\frac{J_1\left[kr_0\sin(\theta)\right]}{kr_0\sin(\theta)}\right\}, \tag{5.4}$$

where A_p is the area of any circular source with a radius of r_0 given by

$$A_p = \pi r_0^{\,2}\,. \tag{5.5}$$

5.1.2 Acoustic Power Radiation

5.1.2.1 Far-field Integration Approach

The magnitude of the far-field pressure distribution, given by Eq. (5.4), is

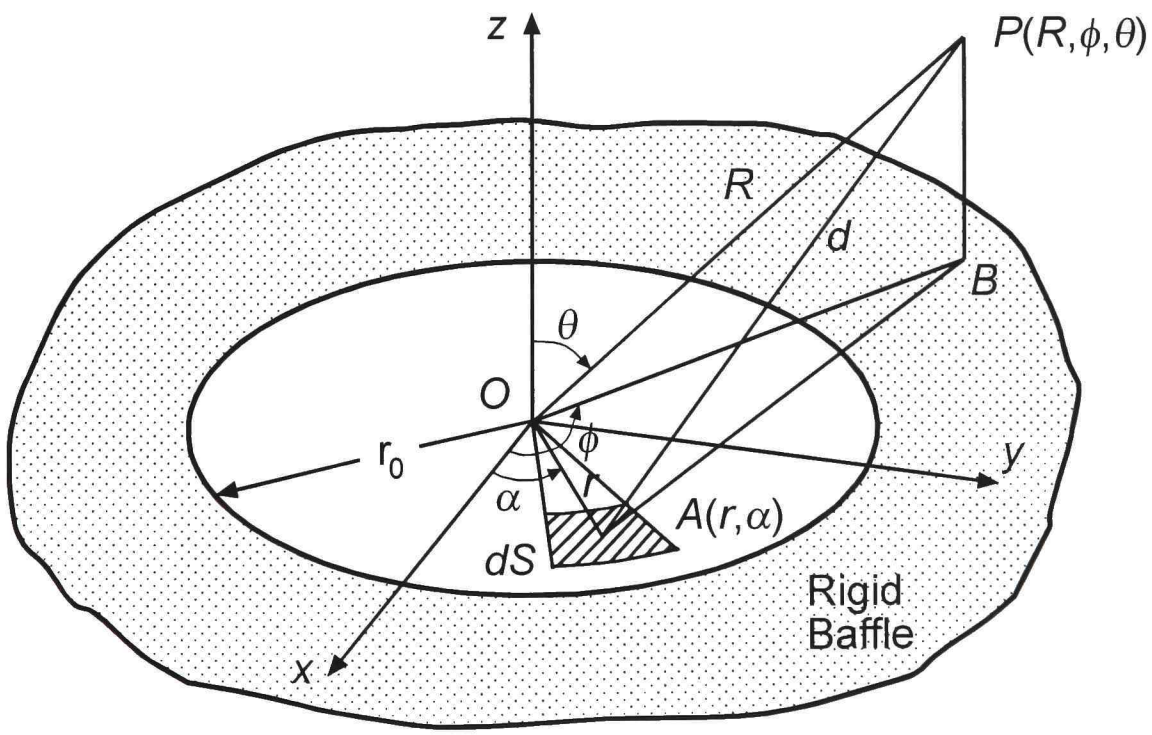

Figure 5.1. A Circular Piston and the Coordinate System.

$$\left|p(R,\theta)\right| = \frac{\rho\omega^2 W_0 A_p}{\pi R}\left\{\frac{J_1\left[kr_0\sin(\theta)\right]}{kr_0\sin(\theta)}\right\}. \tag{5.6}$$

Using this pressure magnitude in Eq. (2.10), the acoustic intensity is obtained as

$$I(R,\theta) = \frac{\rho\omega^4 {W_0}^2 {A_p}^2}{2\pi^2 R^2 c}\left\{\frac{J_1\left[kr_0\sin(\theta)\right]}{kr_0\sin(\theta)}\right\}^2. \tag{5.7}$$

Substituting this intensity into Eq. (2.11) one can get

$$\Pi = \frac{\rho\omega^4 {W_0}^2 {A_p}^2}{4\pi c}\left\{\frac{2}{\pi}\int_{\theta=0}^{\pi/2}\left(\int_{\phi=0}^{2\pi} d\phi\right)\frac{\left\{J_1\left[kr_0\sin(\theta)\right]\right\}^2}{(kr_0)^2\sin(\theta)}d\theta\right\}.$$

Evaluating the inner integral, the acoustic power radiation becomes

$$\Pi = \frac{\rho\omega^4 {W_0}^2 {A_p}^2}{4\pi c}\int_{\theta=0}^{\pi/2}\frac{4\left\{J_1\left[kr_0\sin(\theta)\right]\right\}^2}{(kr_0)^2\sin(\theta)}d\theta. \tag{5.8}$$

This integral is impossible to evaluate in this form, therefore the series expansion of the Bessel function can be used. The Bessel function of the first kind of order n is defined as

$$J_n(x) = \sum_{s=0}^{\infty}\frac{(-1)^s x^{n+2s}}{2^{n+2s}\,s!(n+s)!}. \tag{5.9}$$

If $n=1$ is substituted into this equation one can get

$$J_1(x) = \sum_{s=0}^{\infty}\frac{(-1)^s x^{2s+1}}{2^{2s+1}(s+1)(s!)^2}. \tag{5.10}$$

Then, its square can be written as

$${J_1}^2(x) = \sum_{q=0}^{\infty}\sum_{s=0}^{\infty}\frac{(-1)^{q+s}x^{2(q+s+1)}}{2^{2(q+s+1)}(q+1)(s+1)(q!)^2(s!)^2}.$$

Replacing x with $-kr_0\sin(\theta)$ gives

$${J_1}^2\left[kr_0\sin(\theta)\right] = \sum_{q=0}^{\infty}\sum_{s=0}^{\infty}\frac{(-1)^{q+s}(kr_0)^{2(q+s+1)}\sin^{2(q+s+1)}(\theta)}{2^{2(q+s+1)}(q+1)(s+1)(q!)^2(s!)^2}.$$

Plugging this result into Eq. (5.8) and simplifying, the acoustic power expression for a circular piston of radius r_0 can be found as

$$\Pi = \frac{\rho\omega^4 W_0^{\,2} A_p^{\,2}}{4\pi c} \sum_{q=0}^{\infty}\sum_{s=0}^{\infty} \frac{(-1)^{q+s}(kr_0)^{2(q+s)}}{4^{(q+s)}(q+1)(s+1)(q!)^2(s!)^2} \int_{\theta=0}^{\pi/2} \sin^{2(q+s)+1}(\theta)d\theta \,. \qquad (5.11)$$

If only the first values of the indices are taken into account, the only possible combination is $(q,s)=(0,0)$. Substituting this combination into Eq. (5.11), the acoustic power becomes

$$\Pi \cong \frac{\rho\omega^4 W_0^{\,2} A_p^{\,2}}{4\pi c}$$

which was an expected result as the dominant power term .

If the first two terms of the indices are considered, there are four different combinations of them and they are $(q,s)=(0,0)$, $(0,1)$, $(1,0)$, and $(1,1)$. Substituting these combinations into Eq. (5.11) separately, integrating, adding them up, and simplifying, the total approximate acoustic power can be obtained as

$$\Pi \cong \frac{\rho\omega^4 W_0^{\,2} A_p^{\,2}}{4\pi c}\left[1-\frac{1}{6}(kr_0)^2+\frac{1}{120}(kr_0)^4\right]. \qquad (5.12)$$

All of the arguments on the acoustic power results presented in Section 4.1.2.1 are also applicable to the present case.

5.1.2.2 Surface Integration Approach

The use of polar coordinates is preferred for this analysis also. Therefore, substituting the velocity given by Eq. (3.2) into Eq. (2.30), integrating, and simplifying, the dominant power term becomes

$$\Pi_0 = \frac{\rho\omega^4 W_0^{\,2} A_p^{\,2}}{4\pi c}$$

which is the same as in the previous cases and A_p is given by Eq. (5.5).

Substituting the velocity into Eqs. (2.31) to (2.36), integrating, adding them together, and simplifying, the second term of the acoustic power can be obtained as

$$\Pi_1 = \frac{\rho\omega^4 W_0^{\,2} A_p^{\,2}}{4\pi c}\left[-\frac{1}{6}(kr_0)^2\right]. \qquad (5.13)$$

Finally, the total approximate acoustic power can be written as

$$\Pi \cong \frac{\rho\omega^4 W_0^2 A_p^2}{4\pi c}\left[1-\frac{1}{6}(kr_0)^2\right]. \tag{5.14}$$

It can be seen that the first two terms of Eqs. (5.12) and (5.14) are the same.

5.2 Circular Plates

The far-field acoustic pressure, the acoustic intensity, and the acoustic power expressions will be obtained for a clamped and simply supported circular plate vibrating freely and with a uniform forcing function.

5.2.1 Vibration Analysis

5.2.1.1 Free Vibrations

The differential equation of motion for the transverse displacement w of a plate is given by Eq. (4.11).

When free harmonic vibrations are considered, the displacement function is given by

$$w = W\exp(-i\omega t) \tag{5.15}$$

where W is a position dependent deflection function and ω is the circular frequency expressed in rad/s.

Substituting w given by Eq. (5.15) into Eq. (4.11) yields

$$(\nabla^4 - \lambda^4)W = 0, \tag{5.16}$$

where λ is a parameter defined as

$$\lambda^4 = \frac{\rho_p\omega^2}{D}. \tag{5.17}$$

Eq. (5.16) can also be written as

$$(\nabla^2 + \lambda^2)(\nabla^2 - \lambda^2)W = 0. \tag{5.18}$$

The general solution of Eq. (5.18) is the sum of the solutions of the individual equations

$$\nabla^2 W_1 + \lambda^2 W_1 = 0 \tag{5.19a}$$

and

$$\nabla^2 W_2 - \lambda^2 W_2 = 0. \tag{5.19b}$$

The Laplacian operator in polar coordinates is given by

$$\nabla^2 = \frac{\partial^2}{\partial r^2} + \frac{1}{r}\frac{\partial}{\partial r} + \frac{1}{r^2}\frac{\partial^2}{\partial \alpha^2}. \tag{5.20}$$

Substituting ∇^2 from Eq. (5.20) into Eqs. (5.19) yields

$$\frac{\partial^2 W_1}{\partial r^2} + \frac{1}{r}\frac{\partial W_1}{\partial r} + \frac{1}{r^2}\frac{\partial^2 W_1}{\partial \alpha^2} + \lambda^2 W_1 = 0 \tag{5.21a}$$

and

$$\frac{\partial^2 W_2}{\partial r^2} + \frac{1}{r}\frac{\partial W_2}{\partial r} + \frac{1}{r^2}\frac{\partial^2 W_2}{\partial \alpha^2} - \lambda^2 W_2 = 0. \tag{5.21b}$$

For a circular plate, displacements at any point on the plate are only a function of radius when there are no nodal diameters; therefore, the derivatives with respect to angle vanish and Eqs. (5.21) become

$$\frac{\partial^2 W_1}{\partial r^2} + \frac{1}{r}\frac{\partial W_1}{\partial r} + \lambda^2 W_1 = 0 \tag{5.22a}$$

and

$$\frac{\partial^2 W_2}{\partial r^2} + \frac{1}{r}\frac{\partial W_2}{\partial r} - \lambda^2 W_2 = 0. \tag{5.22b}$$

Eqs. (5.22) are the Bessel and the modified Bessel equations, respectively, and their solutions are

$$W_1(r) = AJ_0(\lambda r) + BY_0(\lambda r) \tag{5.23a}$$

and

$$W_2(r) = CI_0(\lambda r) + DK_0(\lambda r), \tag{5.23b}$$

where J_0, Y_0, I_0, and K_0 are the zeroth order Bessel and modified Bessel functions of the first and second kind, respectively. Then, the general solution of Eq. (5.16) can be written as

$$W(r) = AJ_0(\lambda r) + BY_0(\lambda r) + CI_0(\lambda r) + DK_0(\lambda r), \tag{5.24}$$

where A, B, C, and D are unknown constants which should be determined by using the boundary conditions of the plate.

5.2.1.2 Forced Vibrations

The differential equation of motion is

$$D\nabla^4 w + \rho_p \frac{\partial^2 w}{\partial t^2} = f\,, \tag{5.25}$$

where f is the time-dependent forcing function.

A harmonic forcing function given by

$$f = F\exp(-i\Omega t) \tag{5.26}$$

is chosen, where Ω is the forcing frequency and F is the forcing function which may or may not be uniform over the plate. Recognizing that the steady state response of the system will also be harmonic in time, with the same frequency, the response of the plate can be expressed as (Leissa, 1978)

$$w = W\exp(-i\Omega t)\,. \tag{5.27}$$

Substituting f and w given by Eqs. (5.26) and (5.27) into Eq. (5.25) and simplifying, one can get

$$(\nabla^4 - \mu^4)W = \frac{F}{D}, \tag{5.28}$$

where μ is another parameter given by

$$\mu^4 = \frac{\rho_p \Omega^2}{D}\,. \tag{5.29}$$

Eq. (5.28) is an inhomogeneous one and its homogeneous solution has the same form as in the free vibration case. To obtain the general solution of Eq. (5.28), the particular solution has to be found. By assuming a uniform force distribution over the plate ($F = F_0 = \text{constant}$), the particular solution can be obtained as

$$W_p = -\frac{F_0}{\rho_p \Omega^2}\,. \tag{5.30}$$

Then, the general solution becomes

$$W(r) = AJ_0(\mu r) + BY_0(\mu r) + CI_0(\mu r) + DK_0(\mu r) - \frac{F_0}{\rho_p \Omega^2}\,, \tag{5.31}$$

and, again, the unknown constants A, B, C, and D should be found by using the boundary conditions of the plate.

5.2.2 Clamped Circular Plates

A clamped circular plate, as shown in Fig. 5.2, is studied. The coordinate system used is the same as in Fig. 5.1.

5.2.2.1 Displacement Function and Velocity Distribution

To find the displacement functions, the unknown constants A, B, C, and D in Eqs. (5.24) and (5.31) should be found by using the boundary conditions of the plate. For a clamped circular plate the boundary conditions can be given as

i. the displacement at the center of the plate is finite

$$W \text{ is finite at } r = 0, \tag{5.32}$$

ii. the displacement at the edge of the plate is zero

$$W = 0 \text{ at } r = r_0, \tag{5.33}$$

iii. the slope at the edge of the plate is zero

$$\frac{\partial W}{\partial r} = 0 \text{ at } r = r_0. \tag{5.34}$$

5.2.2.1.1 The Case of Free Vibrations. If the first boundary condition, given by Eq. (5.32), is used in Eq. (5.24), it can be seen that the constants B and D should be zero, because Y_0 and K_0, the zeroth order Bessel and the modified Bessel functions of the second kind, are not bounded at the center. Therefore, the displacement function reduces to

$$W(r) = AJ_0(\lambda r) + CI_0(\lambda r). \tag{5.35}$$

An important point to add at this step is that the first boundary condition applies to all circular plates regardless of the edge boundary conditions and types of vibrations. Therefore, after this analysis, it is logical to ignore the Bessel functions that are unbounded at the center, start with the short form of the displacement functions, and use the remaining boundary conditions to solve for the unknown constants A and C.

Now, if the second boundary condition, given by Eq. (5.33), is used in Eq. (5.35), C can be found in terms of A as

$$C = -\frac{J_0(\lambda r_0)}{I_0(\lambda r_0)} A . \tag{5.36}$$

Substituting C from Eq. (5.36) into Eq. (5.35) and factoring the A's out, W becomes

$$W(r) = A\left[J_0(\lambda r) - \frac{J_0(\lambda r_0)}{I_0(\lambda r_0)} I_0(\lambda r) \right]. \tag{5.37}$$

Applying the last boundary condition, given by Eq. (5.34), to Eq. (5.37), the characteristic equation for λ can be obtained as

$$J_0(\lambda r_0) I_1(\lambda r_0) + J_1(\lambda r_0) I_0(\lambda r_0) = 0 . \tag{5.38}$$

The roots of this equation, λr_0 (or λ for a specified r_0), can be found and it is convenient to name them $\overline{\lambda} r_0$ (or $\overline{\lambda}$). Each of these roots refers to a specific mode of the plate; in other words, the first root refers to the first mode, the second one refers to the second mode, and so on.

After adding the harmonic time-dependence, the displacement function for a specific mode becomes

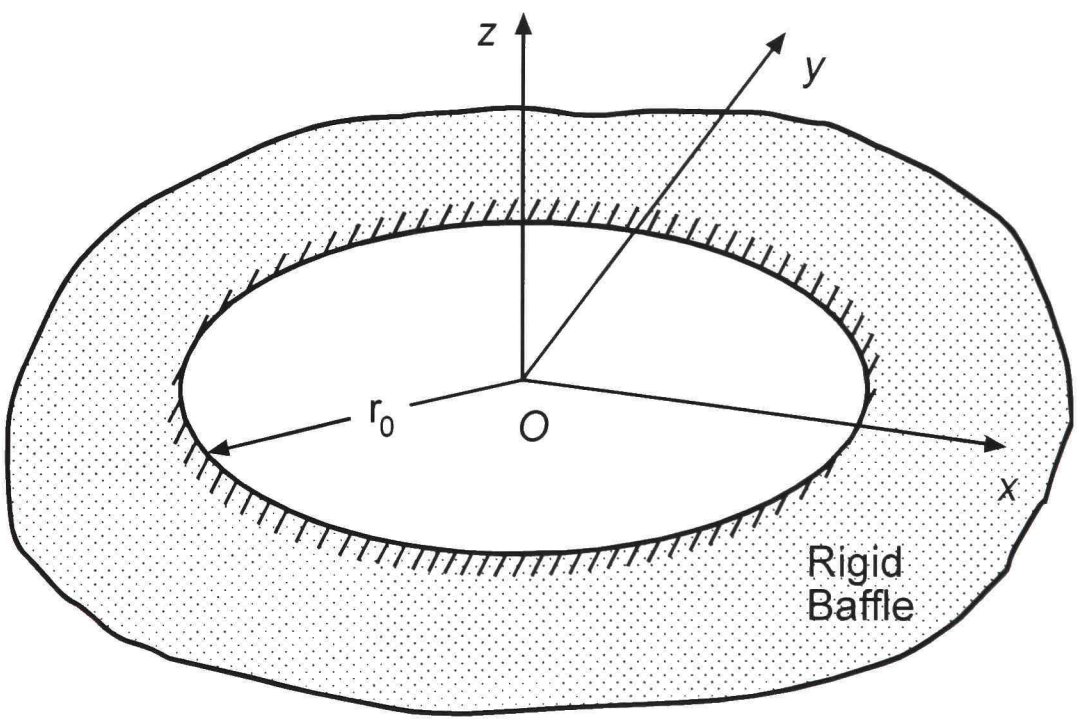

Figure 5.2. A Clamped Circular Plate.

$$w(r,t) = A\left[J_0\left(\overline{\lambda} r\right) - \frac{J_0\left(\overline{\lambda} r_0\right)}{I_0\left(\overline{\lambda} r_0\right)} I_0\left(\overline{\lambda} r\right) \right] \exp(-i\omega t). \tag{5.39}$$

Taking the first time derivative and suppressing $-i\exp(-i\omega t)$ term, the velocity distribution for a specific mode of a clamped circular plate can be obtained as

$$u(r) = A\omega\left[J_0\left(\overline{\lambda} r\right) - \frac{J_0\left(\overline{\lambda} r_0\right)}{I_0\left(\overline{\lambda} r_0\right)} I_0\left(\overline{\lambda} r\right) \right]. \tag{5.40}$$

5.2.2.1.2 The Case of Forced Vibrations. Using the argument about boundedness, which was explained in the free vibration case, along with Eq. (5.31), the displacement function becomes

$$W(r) = AJ_0(\mu r) + CI_0(\mu r) - \frac{F_0}{\rho_p \Omega^2}. \tag{5.41}$$

Then, using the boundary condition given by Eq. (5.33), C in terms of A is expressed as

$$C = \frac{1}{I_0(\mu r_0)}\left[-AJ_0(\mu r_0) + \frac{F_0}{\rho_p \Omega^2} \right]. \tag{5.42}$$

Substituting C into Eq. (5.41) and applying the last boundary condition, given by Eq. (5.34), A can be obtained as

$$A = \frac{F_0 I_1(\mu r_0)}{\rho_p \Omega^2 \left[J_1(\mu r_0) I_0(\mu r_0) + J_0(\mu r_0) I_1(\mu r_0) \right]}. \tag{5.43}$$

Since A and C are known, the velocity distribution that will be obtained from the displacement function given by Eq. (5.41) can be used in all acoustic calculations for the sake of clarity, and afterwards, these constants can be found from Eqs. (5.43) and (5.42), and used in the acoustic results. Therefore, after adding the harmonic time-dependence, the displacement function is written as

$$w(r,t) = \left[AJ_0(\mu r) + CI_0(\mu r) - \frac{F_0}{\rho_p \Omega^2} \right] \exp(-i\Omega t). \tag{5.44}$$

Finally, the velocity distribution can be found as

$$u(r)=\Omega\left[AJ_0(\mu r)+CI_0(\mu r)-\frac{F_0}{\rho_p\Omega^2}\right]. \tag{5.45}$$

5.2.2.2 Far-field Acoustic Pressure Distribution and Acoustic Intensity

5.2.2.2.1 The Case of Free Vibrations. Substituting the velocity distribution given by Eq. (5.40) into Eq. (2.8), rotating x-z plane in Fig. 5.1 to the plane including the far-field point P so that $\phi=0$, and simplifying, the Rayleigh integral reduces to

$$p(R,\theta,t)=-i\frac{\rho\omega^2 A\exp\left[i(-\omega t+kR)\right]}{2\pi R}\times\int_{r=0}^{r_0}\int_{\alpha=0}^{2\pi}\left[J_0(\bar{\lambda}r)-\frac{J_0(\bar{\lambda}r_0)}{I_0(\bar{\lambda}r_0)}I_0(\bar{\lambda}r)\right]r\exp\left[-ik\sin(\theta)r\cos(\alpha)\right]d\alpha dr. \tag{5.46}$$

If these integrals are taken and the area given by Eq. (5.5) is factored out, the far-field pressure distribution for a clamped circular plate becomes

$$p(R,\theta,t)=i\frac{\rho\omega^2 AA_p\exp\left[i(-\omega t+kR)\right]}{\pi R}\times\left\{\begin{array}{l}\dfrac{(\bar{\lambda}r_0)J_1(\bar{\lambda}r_0)J_0\left[kr_0\sin(\theta)\right]-kr_0\sin(\theta)J_0(\bar{\lambda}r_0)J_1\left[kr_0\sin(\theta)\right]}{\left[kr_0\sin(\theta)\right]^2-(\bar{\lambda}r_0)^2}\\ +\dfrac{J_0(\bar{\lambda}r_0)\left\{(\bar{\lambda}r_0)I_1(\bar{\lambda}r_0)J_0\left[kr_0\sin(\theta)\right]+kr_0\sin(\theta)I_0(\bar{\lambda}r_0)J_1\left[kr_0\sin(\theta)\right]\right\}}{I_0(\bar{\lambda}r_0)\left\{\left[kr_0\sin(\theta)\right]^2+(\bar{\lambda}r_0)^2\right\}}\end{array}\right\}. \tag{5.47}$$

Then, its magnitude can be written as

$$\left|p(R,\theta)\right|=\frac{\rho\omega^2 AA_p}{\pi R}\times\left\{\begin{array}{l}\dfrac{(\bar{\lambda}r_0)J_1(\bar{\lambda}r_0)J_0\left[kr_0\sin(\theta)\right]-kr_0\sin(\theta)J_0(\bar{\lambda}r_0)J_1\left[kr_0\sin(\theta)\right]}{\left[kr_0\sin(\theta)\right]^2-(\bar{\lambda}r_0)^2}\\ +\dfrac{J_0(\bar{\lambda}r_0)\left\{(\bar{\lambda}r_0)I_1(\bar{\lambda}r_0)J_0\left[kr_0\sin(\theta)\right]+kr_0\sin(\theta)I_0(\bar{\lambda}r_0)J_1\left[kr_0\sin(\theta)\right]\right\}}{I_0(\bar{\lambda}r_0)\left\{\left[kr_0\sin(\theta)\right]^2+(\bar{\lambda}r_0)^2\right\}}\end{array}\right\}. \tag{5.48}$$

Substituting this magnitude into Eq. (2.10), the acoustic intensity is obtained as

$$I(R,\theta)=\frac{\rho\omega^4 A^2 {A_p}^2}{2\pi^2 R^2 c}$$
$$\times\left\{\begin{array}{l}\dfrac{(\bar{\lambda}r_0)J_1(\bar{\lambda}r_0)J_0[kr_0\sin(\theta)]-kr_0\sin(\theta)J_0(\bar{\lambda}r_0)J_1[kr_0\sin(\theta)]}{[kr_0\sin(\theta)]^2-(\bar{\lambda}r_0)^2}\\ +\dfrac{J_0(\bar{\lambda}r_0)\{(\bar{\lambda}r_0)I_1(\bar{\lambda}r_0)J_0[kr_0\sin(\theta)]+kr_0\sin(\theta)I_0(\bar{\lambda}r_0)J_1[kr_0\sin(\theta)]\}}{I_0(\bar{\lambda}r_0)\{[kr_0\sin(\theta)]^2+(\bar{\lambda}r_0)^2\}}\end{array}\right\}^2. \tag{5.49}$$

5.2.2.2.2 The Case of Forced Vibrations. Substituting the velocity distribution given by Eq. (5.45) into Eq. (2.8) with $\phi=0$, one can get

$$p(R,\theta,t)=-i\frac{\rho\Omega^2\exp[i(-\Omega t+kR)]}{2\pi R}$$
$$\times\int_{r=0}^{r_0}\int_{\alpha=0}^{2\pi}\left[AJ_0(\mu r)+CI_0(\mu r)-\frac{F_0}{\rho_p\Omega^2}\right]r\exp[-ik\sin(\theta)r\cos(\alpha)]d\alpha dr. \tag{5.50}$$

After the integrals are evaluated and the area is factored out, the far-field pressure distribution becomes

$$p(R,\theta,t)=i\frac{\rho\Omega^2 A_p\exp[i(-\Omega t+kR)]}{\pi R}$$
$$\times\left\{\begin{array}{l}A\dfrac{\{(\mu r_0)J_1(\mu r_0)J_0[kr_0\sin(\theta)]-kr_0\sin(\theta)J_0(\mu r_0)J_1[kr_0\sin(\theta)]\}}{[kr_0\sin(\theta)]^2-(\mu r_0)^2}\\ -C\dfrac{\{(\mu r_0)I_1(\mu r_0)J_0[kr_0\sin(\theta)]+kr_0\sin(\theta)I_0(\mu r_0)J_1[kr_0\sin(\theta)]\}}{[kr_0\sin(\theta)]^2+(\mu r_0)^2}\\ +\dfrac{F_0J_1[kr_0\sin(\theta)]}{\rho_p\Omega^2 kr_0\sin(\theta)}\end{array}\right\}, \tag{5.51}$$

where A and C can be found from Eqs. (5.43) and (5.42), respectively.

The magnitude of this pressure is given by

$$\left|p(R,\theta)\right| = \frac{\rho\Omega^2 A_p}{\pi R}\left\{\begin{array}{l} A\dfrac{\left\{(\mu r_0)J_1(\mu r_0)J_0\left[kr_0\sin(\theta)\right] - kr_0\sin(\theta)J_0(\mu r_0)J_1\left[kr_0\sin(\theta)\right]\right\}}{\left[kr_0\sin(\theta)\right]^2 - (\mu r_0)^2} \\ -C\dfrac{\left\{(\mu r_0)I_1(\mu r_0)J_0\left[kr_0\sin(\theta)\right] + kr_0\sin(\theta)I_0(\mu r_0)J_1\left[kr_0\sin(\theta)\right]\right\}}{\left[kr_0\sin(\theta)\right]^2 + (\mu r_0)^2} \\ +\dfrac{F_0 J_1\left[kr_0\sin(\theta)\right]}{\rho_p\Omega^2 kr_0\sin(\theta)} \end{array}\right\}. \quad (5.52)$$

Finally, the acoustic intensity is obtained as

$$I(R,\theta) = \frac{\rho\Omega^4 {A_p}^2}{2\pi^2 R^2 c} \times \left\{\begin{array}{l} A\dfrac{\left\{(\mu r_0)J_1(\mu r_0)J_0\left[kr_0\sin(\theta)\right] - kr_0\sin(\theta)J_0(\mu r_0)J_1\left[kr_0\sin(\theta)\right]\right\}}{\left[kr_0\sin(\theta)\right]^2 - (\mu r_0)^2} \\ -C\dfrac{\left\{(\mu r_0)I_1(\mu r_0)J_0\left[kr_0\sin(\theta)\right] + kr_0\sin(\theta)I_0(\mu r_0)J_1\left[kr_0\sin(\theta)\right]\right\}}{\left[kr_0\sin(\theta)\right]^2 + (\mu r_0)^2} \\ +\dfrac{F_0 J_1\left[kr_0\sin(\theta)\right]}{\rho_p\Omega^2 kr_0\sin(\theta)} \end{array}\right\}^2. \quad (5.53)$$

5.2.2.3 Acoustic Power Radiation

5.2.2.3.1 The Case of Free Vibrations. Substituting the velocity distribution given by Eq. (5.40) into Eq. (2.30) and rearranging yields

$$\Pi_0 = \frac{\rho\omega^4 A^2}{4\pi c}\int_0^{r_0}\int_0^{2\pi}\left[J_0\left(\bar{\lambda}r'\right) - \frac{J_0\left(\bar{\lambda}r_0\right)}{I_0\left(\bar{\lambda}r_0\right)}I_0\left(\bar{\lambda}r'\right)\right]r'd\alpha' dr' \times \int_0^{r_0}\int_0^{2\pi}\left[J_0\left(\bar{\lambda}r\right) - \frac{J_0\left(\bar{\lambda}r_0\right)}{I_0\left(\bar{\lambda}r_0\right)}I_0\left(\bar{\lambda}r\right)\right]rd\alpha dr. \quad (5.54)$$

Integrating, factoring the square of the area out, and simplifying, the dominant acoustic power term is obtained as

$$\Pi_0 = \frac{\rho\omega^4 A^2 {A_p}^2}{4\pi c}\left\{\frac{2\left[J_1\left(\bar{\lambda}r_0\right)I_0\left(\bar{\lambda}r_0\right) - J_0\left(\bar{\lambda}r_0\right)I_1\left(\bar{\lambda}r_0\right)\right]}{\left(\bar{\lambda}r_0\right)I_0\left(\bar{\lambda}r_0\right)}\right\}^2. \quad (5.55)$$

The second term of the acoustic power can be found by substituting the velocity into Eqs. (2.31) to (2.36), integrating, adding them together, and making the usual simplifications. It is given in Appendix H.

5.2.2.3.2 The Case of Forced Vibrations. Substituting the velocity given by Eq. (5.45) into Eq. (2.30), and rearranging, one can get

$$\Pi_0 = \frac{\rho\Omega^4}{4\pi c}\int_0^{r_0}\int_0^{2\pi}\left[AJ_0(\mu r') + CI_0(\mu r') - \frac{F_0}{\rho_p\Omega^2}\right]r'd\alpha' dr' \times \int_0^{r_0}\int_0^{2\pi}\left[AJ_0(\mu r) + CI_0(\mu r) - \frac{F_0}{\rho_p\Omega^2}\right]rd\alpha dr. \tag{5.56}$$

Integrating and simplifying, the dominant power term becomes

$$\Pi_0 = \frac{\rho\Omega^4 A_p{}^2}{4\pi c}\left\{\frac{2\left[AJ_1(\mu r_0) + CI_1(\mu r_0)\right]}{(\mu r_0)} - \frac{F_0}{\rho_p\Omega^2}\right\}^2, \tag{5.57}$$

where A and C are found from Eqs. (5.43) and (5.42), respectively.

The second term of the acoustic power can be obtained in the same way as in the previous cases and it is given in Appendix H.

5.2.3 Simply Supported Circular Plates

A simply supported circular plate, as shown in Fig. 5.3, is studied, and the coordinate system used is shown in Fig. 5.1.

5.2.3.1 Displacement Function and Velocity Distribution

The first two boundary conditions of a simply supported circular plate are the same as in the clamped circular plate and they are given by Eqs. (5.32) and (5.33). But, the third boundary condition is different, and, initially, it is given as

iii. the bending moment at the edge of the plate is zero

$$M = 0 \text{ at } r = r_0. \tag{5.58}$$

The bending moment in polar coordinates is expressed as

$$M = -D\left[\frac{\partial^2 W}{\partial r^2} + \upsilon\left(\frac{1}{r}\frac{\partial W}{\partial r} + \frac{1}{r^2}\frac{\partial^2 W}{\partial \alpha^2}\right)\right], \tag{5.59}$$

where D is the flexural rigidity given by Eq. (4.12).

Since the derivatives with respect to angle vanish for circular plates having no nodal diameters, Eq. (5.59) reduces to

$$M = -D\left(\frac{\partial^2 W}{\partial r^2} + \frac{\upsilon}{r}\frac{\partial W}{\partial r}\right). \tag{5.60}$$

Therefore, the third boundary condition becomes

iii. $$\frac{\partial^2 W}{\partial r^2} + \frac{\upsilon}{r}\frac{\partial W}{\partial r} = 0 \text{ at } r = r_0. \tag{5.61}$$

5.2.3.1.1 The Case of Free Vibrations. Upon applying the first two boundary conditions to the displacement function given by Eq. (5.24), it becomes exactly the same as in Eq. (5.37). But, after applying the last boundary condition given above to this equation, the characteristic equation becomes

$$\left[2J_0(\lambda r_0) + \frac{2\upsilon}{(\lambda r_0)}J_1(\lambda r_0) - J_2(\lambda r_0)\right] + \frac{J_0(\lambda r_0)}{I_0(\lambda r_0)}\left[\frac{2\upsilon}{(\lambda r_0)}I_1(\lambda r_0) + I_2(\lambda r_0)\right] = 0 \tag{5.62}$$

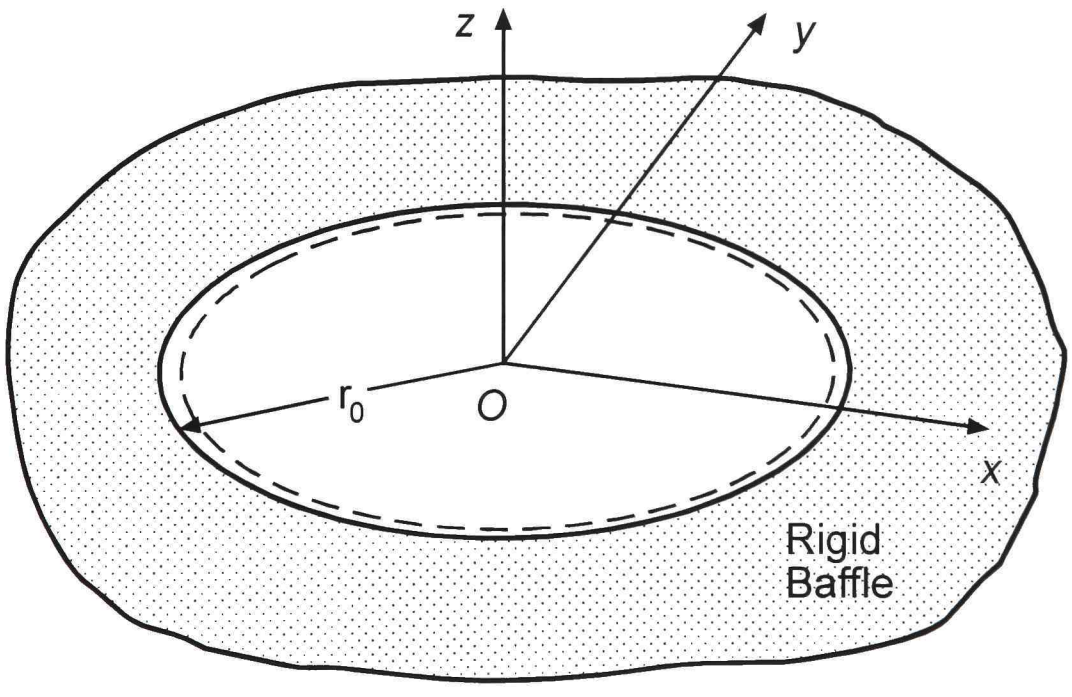

Figure 5.3. A Simply Supported Circular Plate.

the roots, $\overline{\lambda} r_0$ (or $\overline{\lambda}$ for a specified r_0), of which refer to different modes of the plate.

Eq. (5.62) includes υ, the Poisson's ratio, therefore $\overline{\lambda}$, the frequency parameter for a simply supported circular plate, is a material dependent quantity.

More importantly, the form of the displacement function and therefore the velocity distribution are the same as in the free vibration of a clamped circular plate and they are given by Eqs. (5.39) and (5.40), respectively. This is a big step towards calculating the acoustic quantities for a simply supported circular plate as will be seen in Sections 5.2.3.2 and 5.2.3.3.

5.2.3.1.2 The Case of Forced Vibrations. This time applying the first two boundary conditions to Eq. (5.31) yields the displacement function given by Eq. (5.41) and C in terms of A, given by Eq. (5.42). Next, if the last boundary condition, given by Eq. (5.61), is used along with Eq. (5.41) in which Eq. (5.42) is used in writing C, A can be obtained as

$$A = \frac{\dfrac{F_0}{\rho_p \Omega^2}\left[1+\dfrac{I_2(\mu r_0)}{I_0(\mu r_0)}+\dfrac{2\upsilon}{(\mu r_0)}\dfrac{I_1(\mu r_0)}{I_0(\mu r_0)}\right]}{\left\{\left[2J_0(\mu r_0)-J_2(\mu r_0)+\dfrac{J_0(\mu r_0)I_2(\mu r_0)}{I_0(\mu r_0)}\right]+\dfrac{2\upsilon}{(\mu r_0)}\left[J_1(\mu r_0)+\dfrac{J_0(\mu r_0)I_1(\mu r_0)}{I_0(\mu r_0)}\right]\right\}}. \qquad (5.63)$$

Naturally, C can be found by substituting the given A into Eq. (5.42). At this point it is convenient to use Eq. (5.45) as the velocity distribution for the forced vibration of a simply supported circular plate, because now both A and C are known. This makes everything simpler from acoustics point of view.

5.2.3.2 Far-field Acoustic Pressure Distribution and Acoustic Intensity

For the free and the forced vibrations of a simply supported circular plate, one can use the far-field acoustic pressure and acoustic intensity results for the free and the forced vibrations of a clamped circular plate, respectively. This is because for both of the cases, the corresponding forms of the velocity distributions are the same. But, in the results different parameters or constants have to be used. For the free vibration, $\overline{\lambda}$, the frequency

parameter, have to be calculated from Eq. (5.62) and substituted into the pressure expressions instead of using Eq. (5.38). Also, for the forced vibration, A has to be obtained from Eq. (5.63) instead of Eq. (5.43).

5.2.3.3 Acoustic Power Radiation

Again, all of the acoustic power results obtained for a clamped circular plate are applicable to a simply supported circular plate with exactly the same limitations given above.

CHAPTER VI
ELLIPTICAL GEOMETRY

Elliptical pistons and clamped elliptical plates are studied in this chapter.

6.1 Elliptical Pistons

The far-field acoustic pressure and the acoustic power expressions are obtained for an elliptical piston, as shown in Fig. 6.1. The rectangular coordinate system is used in the analysis.

6.1.1 Far-field Acoustic Pressure Distribution

Before using the Rayleigh integral given by Eq. (2.9) to determine the far-field pressure distribution, the integration limits should be specified. The equation of an ellipse is given by

$$\frac{x^2}{a_1^{\,2}}+\frac{y^2}{b_1^{\,2}}=1, \tag{6.1}$$

where a_1 and b_1 denote the semi-major and semi-minor axes of the ellipse.

From Eq. (6.1), y can be written in terms of x as

$$y=\pm\frac{b_1}{a_1}\sqrt{a_1^{\,2}-x^2}\,. \tag{6.2}$$

Therefore, in the Rayleigh integral, y varies between $-\frac{b_1}{a_1}\sqrt{a_1^{\,2}-x^2}$ and $\frac{b_1}{a_1}\sqrt{a_1^{\,2}-x^2}$

while x varies between $-a_1$ and a_1.

Substituting the velocity given by Eq. (3.2) into Eq. (2.9), using the given integration limits, and simplifying, one can get

$$p(R,\phi,\theta,t)=-i\frac{\rho\omega^2 W_0\exp\left[i(-\omega t+kR)\right]}{2\pi R}\int_{-a_1}^{a_1}\left[\int_{-\frac{b_1}{a_1}\sqrt{a_1^{\,2}-x^2}}^{\frac{b_1}{a_1}\sqrt{a_1^{\,2}-x^2}}\exp(-i\psi_2 y)dy\right]\exp(-i\psi_1 x)dx\,, \tag{6.3}$$

where ψ_1 and ψ_2 are given by Eqs. (3.6) and (3.7), respectively.

Evaluating the inner integral and simplifying yields

$$p(R,\phi,\theta,t) = -i\frac{\rho\omega^2 W_0 \exp\left[i(-\omega t + kR)\right]}{\pi R}\int_{-a_1}^{a_1}\frac{\sin\left(\frac{\psi_2 b_1\sqrt{a_1^{\,2}-x^2}}{a_1}\right)\exp(-i\psi_1 x)}{\psi_2}dx\,. \tag{6.4}$$

This integral is impossible to evaluate in closed form, therefore series expansions of the functions are substituted into it. If this is done and simplifications are made, the far-field pressure distribution becomes

$$\begin{aligned} p(R,\phi,\theta,t) = {} & \frac{\rho\omega^2 W_0 A_p \exp\left[i(-\omega t + kR)\right]}{\pi^2 R} \\ & \times\sum_{s=0}^{\infty}\sum_{q=0}^{\infty}\frac{(-1)^{s+q+1} i^{q+1} R_a^{\,2s}\psi_2^{\,2s}\psi_1^{\,q}}{a_1^{\,2}(2s+1)!\,q!}\int_{-a_1}^{a_1} x^q\left(a_1^{\,2}-x^2\right)^{s+\frac{1}{2}}dx, \end{aligned} \tag{6.5}$$

where s and q are the indices for sinusoidal and exponential functions, respectively, A_p is the area of the elliptical source given by

$$A_p = \pi a_1 b_1\,, \tag{6.6}$$

and R_a is the aspect ratio of the ellipse defined as

$$R_a = \frac{b_1}{a_1}\,. \tag{6.7}$$

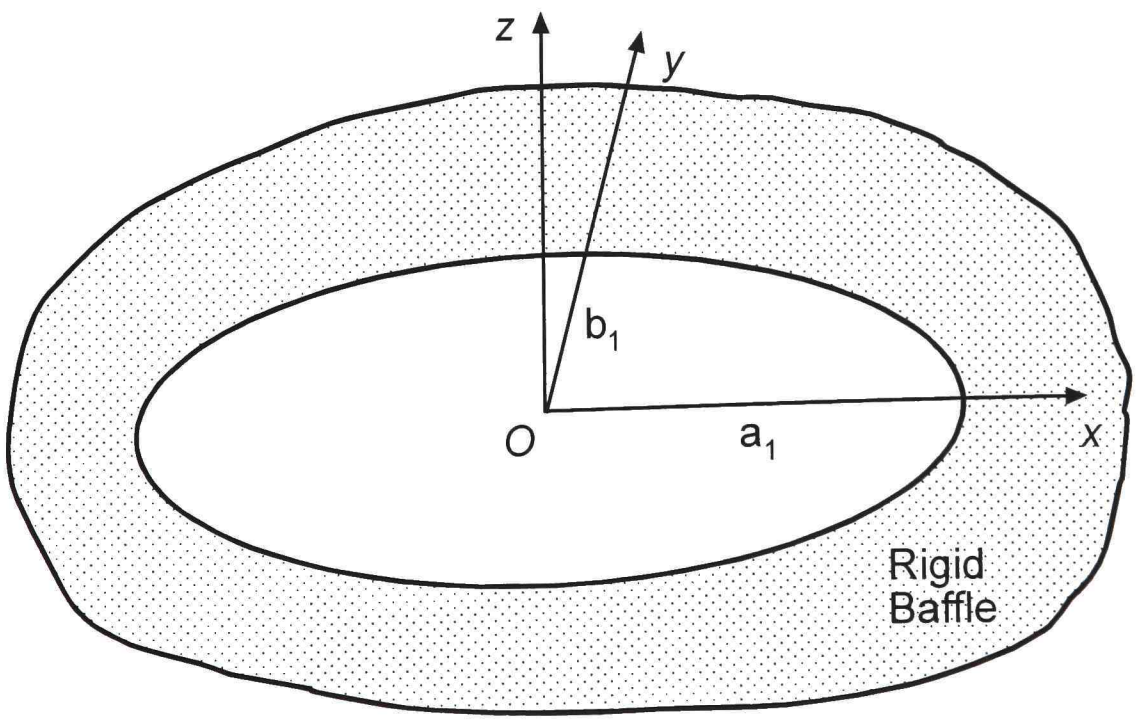

Figure 6.1. An Elliptical Piston.

It is possible to check this expression. When $(q,s)=(0,0)$, the first term of the above expression can be obtained as

$$p_0 = -i\frac{\rho\omega^2 W_0 A_p \exp\left[i(-\omega t + kR)\right]}{2\pi R}. \tag{6.8}$$

Since a circle is a specific case of an ellipse, the result given by Eq. (6.8) has to be the same as the first term of Eq. (5.4) which is the exact far-field pressure distribution originally derived for a circular piston. If one expands the Bessel function in Eq. (5.4) in series, the first term of this equation reduces to Eq. (6.8) making the expression given by Eq. (6.5) correct.

6.1.2 Acoustic Power Radiation

Substituting the velocity given by Eq. (3.2) into Eq. (2.20), integrating by using the given limits of integration, and factoring the square of the area given by Eq. (6.6) out, the dominant acoustic power term becomes

$$\Pi_0 = \frac{\rho\omega^4 W_0^{\,2} A_p^{\,2}}{4\pi c},$$

which is always an expected result for piston radiators.

The second acoustic power term can be obtained in the same way as in the previous geometric shapes and it is expressed as

$$\Pi_1 = \frac{\rho\omega^4 W_0^{\,2} A_p^{\,2}}{4\pi c}\left[-\frac{\left(1+R_a^{\,2}\right)}{12}(ka_1)^2\right], \tag{6.9}$$

where R_a is given by Eq. (6.7)

Finally, the total approximate acoustic power can be written as

$$\Pi \cong \frac{\rho\omega^4 W_0^{\,2} A_p^{\,2}}{4\pi c}\left[1-\frac{\left(1+R_a^{\,2}\right)}{12}(ka_1)^2\right]. \tag{6.10}$$

This result can also be verified. The result obtained by substituting $R_a = 1$ into Eq. (6.10) and the result given by Eq. (5.14), which was originally obtained for a circular piston, should be the same. If this is done, it can be seen that they are the same.

6.2 Clamped Elliptical Plates

A clamped elliptical plate, as shown in Fig. 6.2, is studied.

6.2.1 Displacement Function and Velocity Distribution

Free vibrations of clamped elliptical plates were studied extensively. Among the researchers Shibaoka (1956) used two methods of solution. In the first one, Mathieu functions were used which exactly satisfied the differential equation of free vibration, boundary conditions of the plate were satisfied by an infinite determinant, and numerical convergence was investigated for determinant truncations of various sizes. In the second method, a simple Rayleigh type solution utilizing the displacement function

$$W(x,y) = A\left[A_0\left(1-\frac{x^2}{a_1^{\,2}}-\frac{y^2}{b_1^{\,2}}\right)^2\right], \tag{6.11}$$

where A and A_0 are constants, was used.

McNitt (1962) used the Galerkin method and the two-term displacement function

$$W(x,y) = A\left[A_1\left(\frac{x^2}{a_1^{\,2}}+\frac{y^2}{b_1^{\,2}}-1\right)^2 + A_2\left(\frac{x^2}{a_1^{\,2}}+\frac{y^2}{b_1^{\,2}}-1\right)^3\right] \tag{6.12}$$

where A, A_1, and A_2 are also constants.

The use of Mathieu functions is not preferred in this study because this way of solution is well-suited for a numerical study, not for an approximate analytic one. Also, to begin with the acoustic problem, a velocity distribution, and therefore a displacement function is needed and the assumed displacement functions by Shibaoka and McNitt may provide a good starting point. Of course, in deciding which one of these functions to use we should have good reasons and one of these comes from Leissa (1969). He states that the use of the two-term displacement function gives slightly better frequency results. The author has another reason to justify the use of the two-term function. If elliptical plate is a circular one ($b_1 = a_1$), Eqs. (6.11) and (6.12) reduce to

$$W(r) = A\left[A_0\left(1-\delta^2\right)^2\right] \tag{6.13}$$

and

$$W(r) = A\left[A_1\left(\delta^2 - 1\right)^2 + A_2\left(\delta^2 - 1\right)^3\right], \tag{6.14}$$

respectively, and δ is the ratio of the distance from the center of the circular plate to the radius of the plate given by

$$\delta = \frac{r}{a_1}. \tag{6.15}$$

Since the exact solution for the displacement function at a specific mode of a clamped circular plate is known from Chapter V and it is given by Eq. (5.39) (excluding the harmonic time-dependence), it is a good idea to compare the assumed functions with this exact solution. But this comparison is only limited to the fundamental (first) mode of the plate. In any event, one may add higher order terms to W's given by Eqs. (6.11) and (6.12) to account for higher modes of the plate. Naturally, this makes the analysis more difficult.

Ignoring the harmonic time-dependence, Eq. (5.39) can be written in a form similar to Eqs. (6.13) and (6.14) as

$$W(r) = A\left\{J_0\left[\left(\overline{\lambda}a_1\right)\delta\right] - \frac{J_0\left(\overline{\lambda}a_1\right)}{I_0\left(\overline{\lambda}a_1\right)} I_0\left[\left(\overline{\lambda}a_1\right)\delta\right]\right\}, \tag{6.16}$$

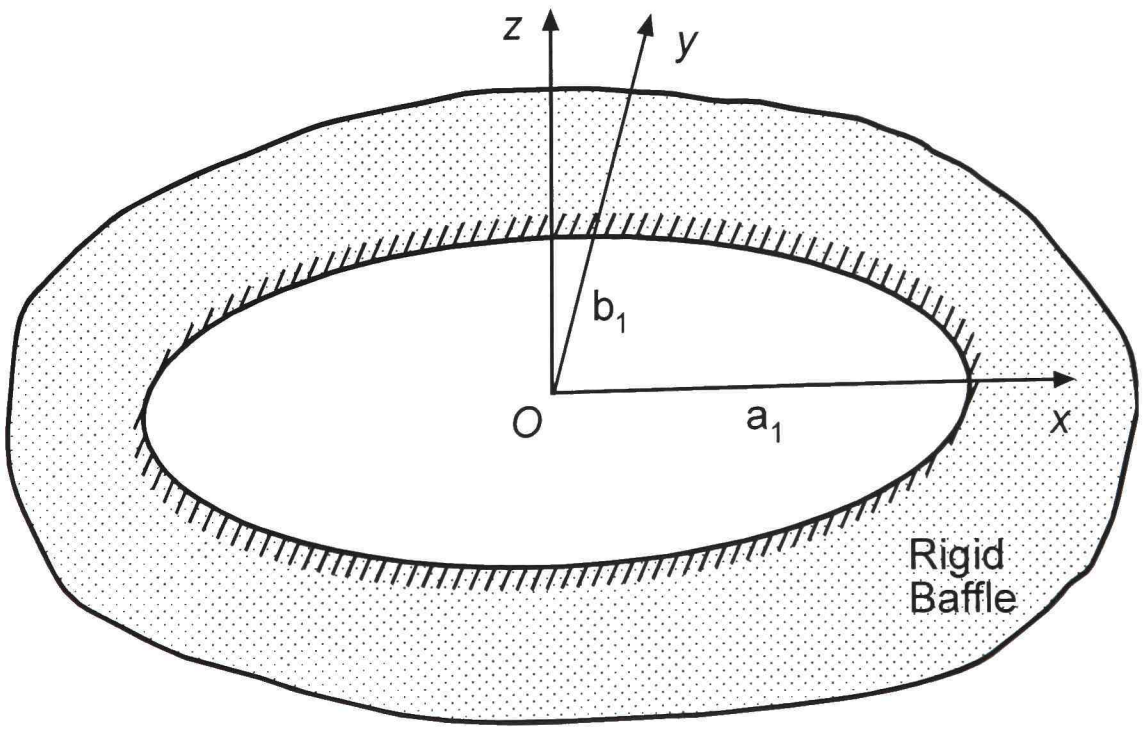

Figure 6.2. A Clamped Elliptical Plate.

where $\overline{\lambda}a_1$ is the first root of Eq. (5.38).

If the constant A is ignored in all three equations (6.13, 6.14, and 6.16), it is possible to graph them in terms of δ, therefore to understand which of Eqs. (6.11) and (6.12) is better to use and also with which constants. The author graphed all three functions and realized that the two-term function can imitate the exact solution in a better way. It was seen that the best value of A_0 was around 1.03, on the other hand, for $(A_1, A_2) = (0.806, -0.249)$ the two-term function and the exact solution were almost indistinguishable. A plot of all three functions with these values of the constants can be seen in Fig. 6.3. In this figure, the solid line shows the exact solution, while the dashed lines refer to the one and two-term approximate functions. Since a unique combination of A_1 and A_2 gives this approximation, Eq. (6.14) is a linear combination of two nonlinear terms, and a circle is essentially an ellipse for which $R_a = 1$, this result can be generalized to an ellipse. Therefore, it is logical to use the displacement function given by Eq. (6.12) for the first mode of the clamped elliptical plate. After adding a harmonic time-dependence to it, one gets

$$w(x,y,t) = A\left[A_1\left(\frac{x^2}{a_1^{\,2}} + \frac{y^2}{b_1^{\,2}} - 1\right)^2 + A_2\left(\frac{x^2}{a_1^{\,2}} + \frac{y^2}{b_1^{\,2}} - 1\right)^3\right]\exp(-i\omega t). \qquad (6.17)$$

Then, the velocity distribution becomes

$$u(x,y) = A\omega\left[A_1\left(\frac{x^2}{a_1^{\,2}} + \frac{y^2}{b_1^{\,2}} - 1\right)^2 + A_2\left(\frac{x^2}{a_1^{\,2}} + \frac{y^2}{b_1^{\,2}} - 1\right)^3\right]. \qquad (6.18)$$

Or, if expanded, it can also be written as

$$u(x,y) = A\omega\left[\begin{array}{l} \dfrac{A_2}{a_1^{\,6}}x^6 + \dfrac{A_2}{b_1^{\,6}}y^6 + \dfrac{3A_2}{a_1^{\,4}b_1^{\,2}}x^4y^2 + \dfrac{3A_2}{a_1^{\,2}b_1^{\,4}}x^2y^4 \\ + \dfrac{(A_1 - 3A_2)}{a_1^{\,4}}x^4 + \dfrac{(A_1 - 3A_2)}{b_1^{\,4}}y^4 + \dfrac{2(A_1 - 3A_2)}{a_1^{\,2}b_1^{\,2}}x^2y^2 \\ + \dfrac{(-2A_1 + 3A_2)}{a_1^{\,2}}x^2 + \dfrac{(-2A_1 + 3A_2)}{b_1^{\,2}}y^2 + (A_1 - A_2) \end{array}\right]. \qquad (6.19)$$

Finally, according to McNitt's analysis the approximate frequency is given by

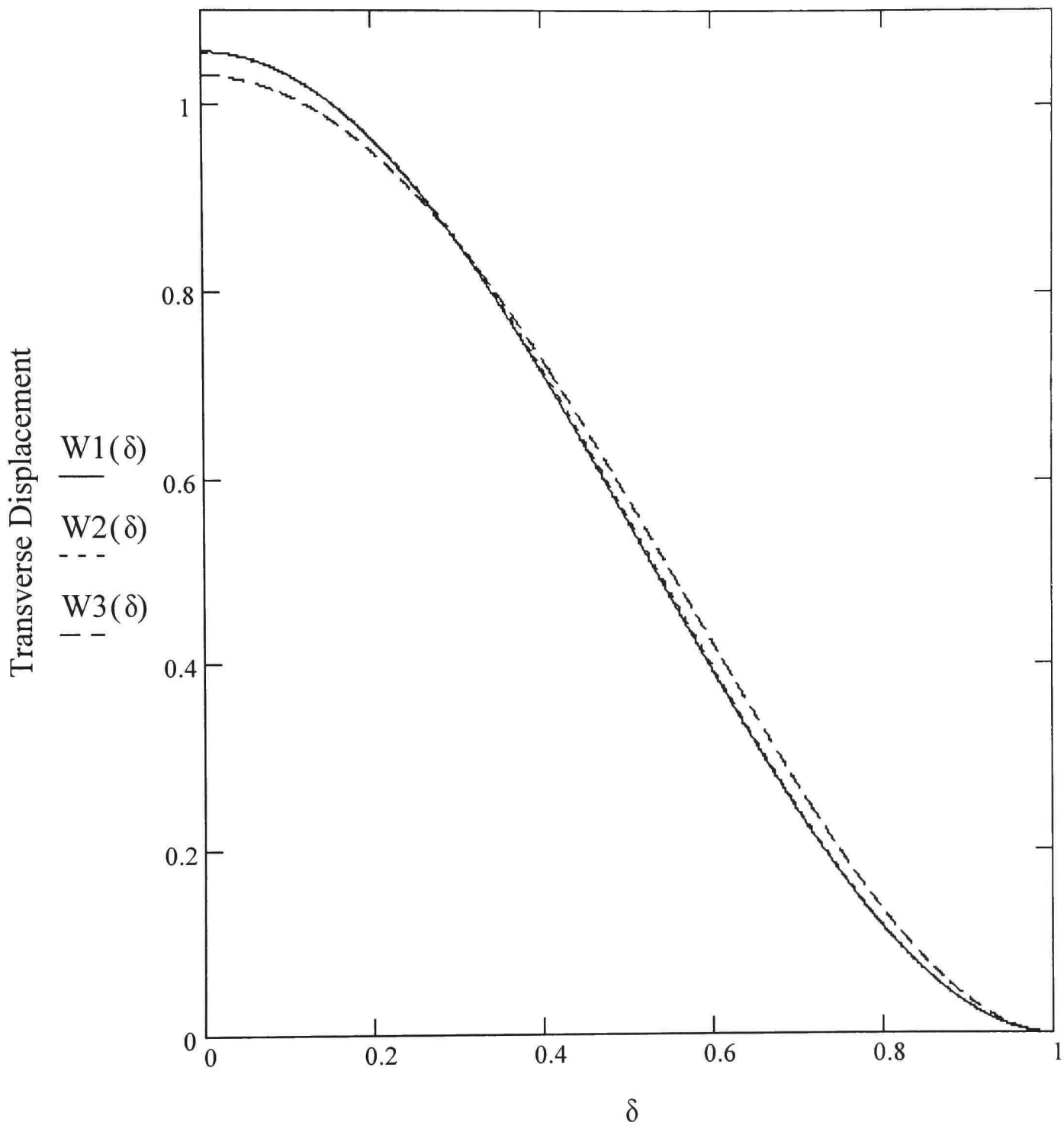

Figure 6.3. Comparison of Assumed and Exact Displacement Functions for a Clamped Circular Plate.

$$\omega \cong \frac{6.262}{a_1^{\,2}}\sqrt{\frac{D}{\rho_p}\left(1+\frac{2}{3R_a^{\,2}}+\frac{1}{R_a^{\,4}}\right)}. \tag{6.20}$$

Since the present analysis is an approximate one and is only limited to one mode of the elliptical plate, the far-field acoustic pressure expression is not derived.

6.2.2 Acoustic Power Radiation

Substituting the velocity distribution, given by Eq. (6.19), into Eq. (2.20), integrating, and simplifying, the dominant acoustic power term becomes

$$\Pi_0 = \frac{\rho\omega^4 A^2 A_p^{\,2}}{4\pi c}\left(\frac{4A_1-3A_2}{12}\right)^2. \tag{6.21}$$

The second term of the acoustic power can be found in the same way as in the previous geometric shapes and it is given as

$$\Pi_1 = \frac{\rho\omega^4 A^2 A_p^{\,2}}{4\pi c}\left[-\frac{(4A_1-3A_2)(5A_1-3A_2)(1+R_a^{\,2})}{4320}\right](ka_1)^2. \tag{6.22}$$

Therefore, the total power can be written as

$$\Pi \cong \frac{\rho\omega^4 A^2 A_p^{\,2}}{4\pi c}\left\{\left(\frac{4A_1-3A_2}{12}\right)^2-\left[\frac{(4A_1-3A_2)(5A_1-3A_2)(1+R_a^{\,2})}{4320}\right](ka_1)^2\right\}. \tag{6.23}$$

Finally, substituting $(A_1, A_2) = (0.806, -0.249)$ into this equation, the total approximate acoustic power is obtained as

$$\Pi \cong \frac{\rho\omega^4 A^2 A_p^{\,2}}{4\pi c}\left[0.1095-0.0044(1+R_a^{\,2})(ka_1)^2\right]. \tag{6.24}$$

The main consequence of this result is that a simple expression for the acoustic power radiation is obtained in terms of the constants used in the two-term displacement function given by Eq. (6.12).

CHAPTER VII
RESULTS AND DISCUSSIONS

In this chapter, the results obtained in previous chapters are discussed. Although the sources with different geometric shapes were studied in different chapters, now it is better to classify them as pistons and plates for comparison purposes. Throughout this chapter the acoustic medium used is air, its density, ρ, is 1.225 kg/m^3, and the speed of sound in air, c, is 340 m/s. These are the values at standard temperature and pressure.

7.1 Pistons

7.1.1 Triangular Pistons

As an example an equilateral triangular piston is considered in this section. The numerical values used are $a_0 = 0.2\ m$, $b_0 = 0.2\ m$, $\beta = 60^\circ$, $W_0 = 0.005\ m$, and $R = 2.5\ m$. The acoustic intensity of a triangular piston is given by Eq. (3.11). Variation of the intensity at a specific point on the imaginary far-field hemisphere ($\phi = 60^\circ$ and $\theta = 30^\circ$) with the frequency of the piston is shown in Fig. 7.1. In this figure, the intensity values are in W/m^2 while the frequency values are in rad/s. From this figure it can be seen that the intensity peak occurs at around 21500 rad/s (around 3400 Hz), and as the frequency increases further, the intensity level starts decreasing. This means that the sound level does not necessarily increase with an increase in the frequency. Fig. 7.2 shows the variation of the intensity with the angle ϕ for $\omega = 20000\ rad/s$ and $\theta = 60^\circ$. In this figure the angle is in rad. It can clearly be seen that the intensity is maximum when ϕ corresponds to the lines passing through the corners of the triangular piston ($\phi = 30^\circ$ and 90°) and it is minimum when ϕ corresponds to the lines parallel to the edges of the piston ($\phi = 0^\circ$, 60° and 120°). Therefore for pistons, corners have an important effect on acoustic intensity, and this is a general result. Fig. 7.3 shows the variation of the intensity with θ for $\omega = 20000\ rad/s$ and $\phi = 45^\circ$. From this figure it

can be deduced that the intensity increases when θ approaches the z-axis ($\theta \to 0^\circ$). This is also a general result for pistons.

The acoustic power radiated by a triangular piston is given by Eq. (3.16). The variation of the power with R_t (the ratio of the lengths of the two specified edges of the piston) and β (the angle between them) is shown in Fig. 7.4. The same numerical values are used as in the intensity plots except for the changing quantities and $\omega = 340\ rad/s$. The unit of the acoustic power is W. The limiting cases are 0 and π rad for β and 0 for R_t. Of course, for these cases the triangle becomes a line and the power is zero. As can be noticed from this figure that for any R_t, the power becomes a maximum when $\beta = 90^\circ$. This is an expected result because this angle gives the maximum area for the two edges previously specified. Fig. 7.5 shows the variation of the power with β and ka_0. This figure shows a similar behavior with Fig. 7.4. Again the surface is symmetric with respect to $\beta = 90^\circ$ and the power increases with increasing ka_0. As can be recalled the acoustic power results presented in this study are limited to low kL values. But as will be proved in Section 7.1.3, for pistons, these results can cover a large frequency range for sufficiently low L values. Therefore, ka_0 values up to 1 was included in Fig. 7.5.

7.1.2 Rectangular Pistons

A square piston is considered as an example of rectangular pistons. The numerical values used are $a = 0.15\ m$, $b = 0.15\ m$, $W_0 = 0.005\ m$, and $R = 2.5\ m$. The acoustic intensity due to a vibrating rectangular piston is given by Eq. (4.4). Fig. 7.6 shows the variation of the intensity with the frequency of vibration for the specific far-field point defined by $\phi = 45^\circ$ and $\theta = 45^\circ$ together with R. As can be noticed, $\phi = 45^\circ$ corresponds to the diagonal of the piston. The behavior seen in this figure is similar to the triangular piston intensity variation shown in Fig. 7.1. Fig. 7.7 shows the variation of the intensity with the angle ϕ for $\omega = 20000\ rad/s$ and $\theta = 45^\circ$. From this figure, it is clear that at far-field points corresponding to the diagonals of the piston, the intensity becomes

maximum, and at points corresponding to the lines parallel to the edges it becomes minimum. This result is the same as in the case of a triangular piston. Fig. 7.8 shows a plot of the intensity versus the angle θ for the same frequency and $\phi = 45^{\circ}$. As can be seen, most of the acoustic radiation is confined to the first half of the θ range, and again the behavior is similar to the one shown in Fig. 7.3.

The acoustic power radiated from a rectangular piston was found by two different approaches; namely, the far-field integration approach and the surface integration approach. They are given by Eqs. (4.8) and (4.10), respectively. The variations with the frequency of vibration are shown in Fig. 7.9. In this figure, the solid line refers to the power found by using the far-field integration approach while the dashed line refers to the one found by the other approach. As can be seen their agreement is good up to 5000 rad/s (around 800 Hz), but after this frequency they start deviating from each other. Especially at higher frequencies, the surface integration approach starts giving negative real power values, which is not possible. Therefore, these power results are reliable only up to $ka = 2.5$ (5000 rad/s refers to an approximate k value of 15, which when multiplied with a gives this value). Naturally, for bigger pistons the frequency range becomes shorter, while for smaller pistons higher frequency ranges can be covered. As stated in previous chapters, to obtain the acoustic power for very high frequency values accurately, a numerical integration of the acoustic intensity over the far-field hemisphere is necessary. This will be done in the next section.

7.1.3 Circular Pistons

The acoustic intensity due to a vibrating circular piston is given by Eq. (5.7). Since a circular shape has symmetry with respect to the angle ϕ, the variation of the intensity with other parameters is investigated. A circular piston of 0.15 m in diameter is considered as an example. Fig. 7.10 shows its variation with θ and k. As seen in this figure, the intensity increases with both of the parameters, but the increase is sharper when θ is around 0. The wavy nature of the intensity is seen more clearly in the next several figures. The variation of the intensity with θ and R is shown in Fig. 7.11. In this figure θ starts with 36° and goes up to 90°. The first 36° is not shown because the

intensity increases sharply in this region, and one misses its wavy dependence on the angle. This figure clearly shows that the intensity decreases with an increase in the radius of the far-field hemisphere. This result is expected. But, it also shows that an increase in θ does not necessarily cause a decrease in the intensity. Fig. 7.12 shows the variation of the intensity with k and r_0. As can be seen from this figure, for any constant piston radius, r_0, when the acoustic wave number, k, increases the intensity may decrease, and the opposite of this statement is also correct. Fig. 7.13 shows the dependence of the intensity on θ and kr_0. The first 30° of θ is not shown. The argument for the previous figure also holds for this figure.

The acoustic power radiated from a circular piston was found by the two methods mentioned earlier. They are given by Eqs. (5.12) and (5.14). Fig. 7.14 shows the variation of the radiated power with the frequency of vibration of the piston. In this figure, Πn shows the power obtained by integrating Eq. (5.8) numerically, Πf shows the result obtained by the far-field integration approach (given by Eq. (5.12)), and Πs shows the result obtained by the surface integration approach (given by Eq. (5.14)). As can be seen, the far-field integration approach shows a better agreement with the numerical integration. Both of Eqs. (5.12) and (5.14) can be used up to around 6000 rad/s. After this frequency, especially, the two-term result obtained by the surface integration approach is not reliable, although the three-term result obtained by the far-field integration approach gives considerably accurate results up to higher frequencies. Again, for smaller pistons the frequency range becomes larger while for bigger pistons this range is narrow.

7.1.4 Elliptical Pistons

The far-field acoustic pressure for an elliptical piston is given by Eq. (6.5). This is an infinite sum of integrals; therefore, one can find a series expansion of the acoustic pressure depending on the number of terms desired. Then, by using its magnitude, the acoustic intensity can be obtained. Naturally, as the number of terms considered increases the frequency range, for which the pressure expression is applicable, gets bigger. The acoustic intensity from an elliptical piston is not analyzed in this study.

The acoustic power from an elliptical piston is given by Eq. (6.10). This is a two-term result obtained by the surface integration approach. Fig. 7.15 shows the variation of the power with the semi-major axis of the ellipse, a_1, and the acoustic wave number, k. The numerical values used in this figure are $W_0 = 0.005\ m$ (vertical displacement) and $R_a = 0.5$ (aspect ratio). It is seen that the power increases with both of the quantities. This behavior is the same as in the previous cases. The dependence of the power on R_a and ka_1 is shown in Fig. 7.16. The behavior is similar with the previous figure; the power increases with both terms, but the increase with ka_1 is sharper. In this figure, for $R_a = 1$ the elliptical piston reduces to a circular piston.

7.2 Plates

Throughout this section aluminum is used as the plate material, and the dependence of the obtained acoustic results on various design parameters is investigated. There are many types of aluminum. The one used here is Aluminum Alloy 1100-H14 (99% Al), and its properties are $\rho_m = 2710\ kg/m^3$ (density), $E = 70\ MPa$ (modulus of elasticity), and $G = 26\ MPa$ (modulus of rigidity) (Beer and Johnston, 1992). By using E and G, the Poisson's ratio is calculated as $\upsilon = 0.346$. Also, to find the mass per unit area of the plate, ρ_p, the mass per unit volume, ρ_m, should be multiplied with the thickness of the plate, h.

7.2.1 Rectangular Plates

A simply supported rectangular plate is considered as an example. The constants used are $W_0 = 0.005\ m$, $R = 2.5\ m$, $a = 0.3\ m$, $b = 0.2\ m$, and $h = 0.001\ m$. The displacement of the plate is given by Eq. (4.21). To see the shape of the plate during the vibration, a specific pair of the numbers of the modal lines in both directions is considered. For $(m,n) = (6,4)$ the shape of the plate is shown in Fig. 7.17. The frequency of vibration for this modal pair should be found from Eqs. (4.18) and (4.19) together with the corresponding frequency coefficients from Table 4.1. This is applicable to all rectangular plates considered in this study. By using the frequency and the other given

constants, the behavior of the acoustic intensity, which is obtained from the pressure expression given by Eq. (4.23), can be investigated. Fig. 7.18 shows the variation of the intensity with the angle ϕ for $\theta = 60^\circ$. ϕ is changed between 0° and 90° since the behavior is the same in all four quadrants of the far-field hemisphere. It can be seen that the intensity is a maximum for $\phi = 0^\circ$, it becomes a minimum at around $\phi = 60^\circ$ (a point of sound cancellation), and levels somewhere in between when $\phi = 90^\circ$. Fig. 7.19 shows the variation of the intensity with ϕ for $\theta = 30^\circ$; everything else is the same. As can be noticed, the magnitude of the intensity drops drastically and the direction of events changes. This is a characteristic of all rectangular plates considered in this study. Also a change in the modal pair would change the behavior totally. Similarly, if the change of the intensity with θ for a constant ϕ is considered, same kind of behavior is observed. As a last example, a very high frequency of vibration is considered referring to the modal pair $(m,n) = (12,8)$. Fig. 7.20 shows the variation of the intensity with ϕ for $\theta = 60^\circ$. It can be deduced that the number of minimum intensity points increase with the increasing number of modal lines. This is a characteristic of higher modes of rectangular plates.

The acoustic power radiated by a simply supported rectangular plate is the sum of the individual power terms given by Eqs. (4.24) and (4.25). As explained before, the acoustic power analysis in this study is limited to low kL values; therefore, for rectangular plates, only the first modal pair $(m,n) = (2,2)$ is considered. A further increase in any of the number of modal lines causes an increase in the frequency of vibration corresponding to that specific mode, which in turn results in high kL values destroying the accuracy. For a constant plate area of 0.06 m^2 the variation of the acoustic power with the aspect ratio is shown in Fig. 7.21. As can be seen from this figure, the acoustic power radiated from a simply supported rectangular plate decreases with an increase in the aspect ratio for the fundamental mode. In other words, out of all simply supported rectangular plates of the same area, the square one radiates the lowest sound in the fundamental mode. Fig. 7.22 shows the dependence of the power on the thickness of the plate. This figure indicates that an increase in the thickness of the plate results in a sharp increase in the acoustic power when all the other parameters are constant.

In Chapter IV, in addition to simply supported rectangular plates, five other plates with different boundary conditions were studied. The far-field acoustic pressure expressions were obtained in closed form. The acoustic intensity for each case can easily be found from them. Also, the acoustic power expressions presented in that chapter can be used for the fundamental modes of the plates. The author analyzed all of these cases and observed that their behavior is very similar to that of the simply supported rectangular plate. Therefore, they are not presented here.

7.2.2 Circular Plates

The numerical values used are $r_0 = 0.2\ m$, $A = 0.005\ m$, $h = 0.001\ m$, and $R = 2.5\ m$. A clamped circular plate is considered first. The displacement functions for the first three modes of the plate are shown in Fig. 7.23. For these modes, the variation of the acoustic intensity with θ is shown in Fig. 7.24. As can be noticed, for the same parameters other than the frequency dependent ones, the first mode is the weakest radiator, and the third mode is the strongest one. Fig. 7.25 shows the acoustic power radiation from the forced vibration of the clamped circular plate. The uniform forcing function is taken to be $100\ N/m^2$. To be able to show the whole behavior a log-log plot is used, and Ω in this figure shows the forcing frequency. The peaks shown correspond to the first two natural frequencies of the plate. This means that when the forcing frequency is equal to one of the plate natural frequencies, resonance conditions are achieved, and the radiated acoustic power increases drastically. Fig. 7.26 shows the displacement functions for the first three modes of a simply supported circular plate with the same constants given above. Fig. 7.27 shows the variation of the acoustic intensity with θ. Almost the same behavior as in the clamped plate is observed. The acoustic power radiation from the forced vibration of the simply supported circular plate is shown in Fig. 7.28. The same forcing function is used. Again, the same behavior as for the clamped plate is observed; when the forcing frequencies becomes equal to the natural frequencies, the power increases sharply. As can be noticed, in the power plots only the first two modes are included because of the previously mentioned limitation of the surface integration approach. Fig. 7.29 shows the acoustic power from the forced vibration of a clamped and a simply supported circular

plate together. This figure indicates that the power curves are very similar for both plates; the only difference is a shift towards the left for the simply supported plate. Finally, Fig. 7.30 shows the power radiated from the free vibration of a clamped or simply supported circular plate. This figure may be a little bit misleading since the radiation from the free vibration should be at a distinct frequency; in other words, it is not possible to obtain a continuous power curve for the free vibration. In any event, it is a function of the frequency, and it can be plotted. But, to find the exact power value from the free vibration of a clamped or a simply supported circular plate, one should know the frequency of vibration for the specific mode considered and find the intersection of the corresponding power curve with this frequency value.

7.2.3 Clamped Elliptical Plates

The acoustic power radiated from a clamped elliptical plate vibrating in its fundamental mode is given by Eq. (6.24). This formula is only approximate, and for very high aspect ratios (more than 3) it may not be very accurate. The variation of the power with the aspect ratio for a constant plate area is shown in Fig. 7.31. This figure indicates that the power radiated for the fundamental mode decreases with an increase in the aspect ratio. The optimum point is a circular plate for which the aspect ratio is 1. This is similar to the rectangular-square plate relation observed in Fig. 7.21. Fig. 7.32 shows the variation of the power with the plate thickness for the fundamental mode of the elliptical plate. From this figure it can be understood that the power increases with the increasing thickness. This behavior is the same as in Fig. 7.22.

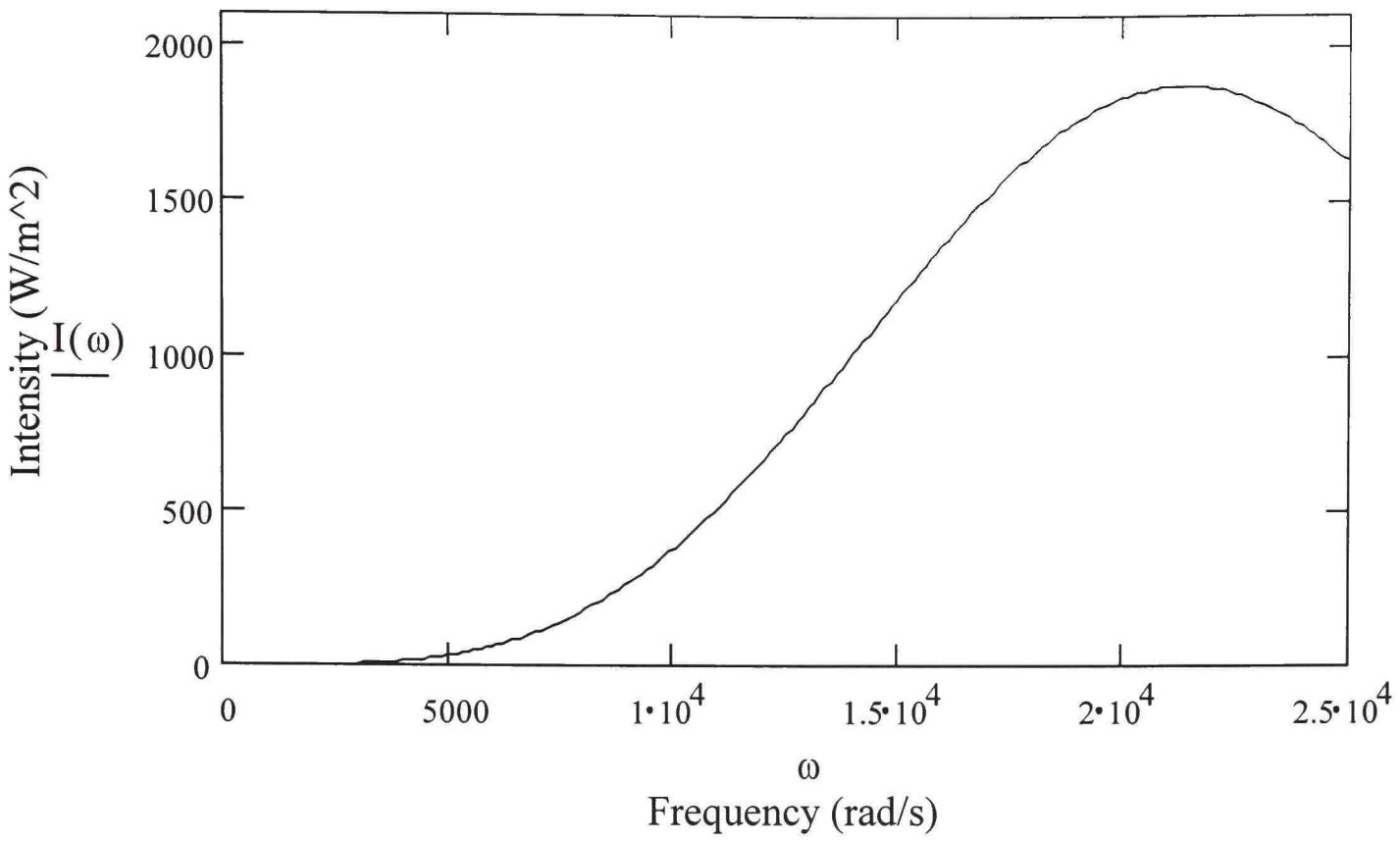

Figure 7.1. Acoustic Intensity versus Frequency for a Triangular Piston for $\phi = 60^{\circ}$ and $\theta = 30^{\circ}$.

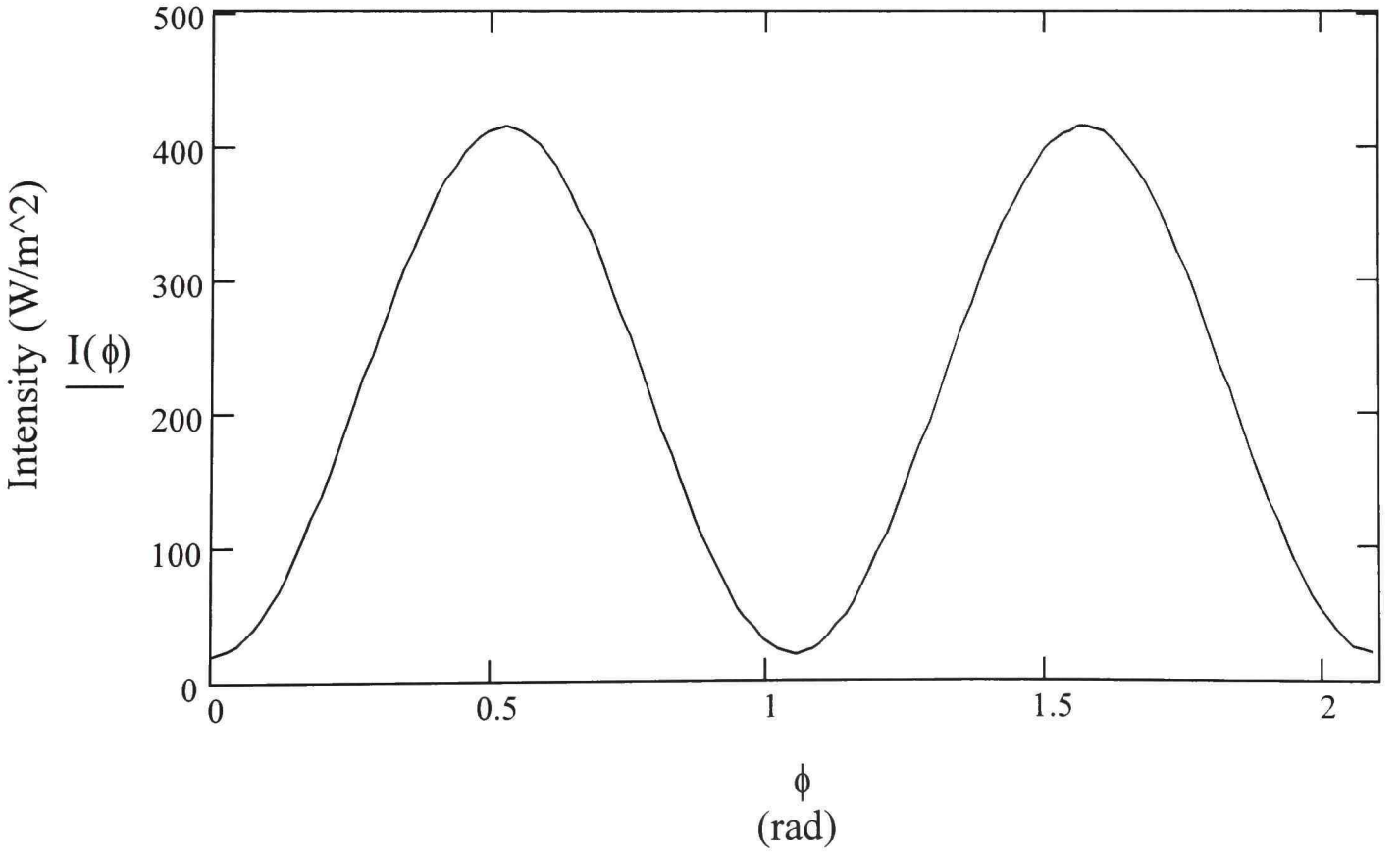

Figure 7.2. Acoustic Intensity versus ϕ for a Triangular Piston for $\omega = 20000\ rad/s$ and $\theta = 60^{\circ}$.

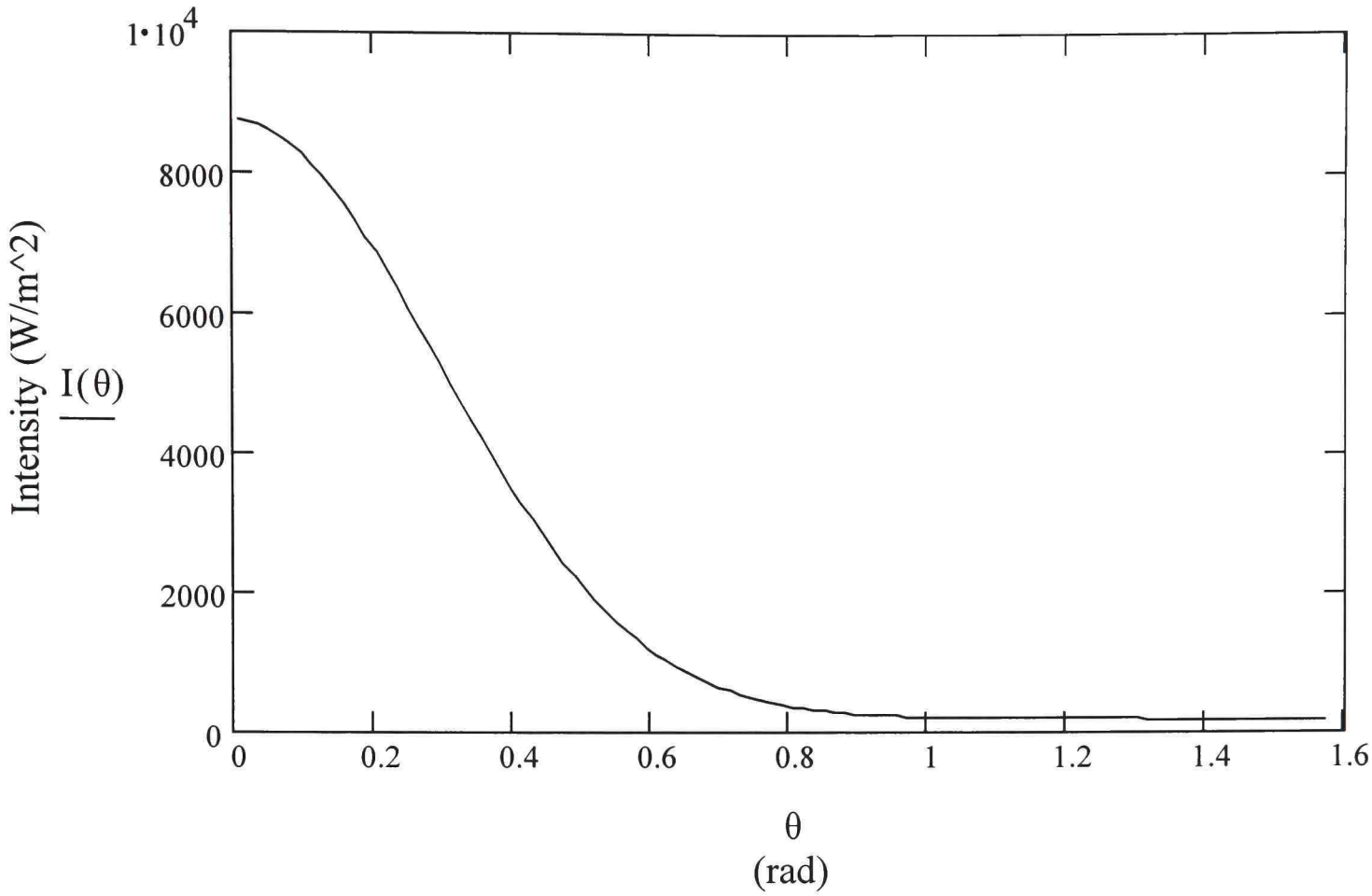

Figure 7.3. Acoustic Intensity versus θ for a Triangular Piston for $\omega = 20000\ rad/s$ and $\phi = 45^\circ$.

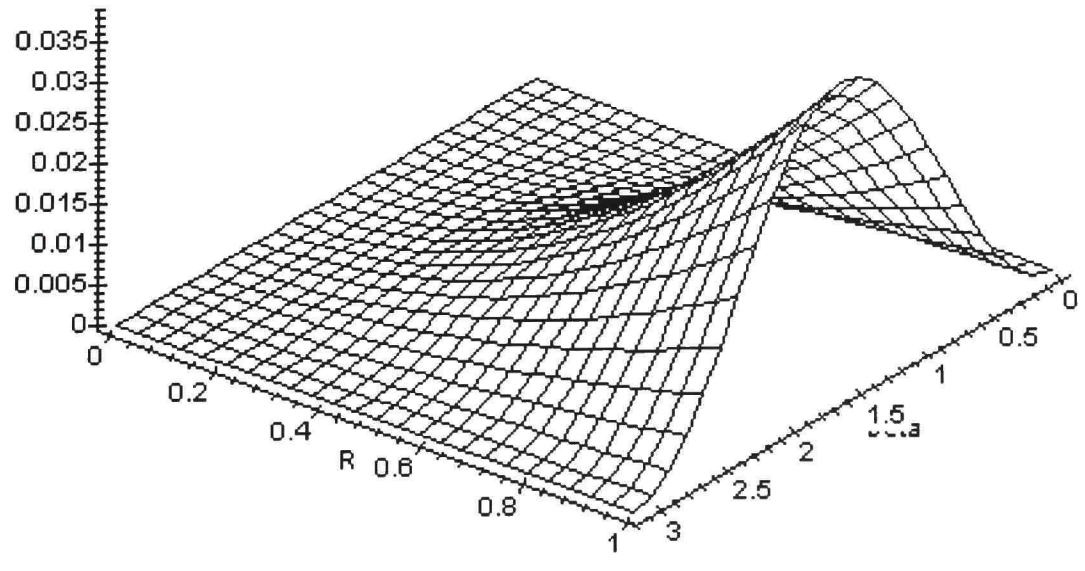

Figure 7.4. Acoustic Power versus R_t and β for a Triangular Piston.

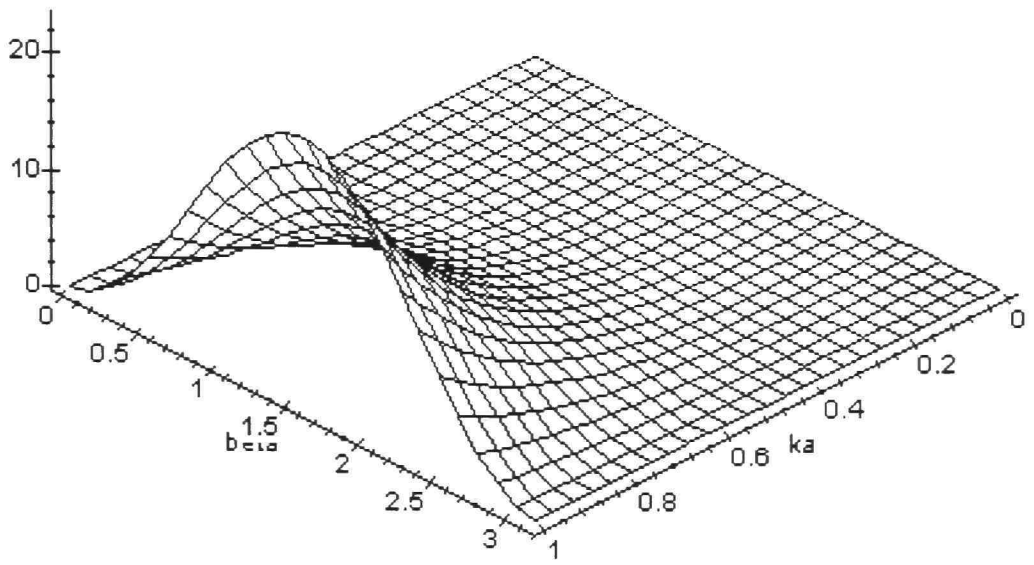

Figure 7.5. Acoustic Power versus β and ka_0 for a Triangular Piston.

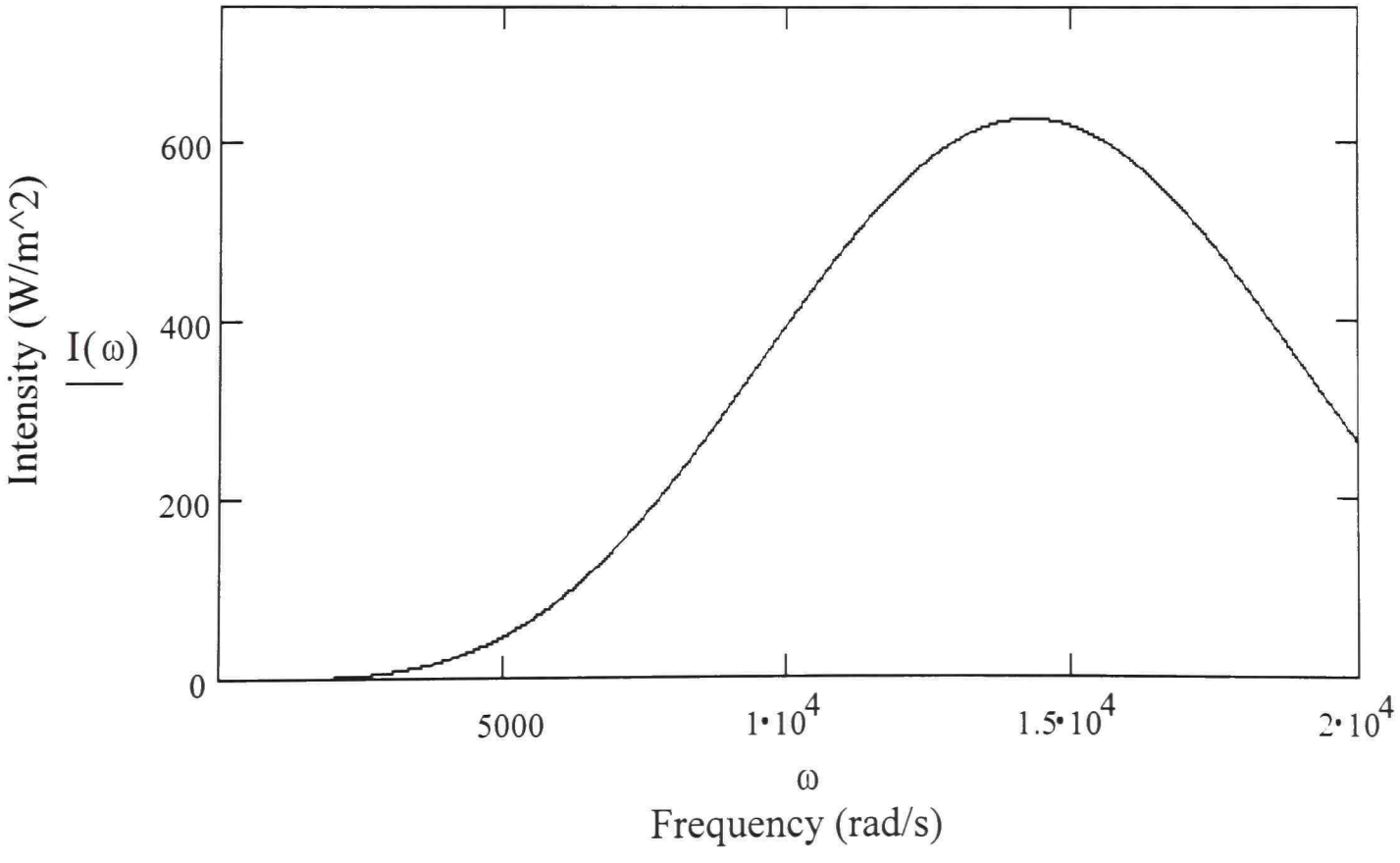

Figure 7.6. Acoustic Intensity versus Frequency for a Rectangular Piston for $\phi = 45^\circ$ and $\theta = 45^\circ$.

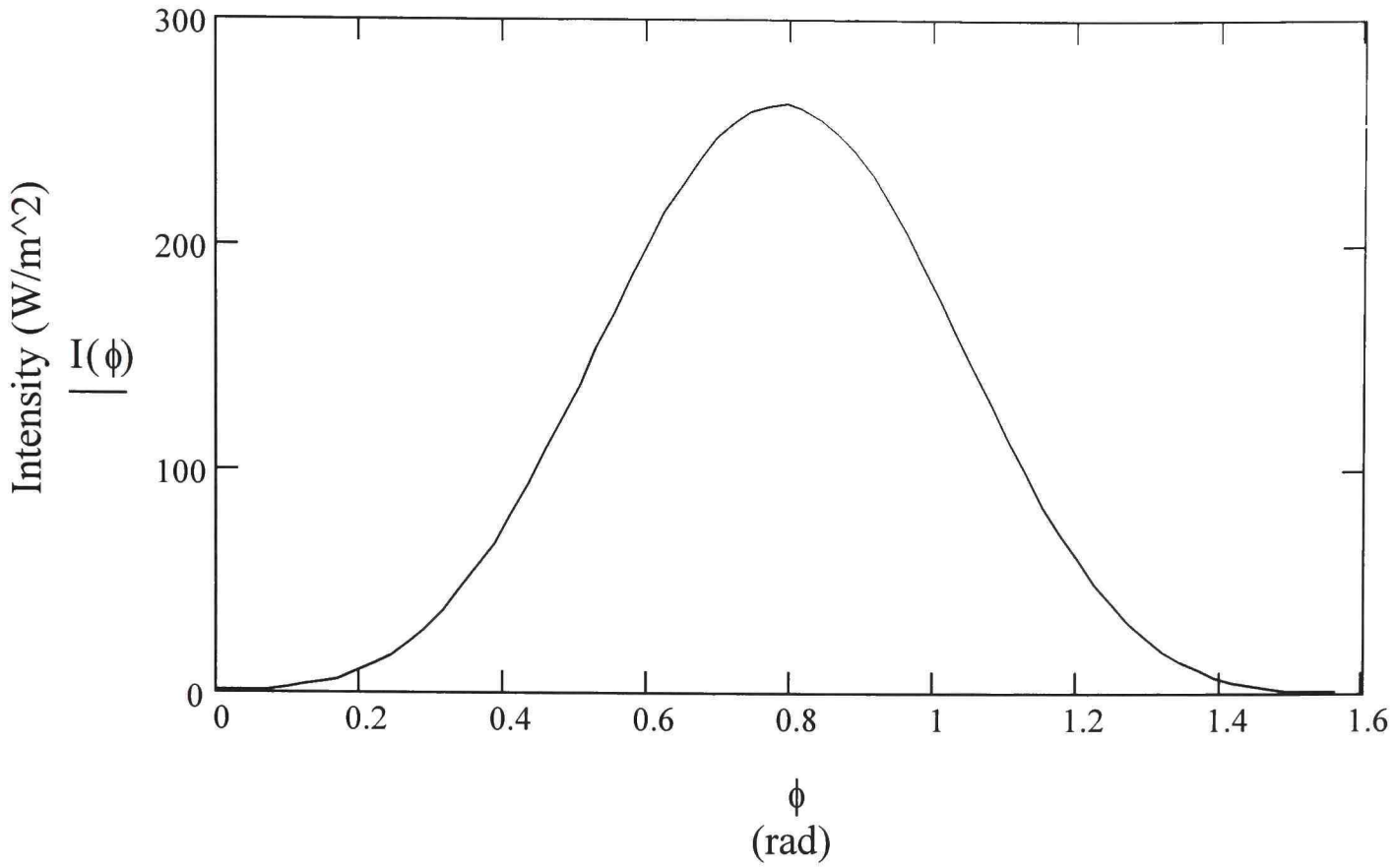

Figure 7.7. Acoustic Intensity versus ϕ for a Rectangular Piston for $\omega = 20000\ rad/s$ and $\theta = 45^\circ$.

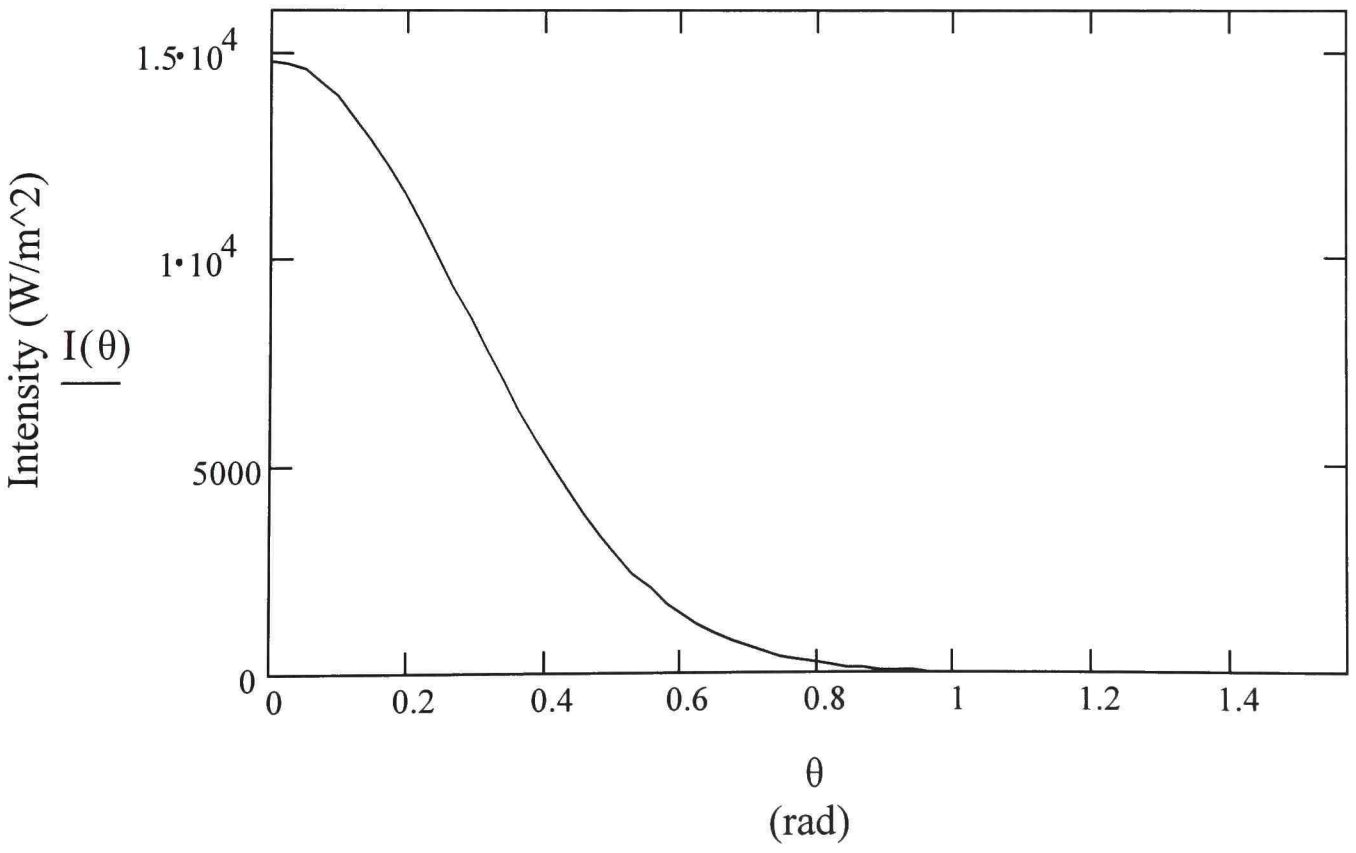

Figure 7.8. Acoustic Intensity versus θ for a Rectangular Piston for $\omega = 20000\ rad/s$ and $\phi = 45^\circ$.

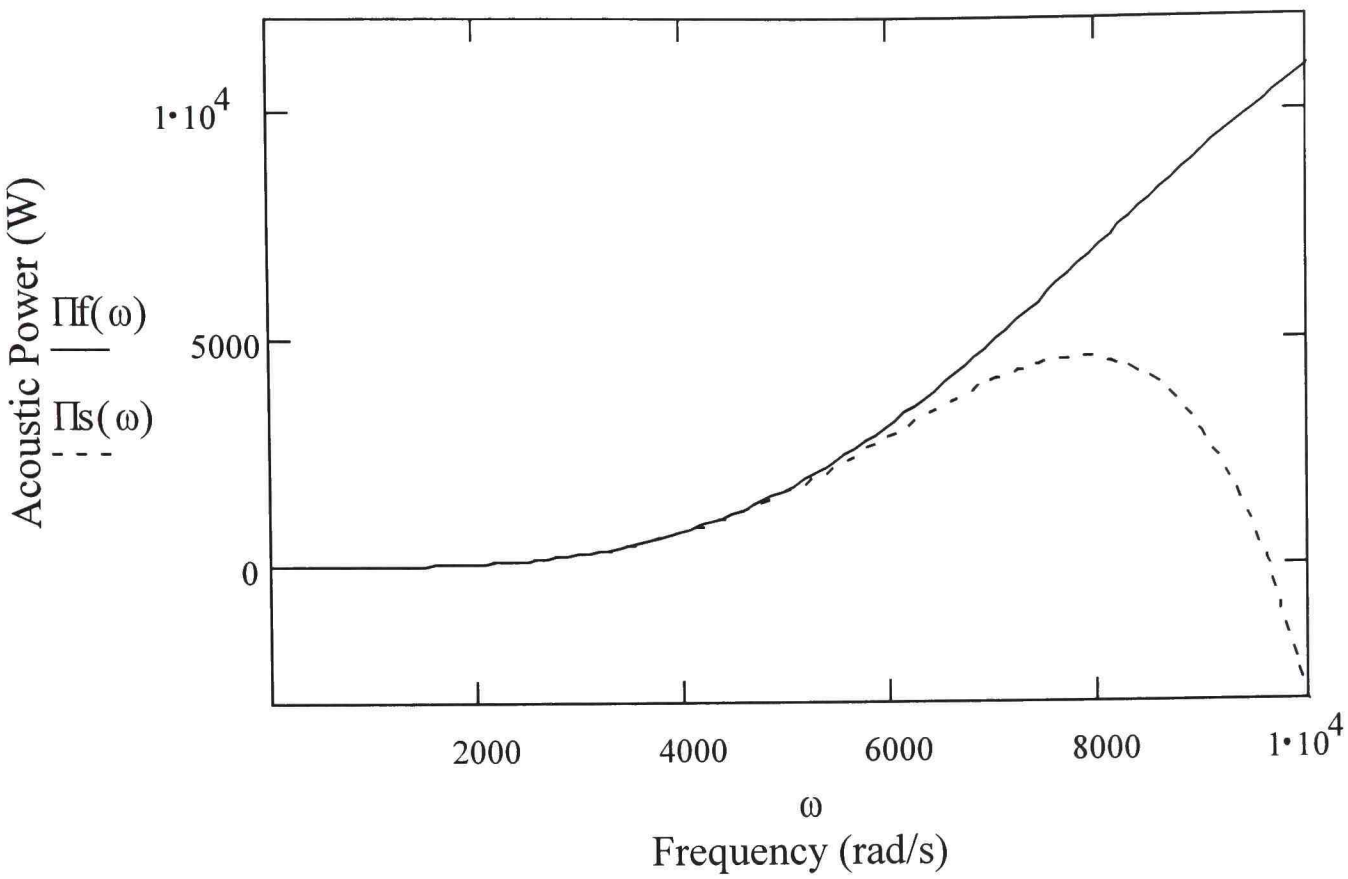

Figure 7.9. Acoustic Power versus Frequency for a Rectangular Piston.

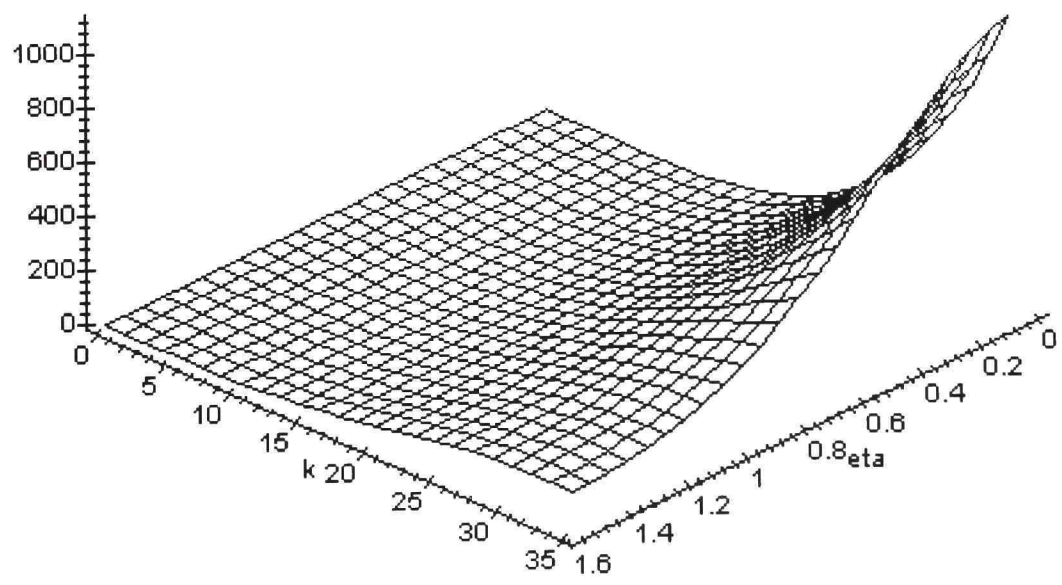

Figure 7.10. Acoustic Intensity versus k and θ for a Circular Piston.

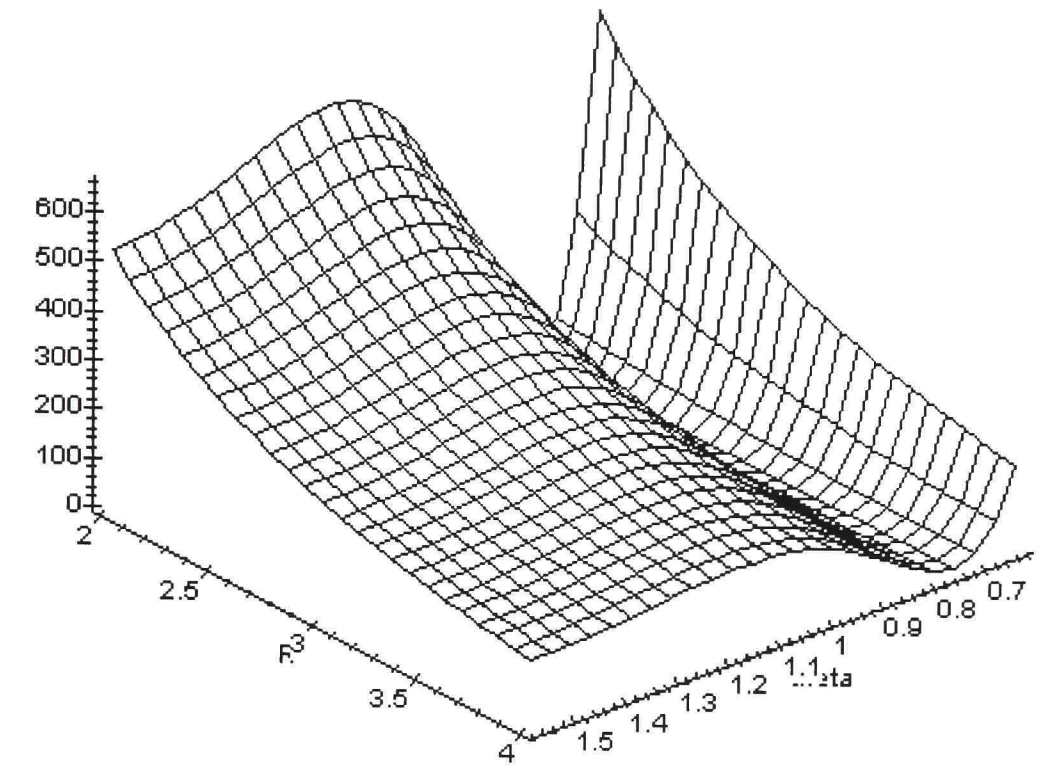

Figure 7.11. Acoustic Intensity versus R and θ for a Circular Piston.

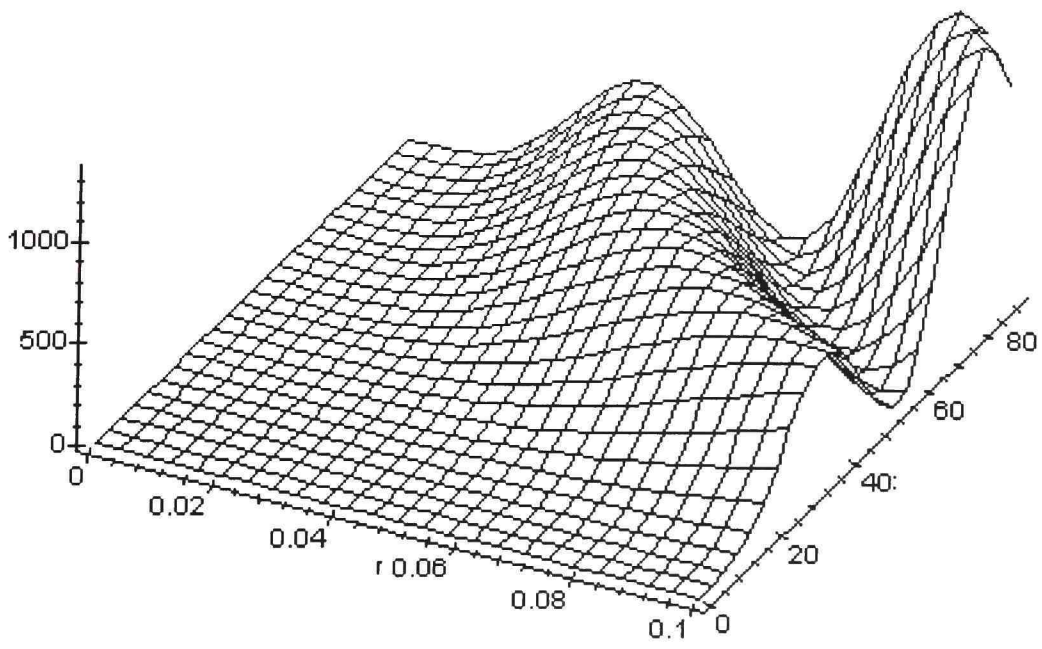

Figure 7.12. Acoustic Intensity versus k and r_0 for a Circular Piston.

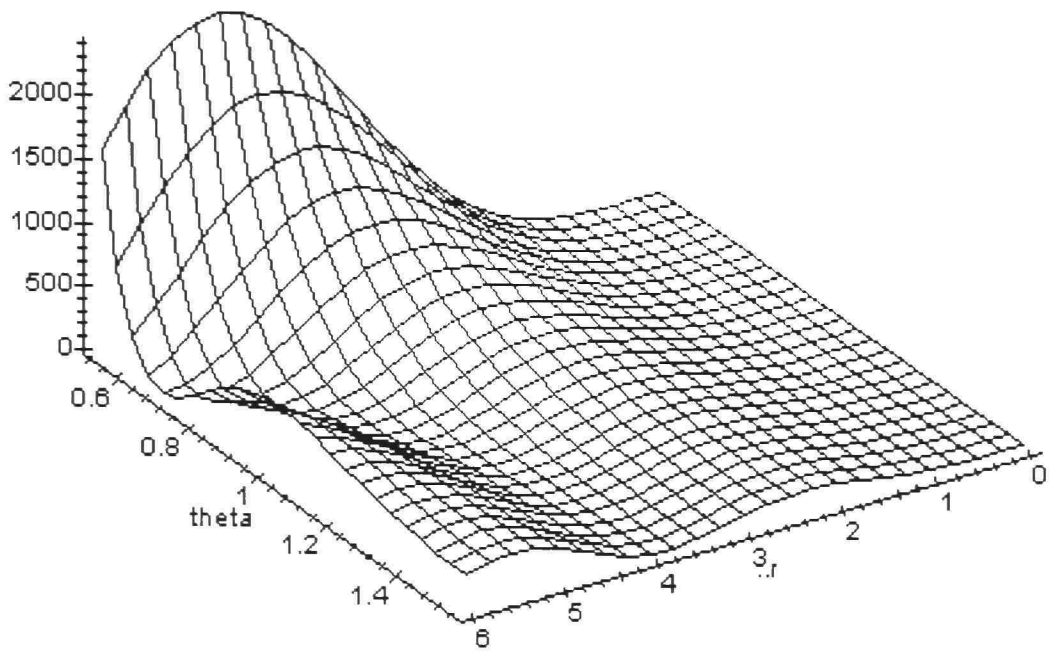

Figure 7.13. Acoustic Intensity versus θ and kr_0 for a Circular Piston.

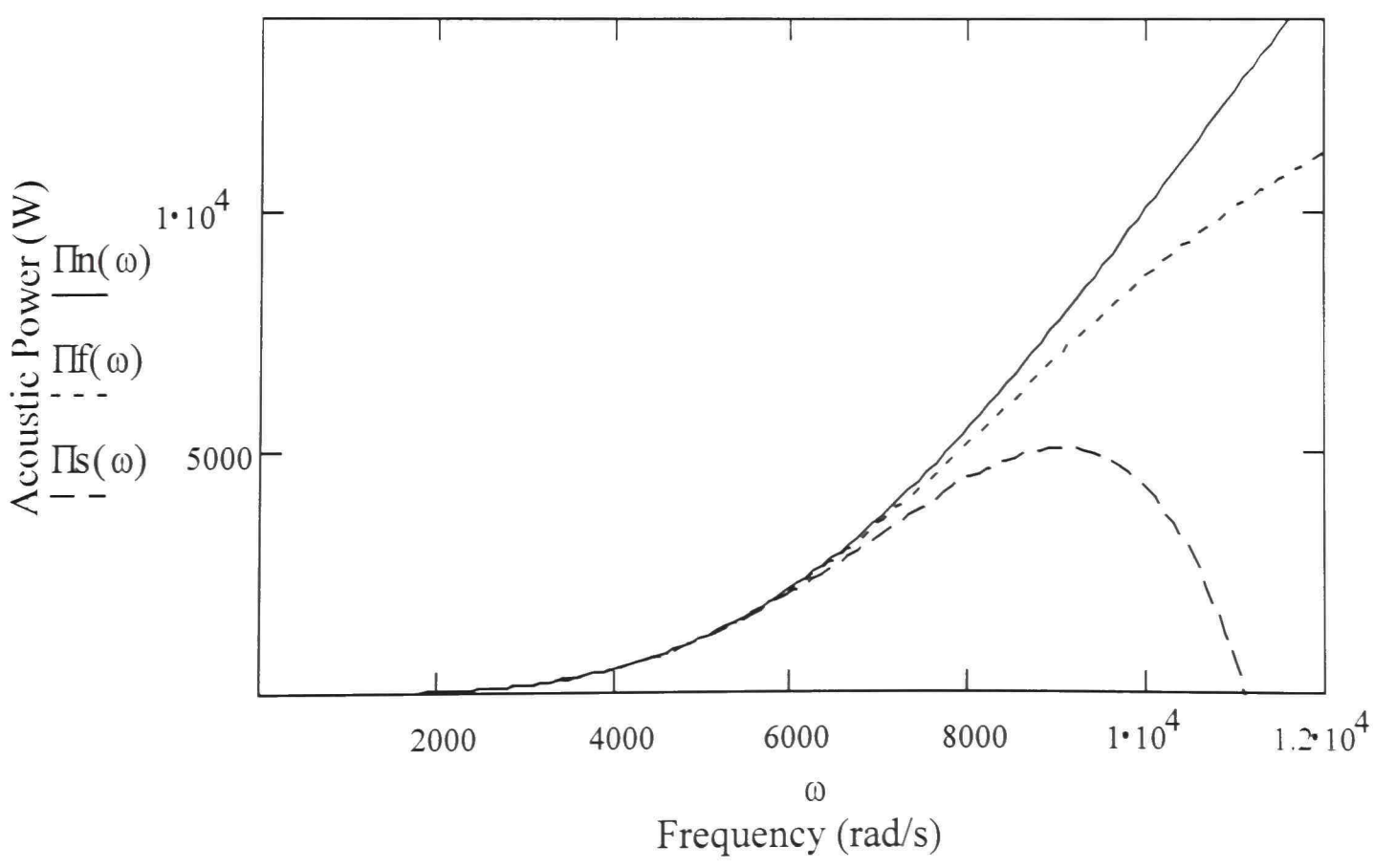

Figure 7.14. Acoustic Power versus Frequency for a Circular Piston.

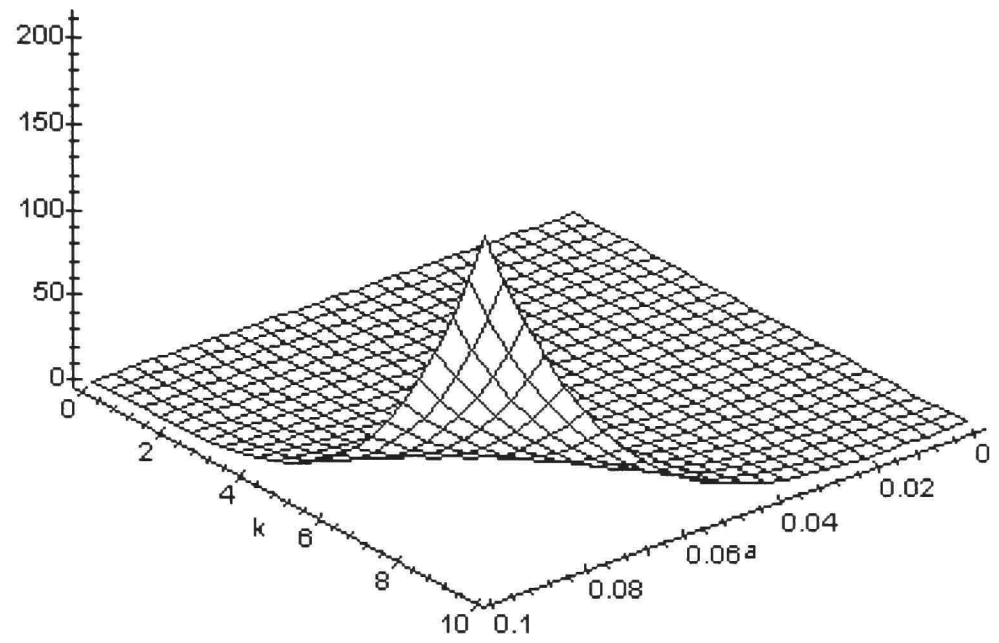

Figure 7.15. Acoustic Power versus k and a_1 for an Elliptical Piston.

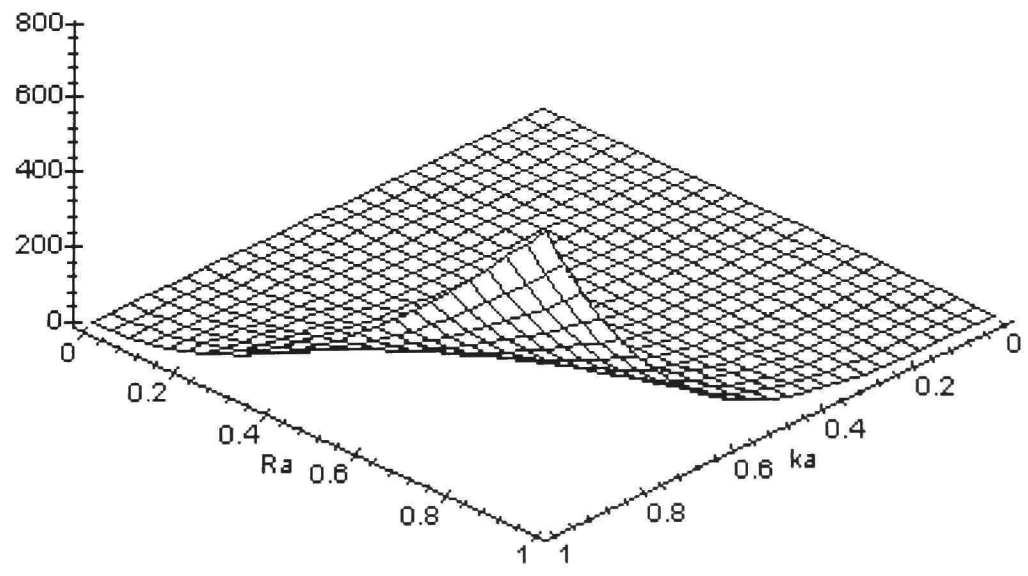

Figure 7.16. Acoustic Power versus ka_1 and R_a for an Elliptical Piston.

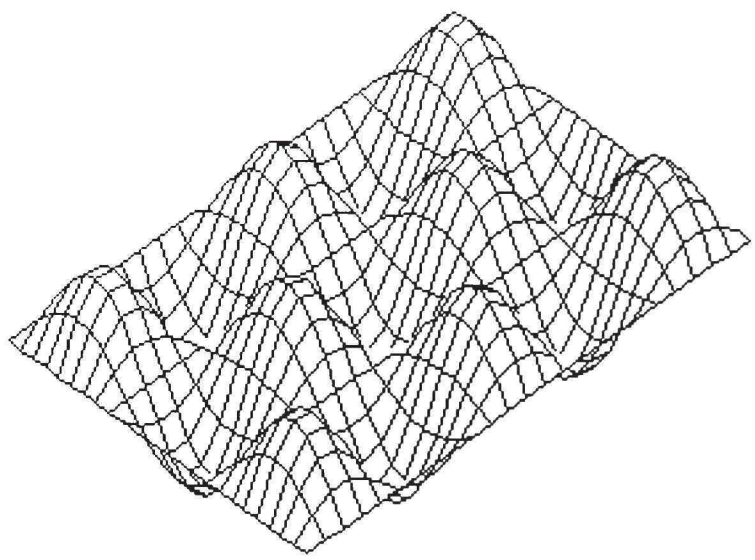

Figure 7.17. Displacement of a Simply Supported Rectangular Plate for $(m,n)=(6,4)$.

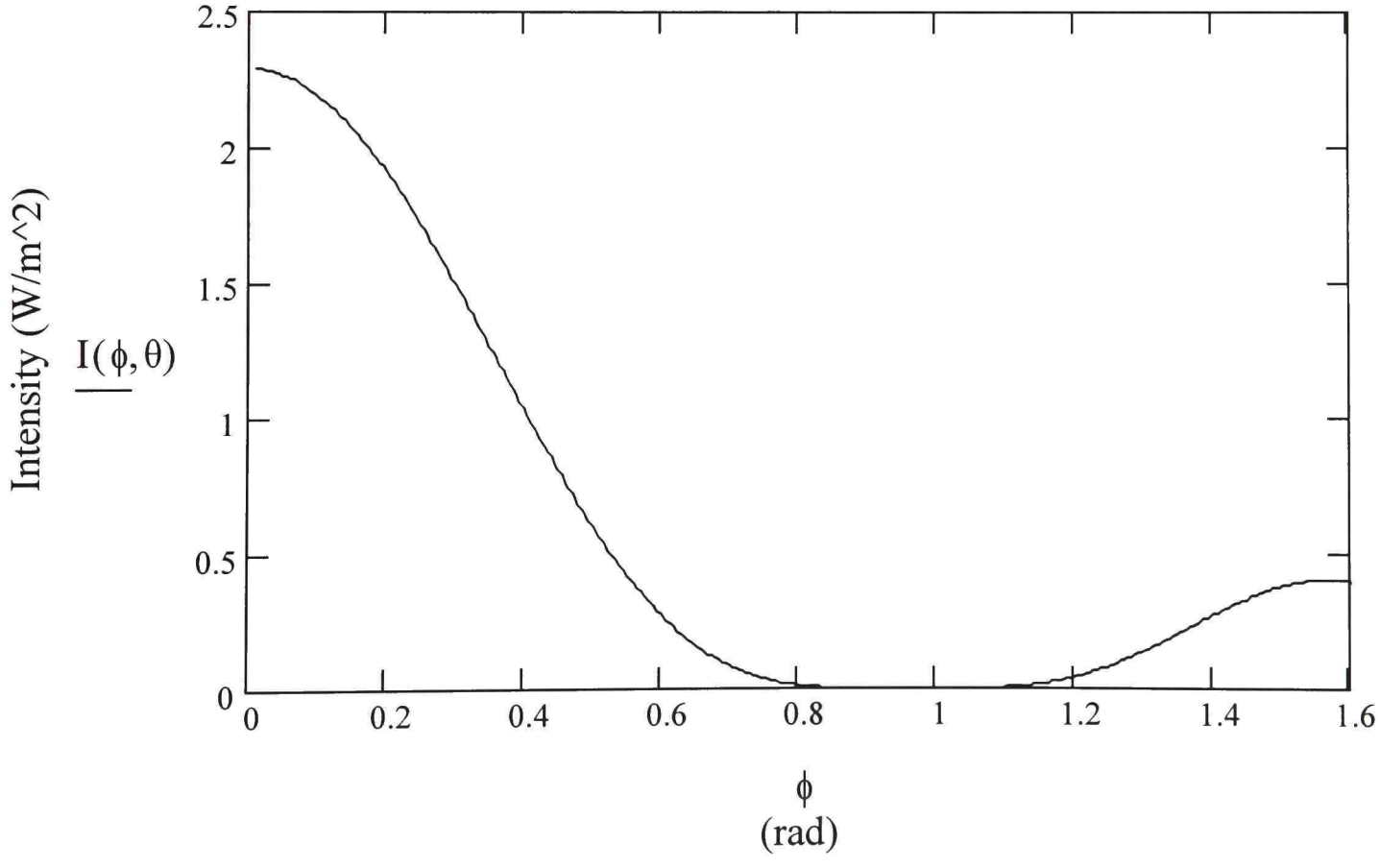

Figure 7.18. Acoustic Intensity versus ϕ for a Simply Supported Rectangular Plate with $(m,n)=(6,4)$ for $\theta=60^{\circ}$.

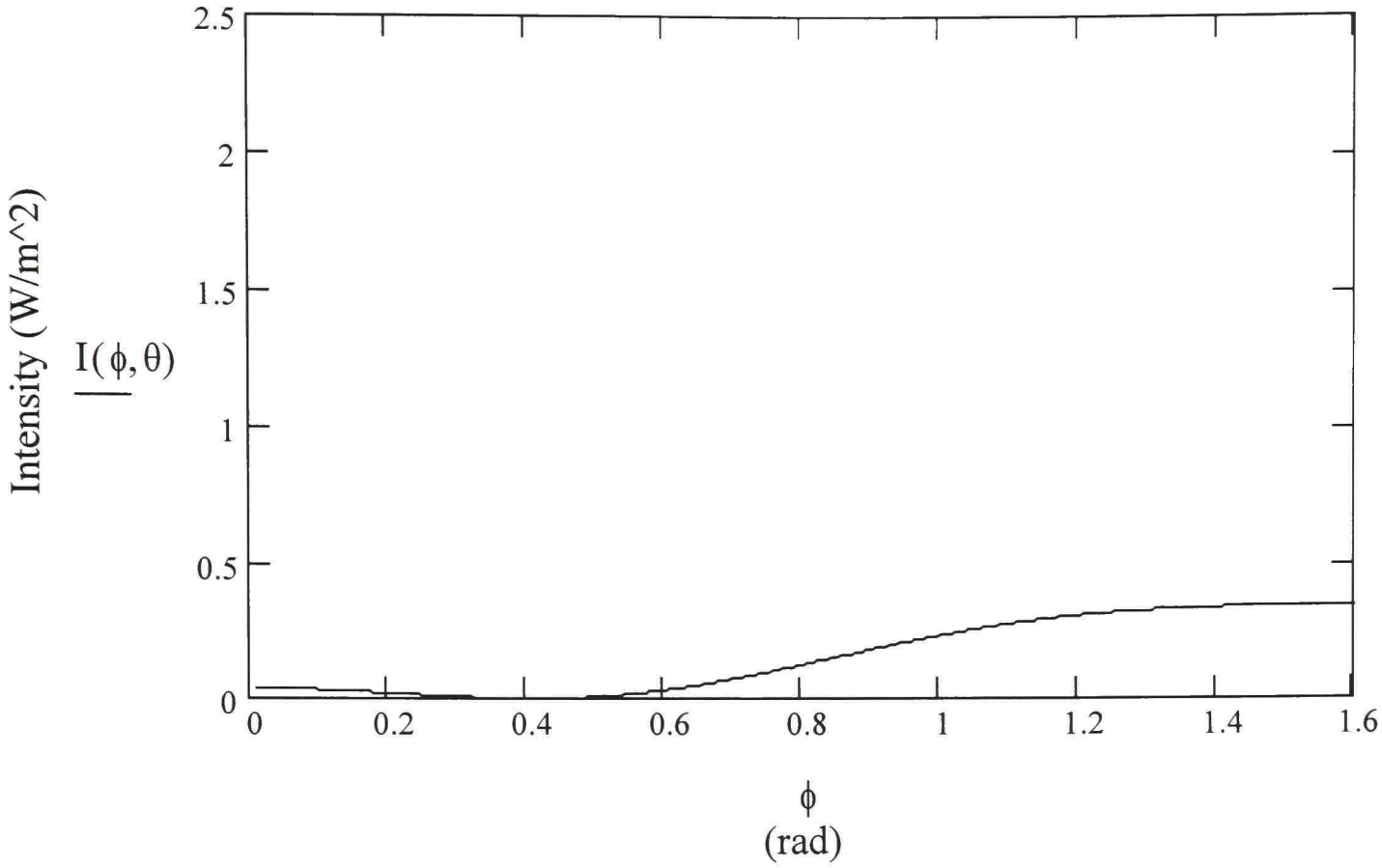

Figure 7.19. Acoustic Intensity versus ϕ for the Simply Supported Rectangular Plate with $(m,n)=(6,4)$ for $\theta=30^{\circ}$.

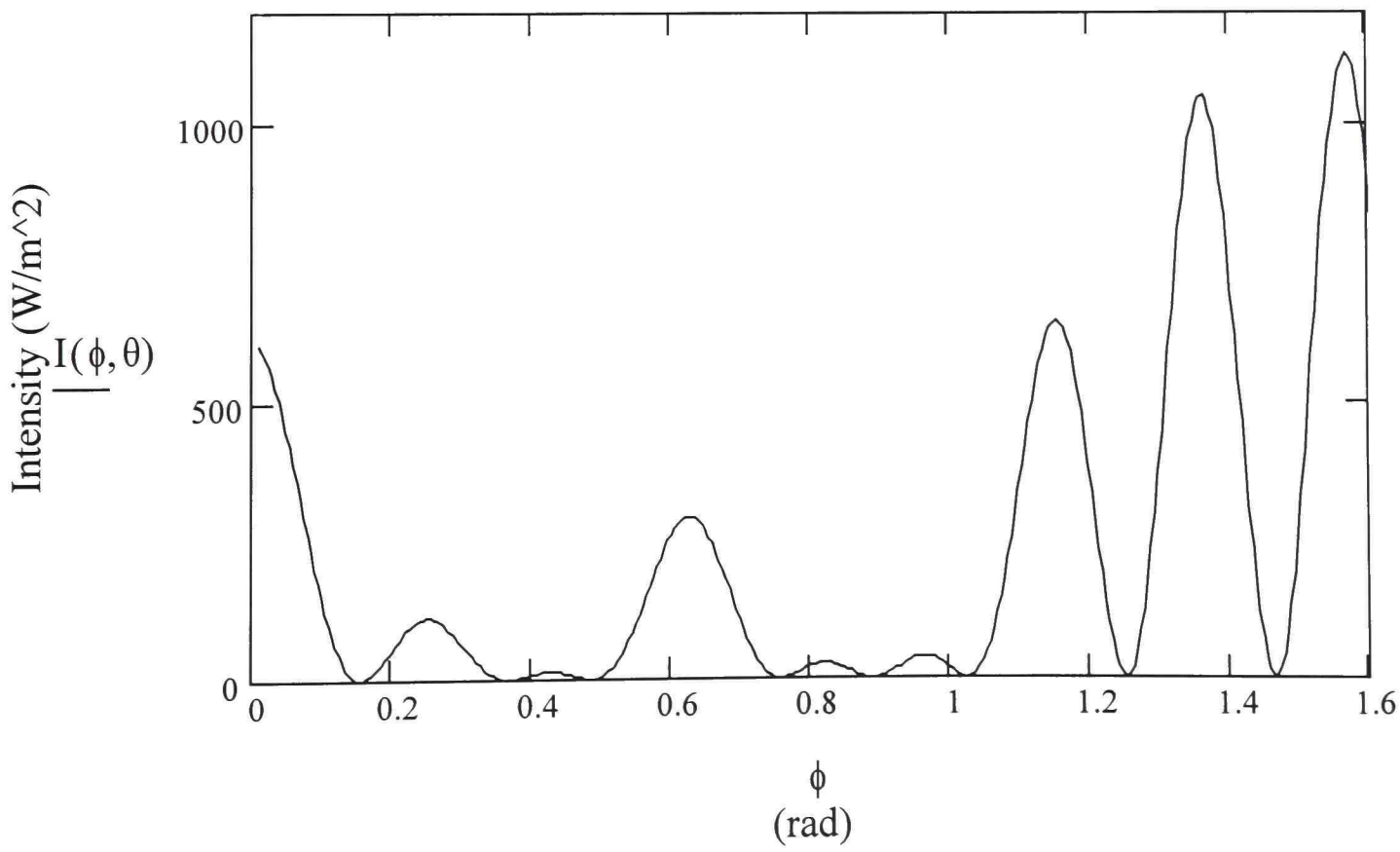

Figure 7.20. Acoustic Intensity versus ϕ for the Simply Supported Rectangular Plate with $(m,n)=(12,8)$ for $\theta=60^{\circ}$.

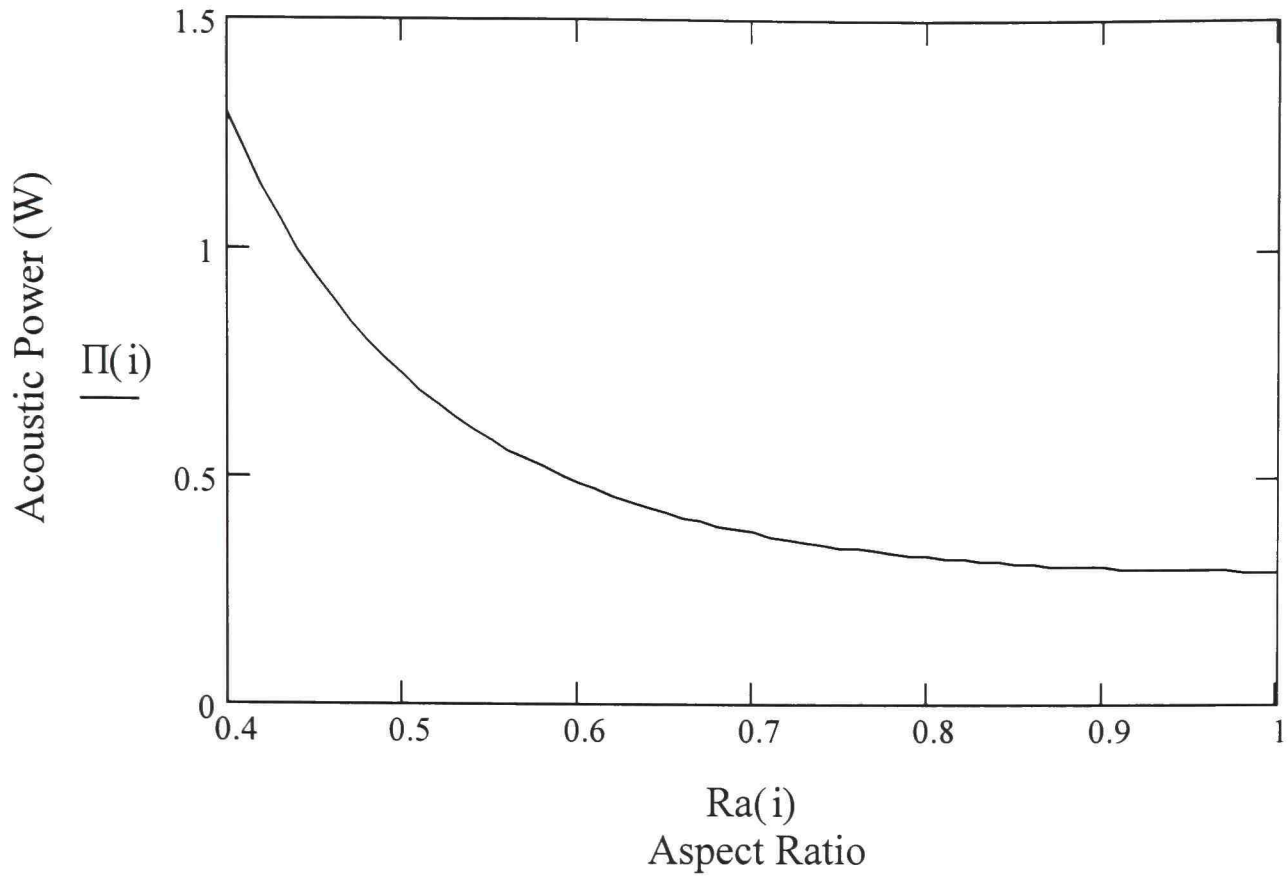

Figure 7.21. Acoustic Power versus R_a for a Simply Supported Rectangular Plate.

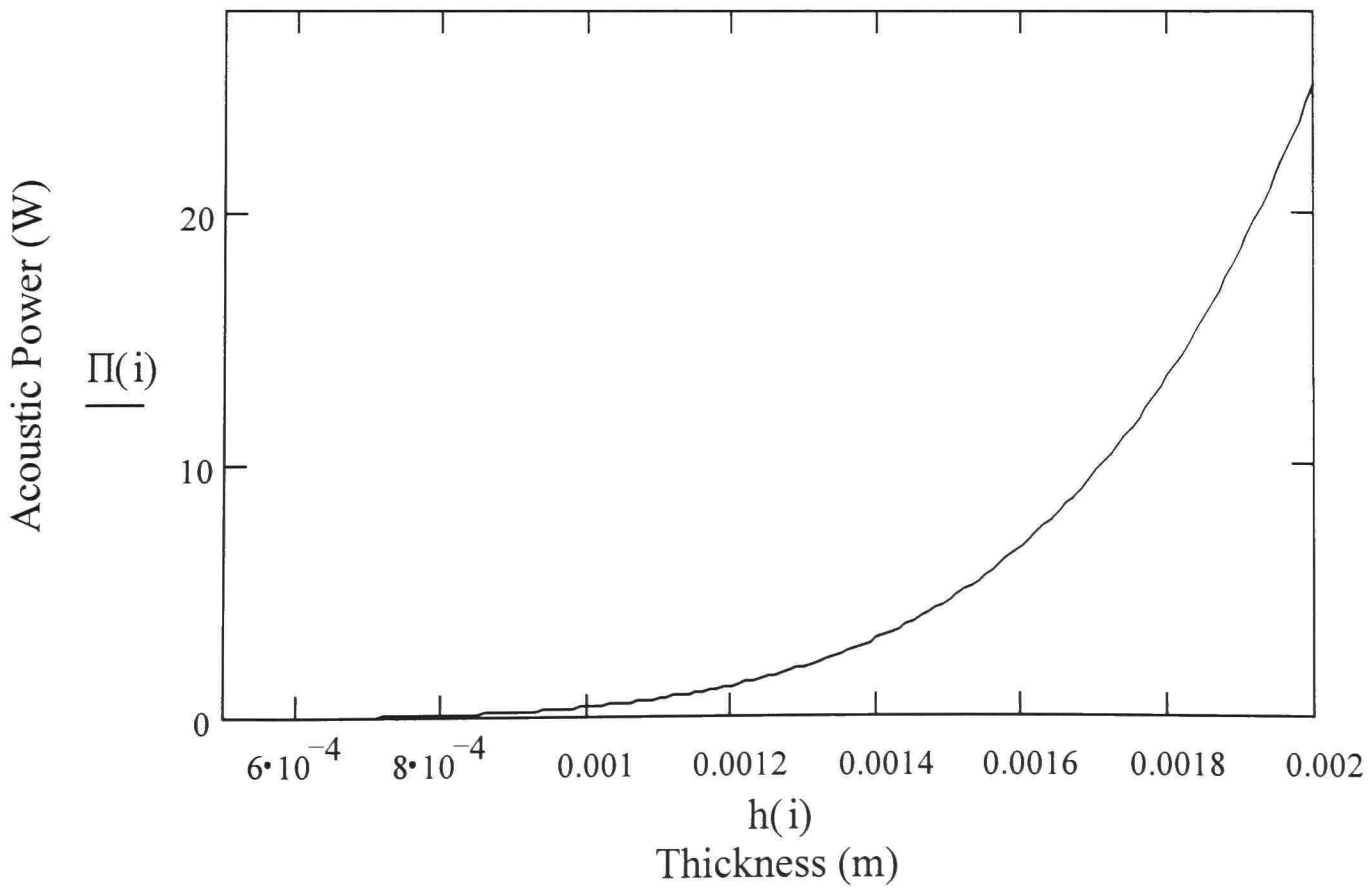

Figure 7.22. Acoustic Power versus h for a Simply Supported Rectangular Plate.

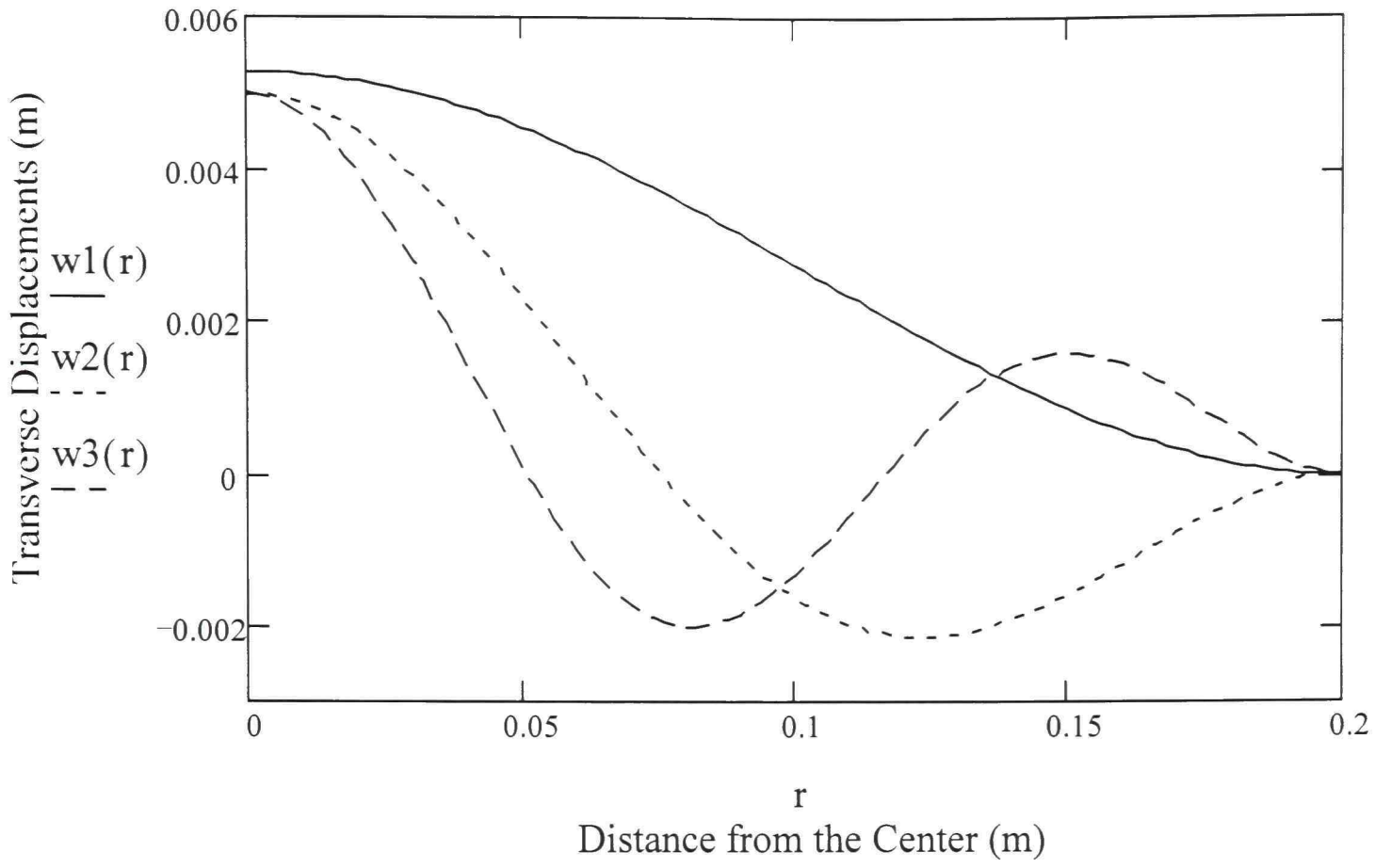

Figure 7.23. Displacement Functions versus r for the First Three Modes of a Clamped Circular Plate.

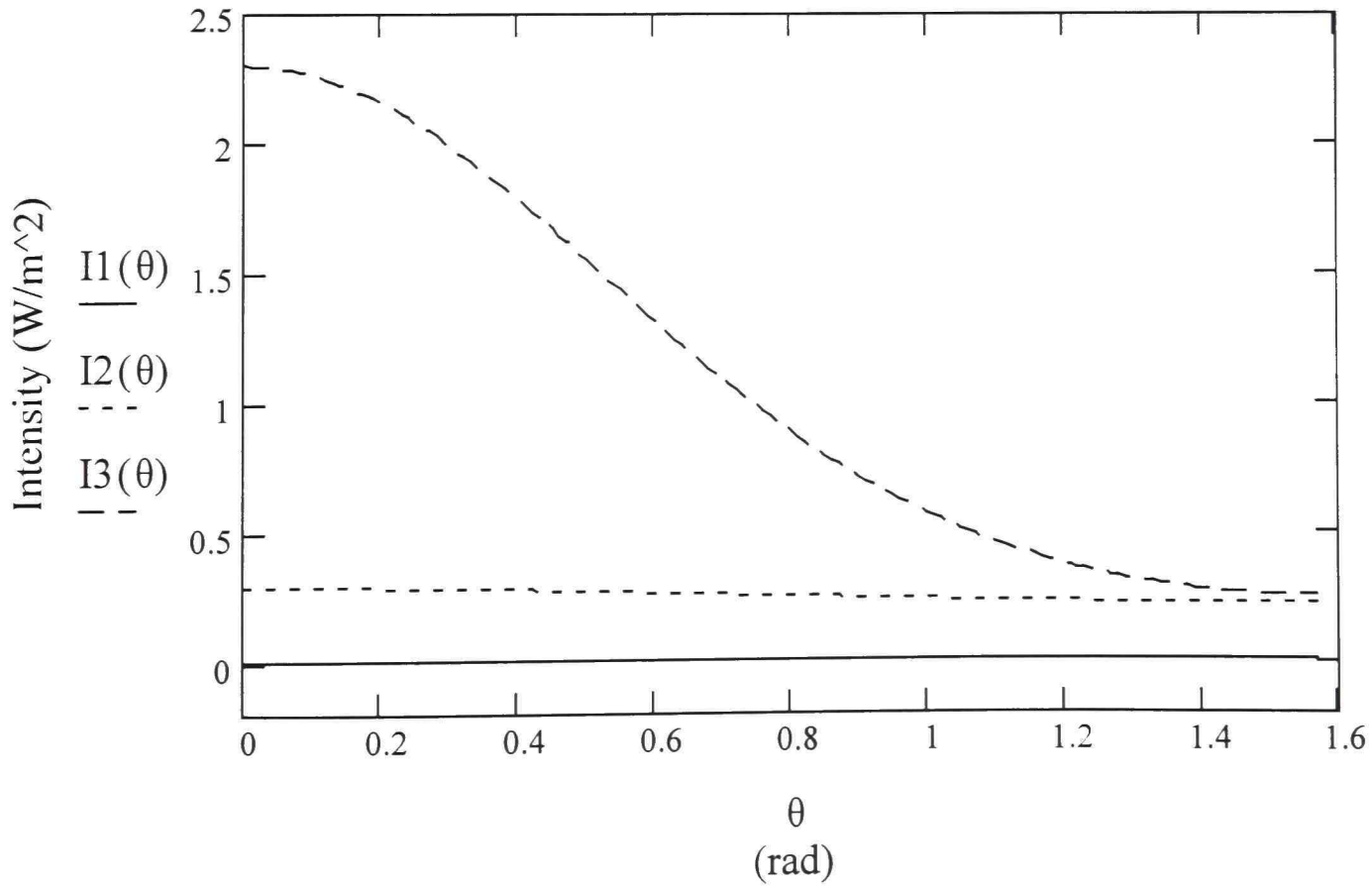

Figure 7.24. Acoustic Intensity versus θ for the First Three Modes of a Clamped Circular Plate.

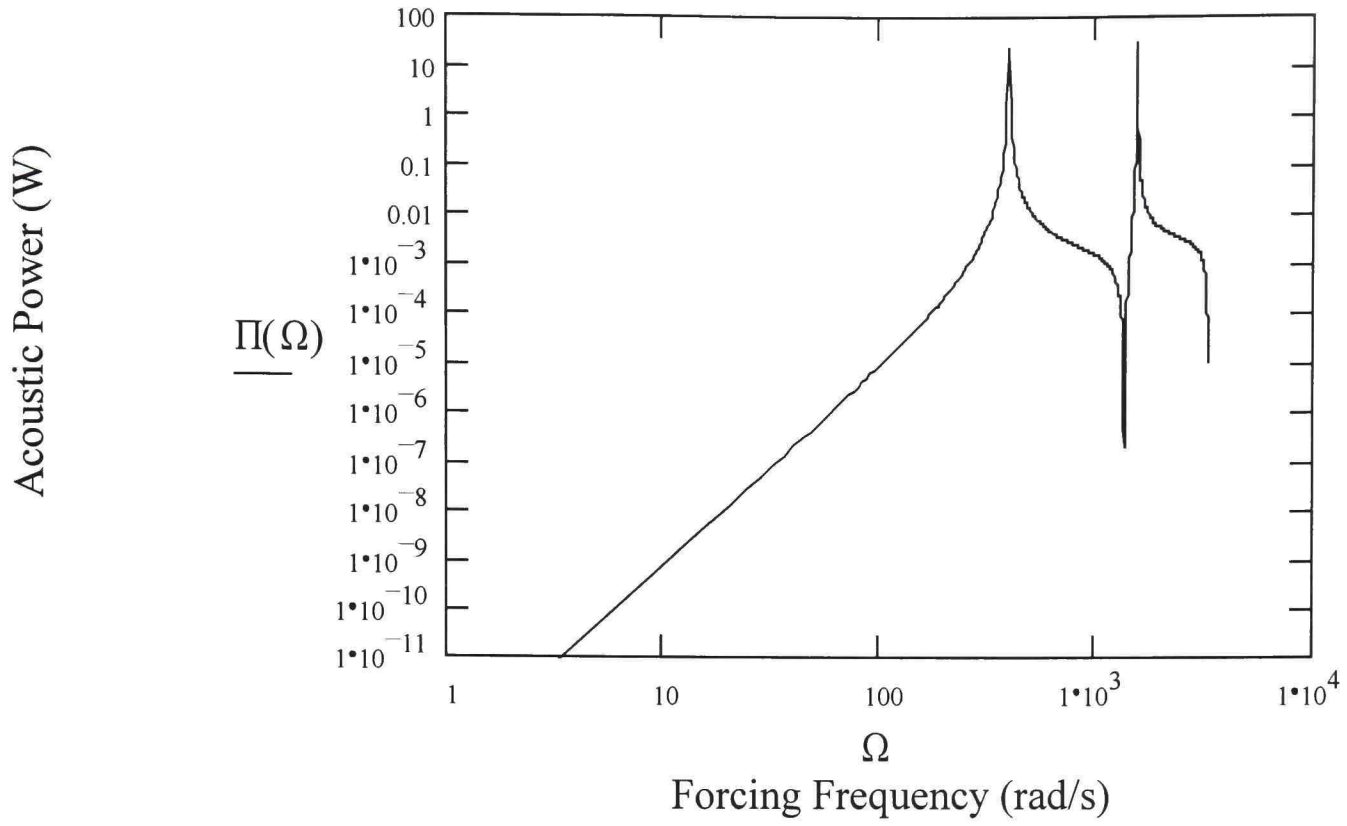

Figure 7.25. Acoustic Power versus Forcing Frequency for a Clamped Circular Plate.

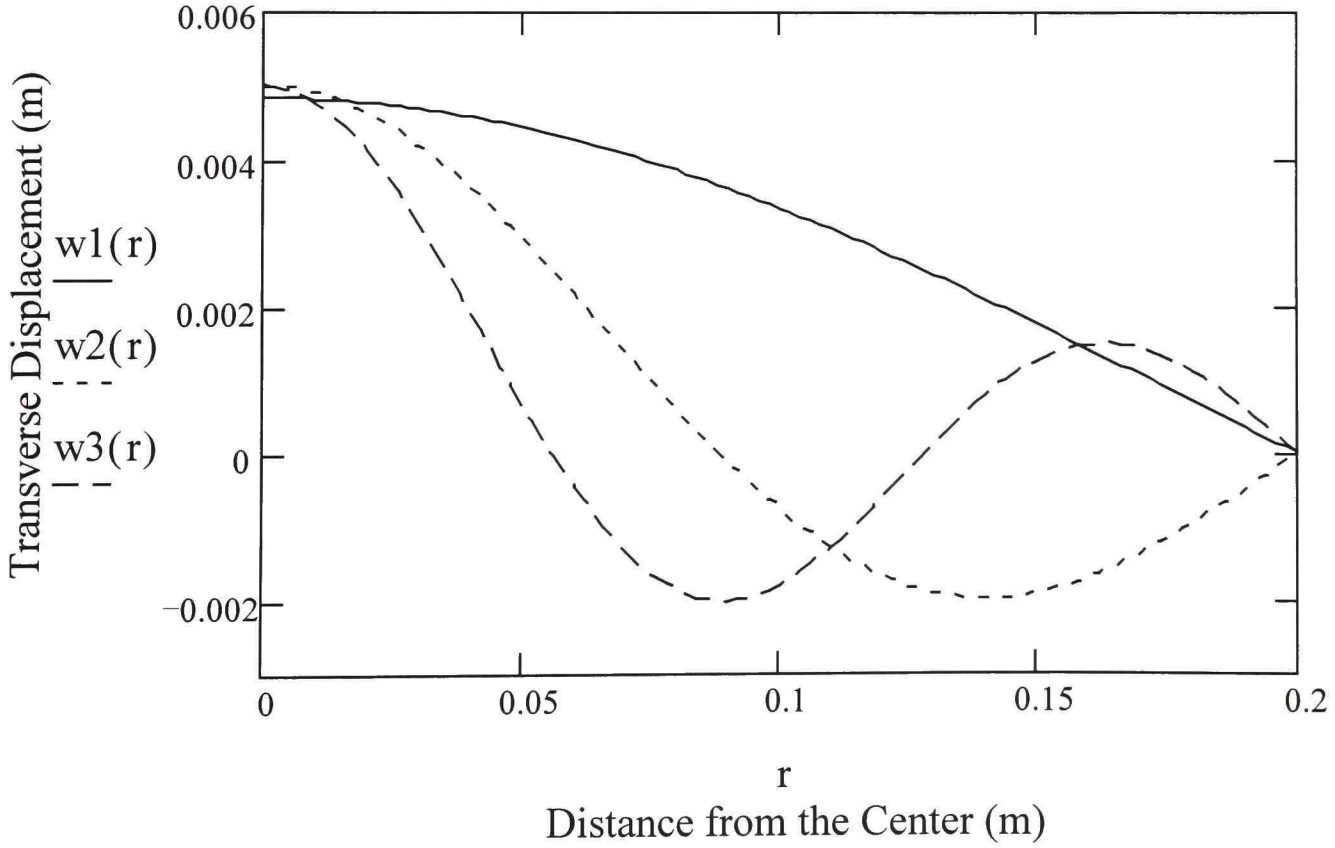

Figure 7.26. Displacement Functions versus r for the First Three Modes of a Simply Supported Circular Plate.

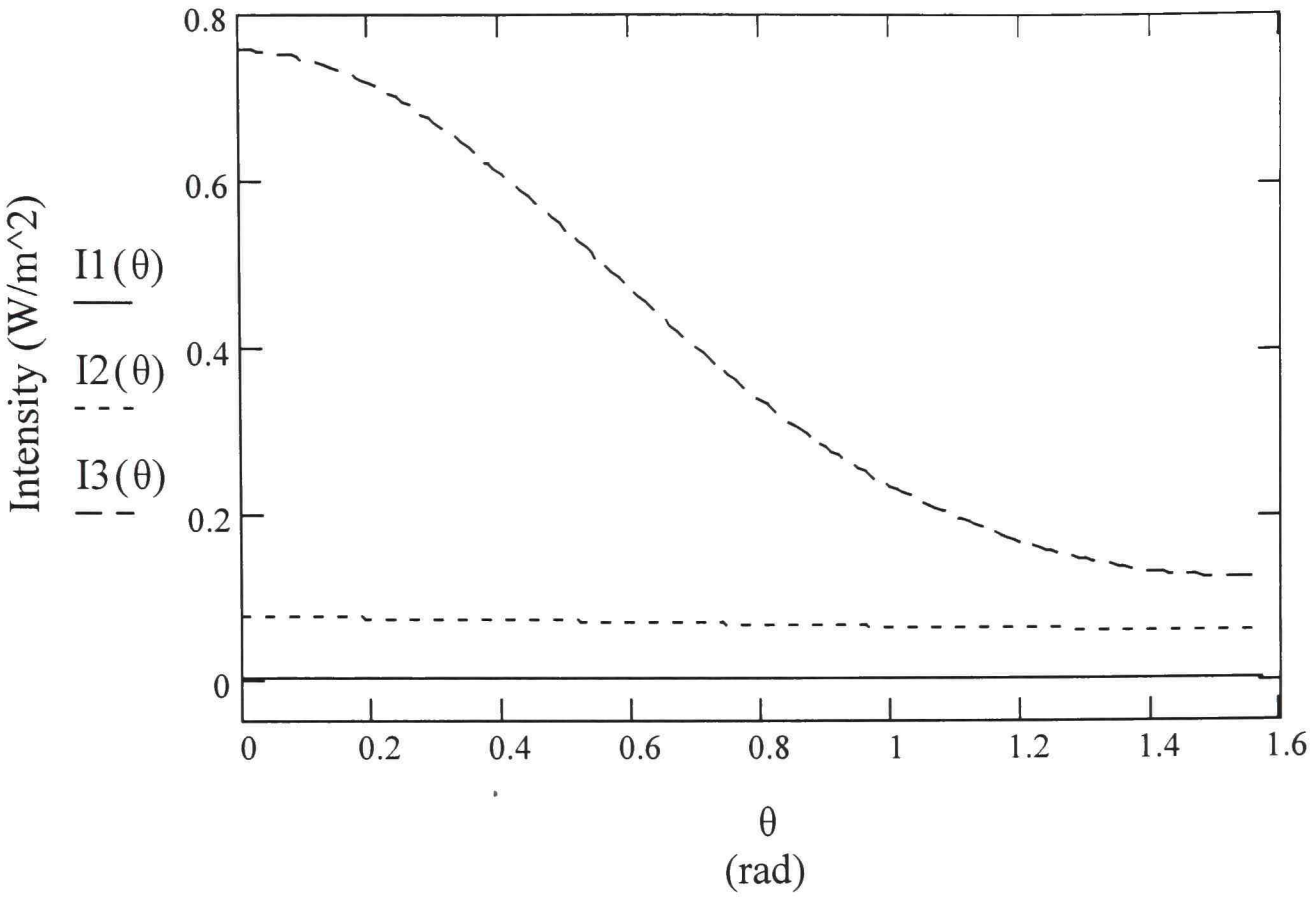

Figure 7.27. Acoustic Intensity versus θ for the First Three Modes of a Simply Supported Circular Plate.

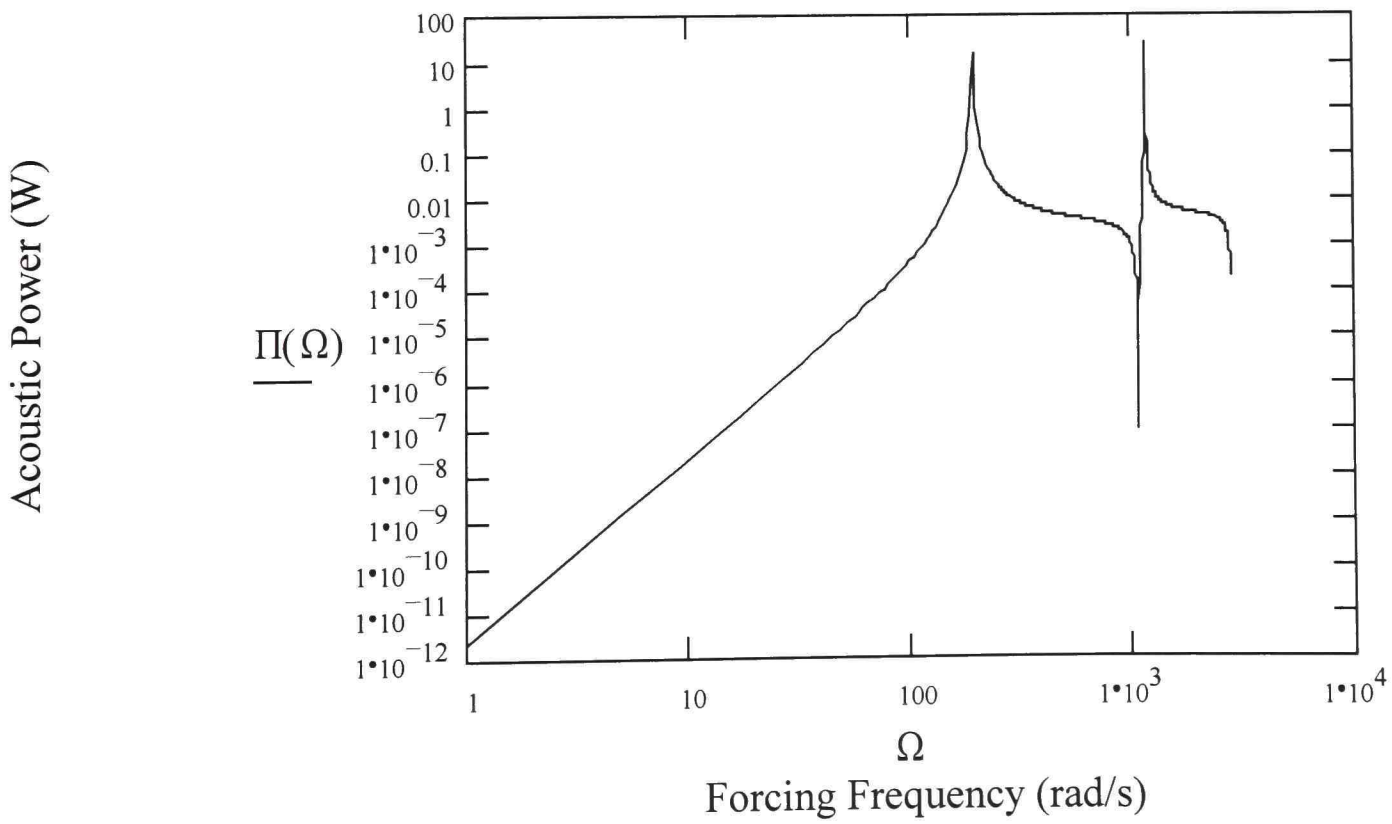

Figure 7.28. Acoustic Power versus Forcing Frequency for a Simply Supported Circular Plate.

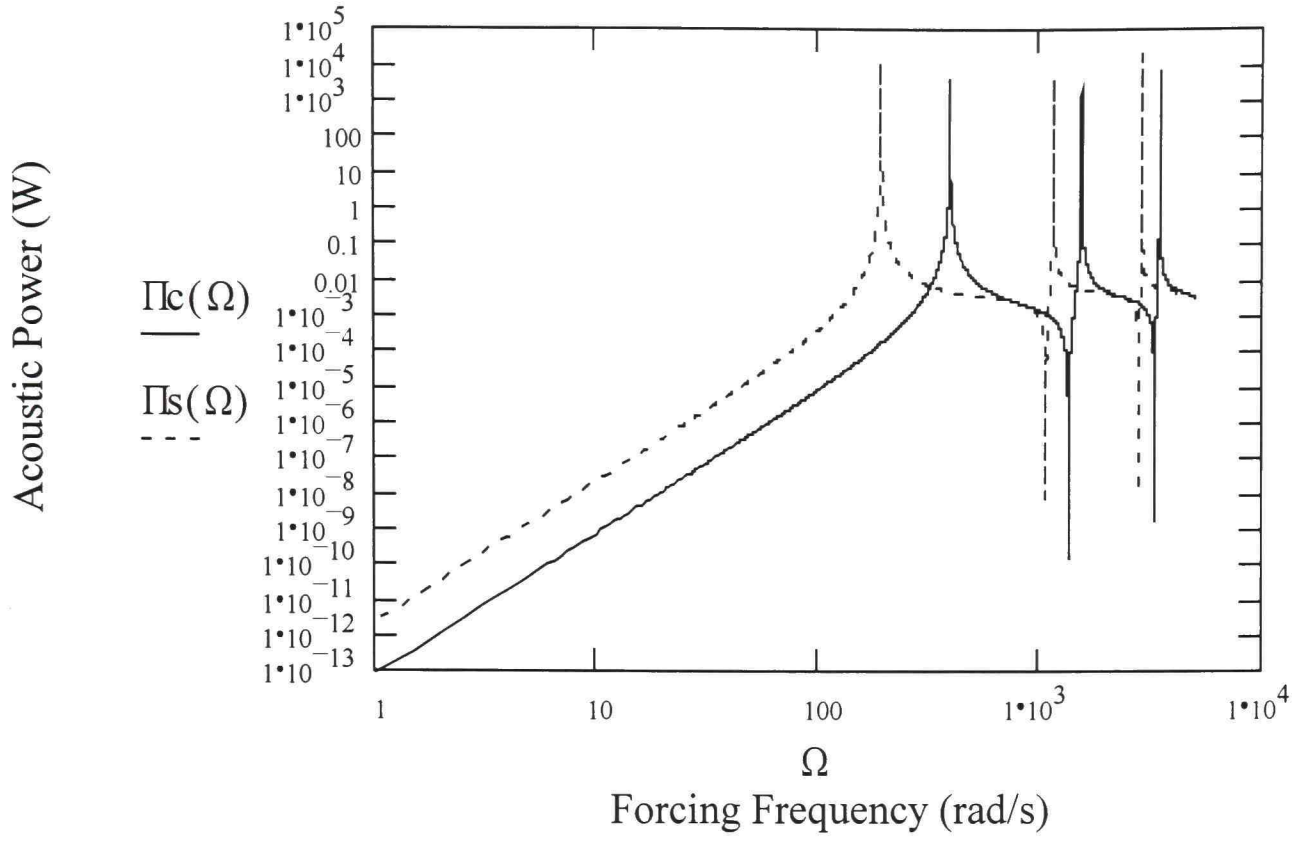

Figure 7.29. Acoustic Power Radiation for the Forced Vibration of a Clamped and a Simply Supported Circular Plate.

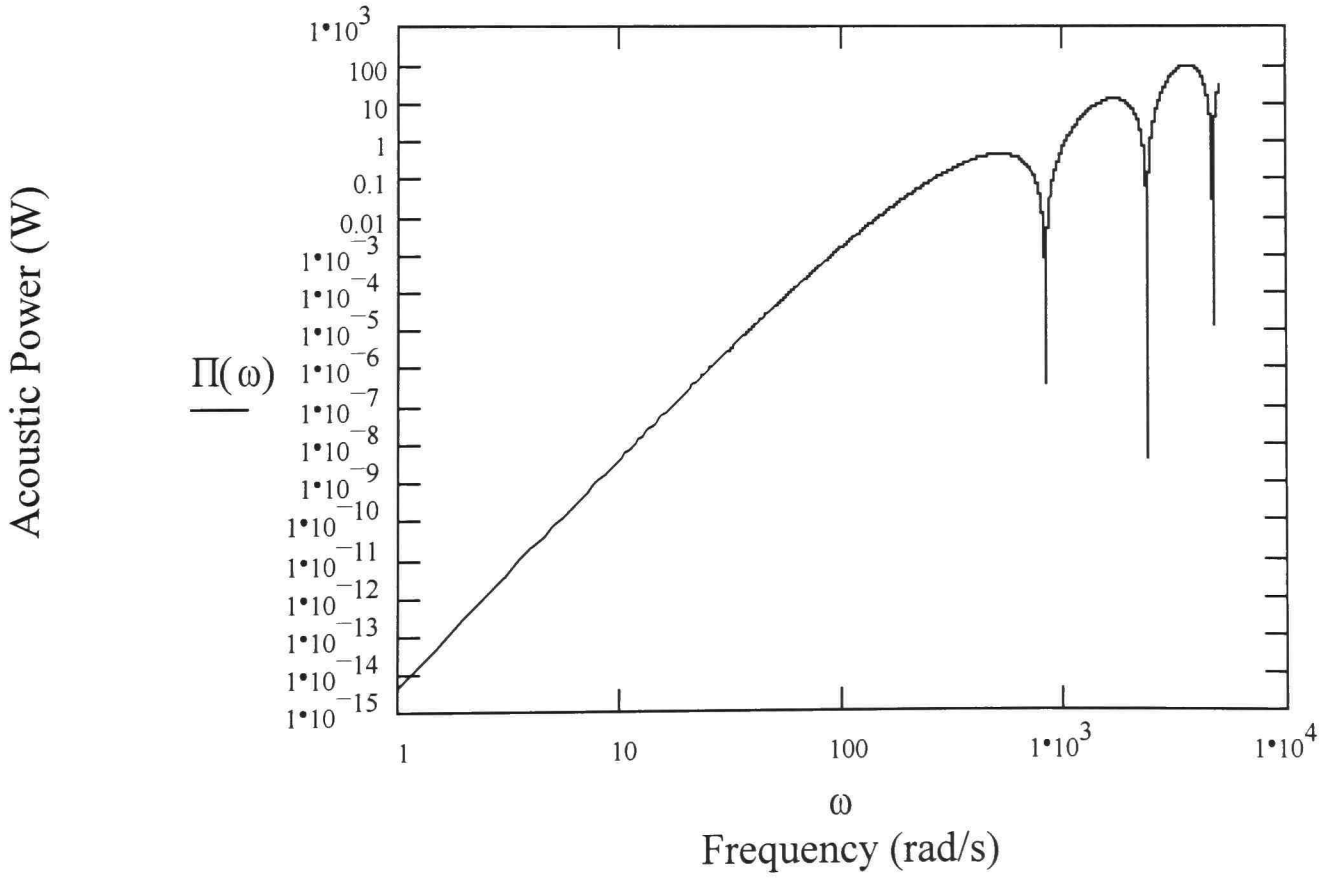

Figure 7.30. Acoustic Power Radiation for the Free Vibration of a Clamped or a Simply Supported Circular Plate.

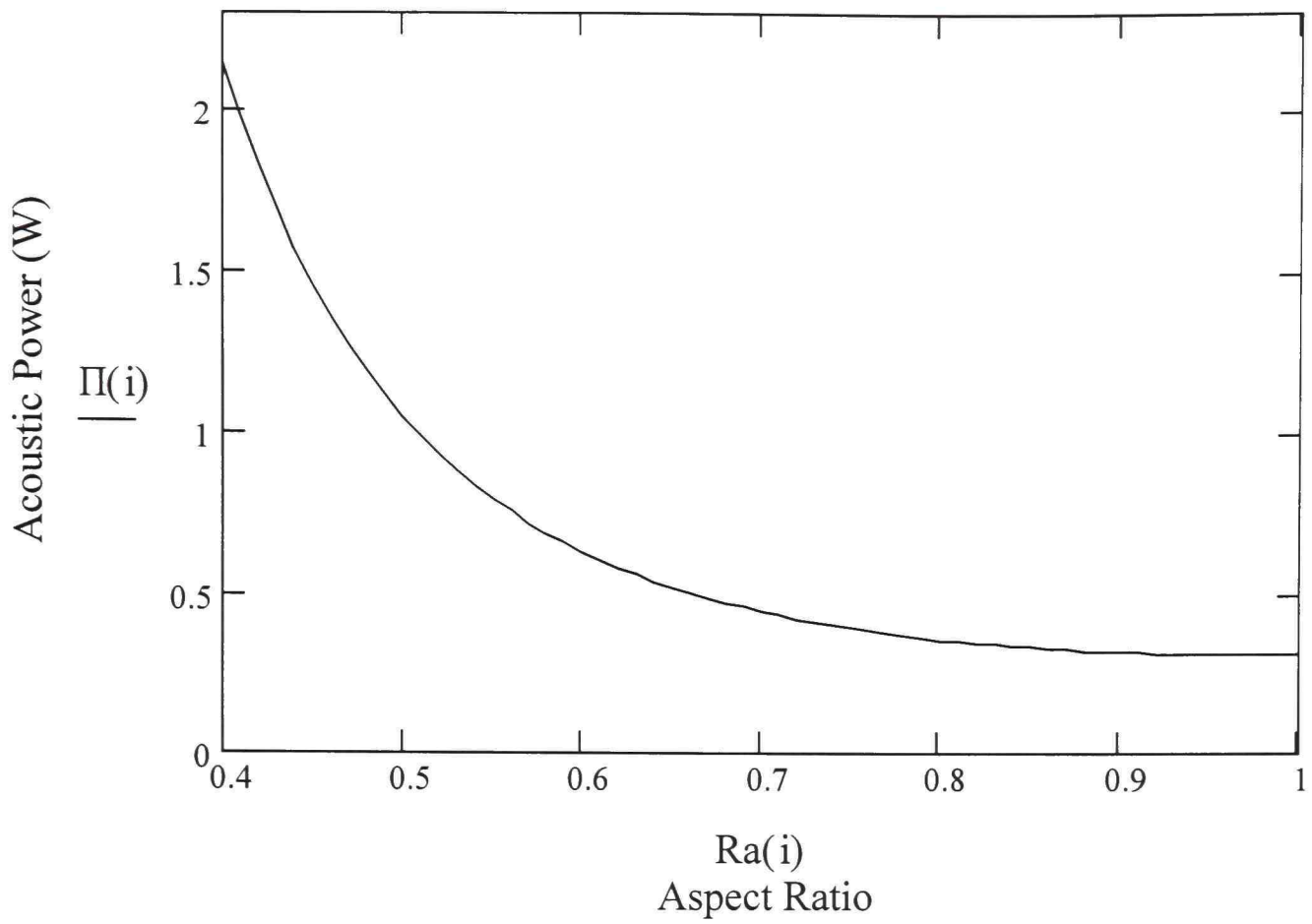

Figure 7.31. Acoustic Power versus Aspect Ratio for a Clamped Elliptical Plate.

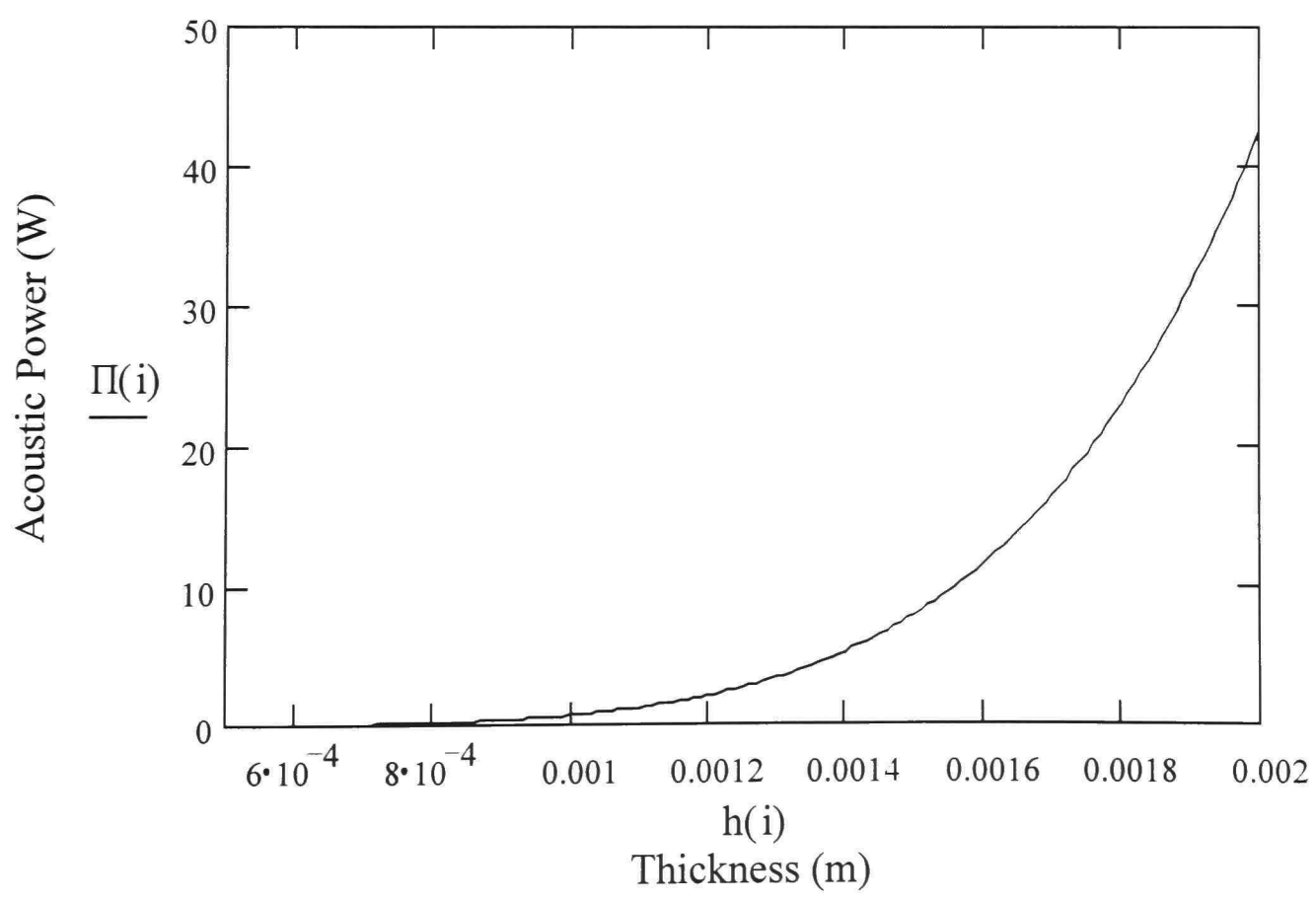

Figure 7.32. Acoustic Power versus Thickness for a Clamped Elliptical Plate.

CHAPTER VIII
CONCLUSIONS AND RECOMMENDATIONS

8.1 Conclusions

The following conclusions can be drawn from this study.

1. Far-field acoustic pressure and acoustic intensity expressions were obtained analytically for most of the source shapes considered. It was seen that the far-field points corresponding to the corners of the pistons have higher acoustic intensity values. Also, in the case of plates, depending on the modes of vibration, very complex intensity distributions are observed.
2. Power series expansions of the acoustic power radiation were obtained by integrating the acoustic intensity over the sources. In this study, this way of solution is called the surface integration approach. It is shown that the results are very reliable for low kL values.
3. The acoustic intensity can also be integrated over an imaginary far-field hemisphere enclosing the source to find the radiated acoustic power. This is called the far-field integration approach. Final power integrals can be evaluated by using the series expansions of their contents; therefore, even better series expansions for the acoustic power can be found. This was shown in the circular piston analysis in this study. To compare the results obtained by the two methods, the final power integral was also integrated numerically providing a basis for accuracy.
4. The acoustic power radiation does not change significantly with shape of pistons having a constant area for low kL values. On the other hand, this is not the case for plates.

8.2 Recommendations

For a further study, the following can be considered.

1. The obtained acoustic intensity results can be integrated numerically for the far-field integration approach; therefore, very accurate acoustic power results for high frequencies of vibration can be obtained.

2. Acoustic radiation from plates with varying thickness, different shapes and boundary conditions can be studied analytically and/or numerically.
3. Acoustics of structures vibrating under general forcing functions can be studied.
4. Radiation from three-dimensional structures, such as shells, can be considered.
5. Problems in which fluid-structure interaction is not negligible can be investigated. An example would be underwater acoustics.
6. The results obtained in this study can be verified experimentally.

REFERENCES

Alper, S. and Magrab, E. B. (1970), "Radiation from the Forced Harmonic Vibrations of a Clamped Circular Plate in an Acoustic Fluid," J. Acoust. Soc. Am., 48(3), 681-691.

Beer, F. P. and Johnston, Jr., E. R. (1992), Mechanics of Materials, McGraw-Hill Inc., London.

Berry, A., Guyader, J.-L., and Nicolas, J. (1990), "A General Formulation for the Sound Radiation from Rectangular, Baffled Plates with Arbitrary Boundary Conditions," J. Acoust. Soc. Am., 88(6), 2792-2802.

Berry, A., Guyader, J.-L., and Nicolas, J. (1992), "Reply to "Comments on 'A general formulation for the sound radiation from rectangular, baffled plates with arbitrary boundary conditions'" [J. Acoust. Soc. Am. 92, 2990 (1992)]," J. Acoust. Soc. Am., 92(5), 2991-2992.

Beyer, R. T. (1999), Sounds of Our Times: Two Hundred Years of Acoustics, Springer-Verlag Inc., New York.

Bhat, R. B. (1985), "Natural Frequencies of Rectangular Plates Using Characteristic Orthogonal Polynomials in Rayleigh-Ritz Method," J. Sound Vib., 102(4), 493-499.

Bhat, R. B., Laura, P. A. A., Gutierrez, R. G., Cortinez, and V. H., Sanzi, H. C. (1990), "Numerical Experiments on the Determination of Natural Frequencies of Transverse Vibrations of Rectangular Plates of Non-Uniform Thickness," J. Sound Vib., 138(2), 205-219.

Chedd, G. (1970), Sound: From Communication to Noise Pollution, Doubleday & Company Inc., Garden City, NY.

Chonan, S. (1978), "Random Vibration of an Elastically Supported Circular Plate with an Elastically Restrained Edge and an Initial Tension," J. Sound Vib., 58(3), 443-454.

Cremer, L., Heckl, M., and Ungar, E. E. (1987), Structure-Borne Sound, Springer-Verlag, Berlin.

Cunefare, K. A. (1991), "The Minimum Multimodal Radiation Efficiency of Baffled Finite Beams," J. Acoust. Soc. Am., 90(5), 2521-2529.

Currey, M. N. and Cunefare, K. A. (1995), "The Radiation Modes of Baffled Finite Plates," J. Acoust. Soc. Am., 98(3), 1570-1580.

Deffayet, C. and Nelson, P. A. (1988), "Active Control of Low-Frequency Harmonic Sound Radiated by a Finite Panel," J. Acoust. Soc. Am., 84(6), 2192-2199.

Dickinson, S. M. and Di Blasio, A. (1986), "On the Use of Orthogonal Polynomials in the Rayleigh-Ritz Method for the Study of the Flexural Vibration and Buckling of Isotropic and Orthotropic Rectangular Plates," J. Sound Vib., 108(1), 51-62.

Fahy, F. J. and Walker, J. G., Edited by (1998), Fundamentals of Noise and Vibration, E & FN Spon, an imprint of Routledge, London.

Ghering, W. L. (1978), Reference Data for Acoustic Noise Control, Ann Arbor Science Publishers, Inc., Ann Arbor, MI.

Hunter, J. L. (1957), Acoustics, Prentice-Hall, Inc., Englewood Cliffs, NJ.

Junger, M. C. and Feit, D. (1972), Sound, Structures, and Their Interaction, The MIT Press, Cambridge, MA.

Kim, C. S. and Dickinson, S. M. (1989), "On the Lateral Vibration of Thin Annular and Circular Composite Plates Subject to Certain Complicating Effects," J. Sound Vib., 130(3), 363-377.

Kinsler, L. E. and Frey, A. R. (1950), Fundamentals of Acoustics, John Wiley & Sons, Inc., New York.

Kompella, K. S. (1994), "Investigation of the Effect of Geometry and Boundary Conditions on Acoustic Power Radiation," M.S. Thesis, Texas Tech Univ., Lubbock.

Lam, K. Y., Liew, K. M., and Chow, S. T. (1992), "Use of Two-Dimensional Orthogonal Polynomials for Vibration Analysis of Circular and Elliptical Plates," J. Sound Vib., 154(2), 261-269.

Laura, P. A. A., Pombo, J. L., and Luisoni, L. E. (1976), "Forced Vibrations of a Circular Plate Elastically Restrained Against Rotation," J. Sound Vib., 45(2), 225-235.

Laura, P. A. A. and Ercoli, L. (1992), "Comments on "A general formulation for the sound radiation from rectangular, baffled plates with arbitrary boundary conditions" [Berry et al., J. Acoust. Soc. Am. 88, 2792-2802 (1990)]," J. Acoust. Soc. Am., 92(5), 2990.

Leissa, A. W. (1967), "Vibration of a Simply Supported Elliptical Plate," J. Sound Vib., 6(1), 145-148.

Leissa, A. W. (1969), Vibration of Plates, NASA SP-160, National Aeronautics and Space Administration, Washington, D. C., MD.

Leissa, A. W. (1978), "A Direct Method for Analyzing the Forced Vibrations of Continuous Systems Having Damping," J. Sound Vib., 56(3), 313-324.

Levine, H. (1984), "On the Short Wave Acoustic Radiation from Planar Panels or Beams of Rectangular Shape," J. Acoust. Soc. Am., 76(2), 608-615.

McLachlan, N. W. (1955), Bessel Functions for Engineers, Oxford University Press, London, England.

McNitt, R. P. (1962), "Free Vibrations of a Clamped Elliptical Plate," J. Aerospace Sci., 29(9), 1124-1125.

Nakayama, I., Nakamura, A., and Takeuchi, R. (1980), "Transient Radiation Field from an Elastic Circular Plate Excited by a Sound Pulse," Acustica, 46, 276-282.

Nayfeh, A. H., Mook, D. T., Lobitz, D. W., and Sridhar, S. (1976), "Vibrations of Nearly Annular and Circular Plates," J. Sound Vib., 47(1), 75-84.

Rahman, Md. K. and Ertas, A. (1994), "Acoustic Power Radiation from a Rectangular Plate with Mixed Boundary Conditions," Thin-Walled Structures, 18, 3-22.

Rettinger, M. (1973), Acoustic Design and Noise Control, Chemical Publishing Co., Inc., New York, NY.

Sato, K. (1972), "Free Flexural Vibrations of an Elliptical Plate with Simply Supported Edge," J. Acoust. Soc. Am., 52(3), 919-922.

Shibaoka, Y. (1956), "On the Transverse Vibration of an Elliptic Plate with Clamped Edge," J. Phys. Soc. Japan, 11(7), 797-803.

Singh, B. and Chakraverty, S. (1992), "Transverse Vibration of Simply Supported Elliptical and Circular Plates Using Boundary Characteristic Orthogonal Polynomials in Two Variables," J. Sound Vib., 152(1), 149-155.

Snyder, S. D. and Tanaka, N. (1995), "Calculating Total Acoustic Power Output Using Modal Radiation Efficiencies," J. Acoust. Soc. Am., 97(3), 1702-1709.

Temkin, S. (1981), Elements of Acoustics, John Wiley & Sons, Inc., New York.

Wallace, C. E. (1972), "Radiation Resistance of a Rectangular Panel," J. Acoust. Soc. Am., 51(3), 946-952.

Warburton, G. B. (1954), "The Vibration of Rectangular Plates," Proc. Inst. Mech. Eng., 168, 371-384.

Williams, E. G. and Maynard, J. D. (1982), "Numerical Evaluation of the Rayleigh Integral for Planar Radiators Using the FFT," J. Acoust. Soc. Am., 72(6), 2020-2030.

Williams, E. G. (1983), "A Series Expansion of the Acoustic Power Radiated from Planar Sources," J. Acoust. Soc. Am., 73(5), 1520-1524.

APPENDIX A
DERIVATIONS OF THE ACOUSTIC INTENSITY AND THE ACOUSTIC POWER FORMULAE GIVEN IN CHAPTER II

It is evident that as compressions pass through an acoustic medium, then there is a transfer of energy from the vibrating source to the space above it. The time-averaged rate at which this energy is transferred is the acoustic intensity. This is defined as

$$I(x) = \frac{1}{T}\int_{-T/2}^{T/2} p(x,t)u(x,t)dt\,, \tag{A.1}$$

where T is the period of one cycle of harmonic motion, and x is used to denote the position-dependency of the quantities. For plane progressive waves, $p(x,t)$ and $u(x,t)$ are simply related by

$$u(x,t) = \frac{p(x,t)}{\rho c}, \tag{A.2}$$

and the pressure can be written as

$$p(x,t) = \mathrm{Re}\left[p(x)\exp(-i\omega t)\right], \tag{A.3}$$

where $p(x)$ is generally complex. Substituting $p_R(x) + ip_I(x)$ for $p(x)$, expanding the exponential term by using Euler's formula, and simplifying gives

$$p(x,t) = p_R(x)\cos(\omega t) + p_I(x)\sin(\omega t)\,. \tag{A.4}$$

Plugging $u(x,t)$ given by Eq. (A.2) into Eq. (A.1), and then using $p(x,t)$ given by Eq. (A.4) yields

$$I(x) = \frac{1}{\rho c T}\int_{-T/2}^{T/2}\left[p_R(x)\cos(\omega t) + p_I(x)\sin(\omega t)\right]^2 dt\,. \tag{A.5}$$

After integrating and simplifying, one can get

$$I(x) = \frac{\left[{p_R}^2(x) + {p_I}^2(x)\right]}{2\rho c}\,. \tag{A.6}$$

As can be noticed, the numerator of Eq. (A.6) is the square of the magnitude of $p(x)$. Therefore, the acoustic intensity becomes

$$I(x) = \frac{|p(x)|^2}{2\rho c}, \tag{A.7}$$

which is the same as Eq. (2.10). It is important to note that, $|p(x)|$ in Eq. (A.7) is the magnitude of the far-field pressure expression without $\exp(-i\omega t)$ term.

In general, the pressure and the velocity are not simply related as given in Eq. (A.2); therefore, it is useful to obtain the acoustic intensity in terms of both $p(x)$ and $u(x)$. Similar to Eq. (A.3), the velocity can be written as

$$u(x,t) = \mathrm{Re}\left[u(x)\exp(-i\omega t)\right] = u_R(x)\cos(\omega t) + u_I(x)\sin(\omega t). \tag{A.8}$$

Substituting this velocity and the pressure given by Eq. (A.4) into Eq. (A.1), integrating, and simplifying gives

$$I(x) = \frac{\left[p_R(x)u_R(x) + p_I(x)u_I(x)\right]}{2}, \tag{A.9}$$

and, it can be seen that, this can also be expressed as

$$I(x) = \frac{1}{2}\mathrm{Re}\left[p^*(x)u(x)\right] = \frac{1}{2}\mathrm{Re}\left[p(x)u^*(x)\right]. \tag{A.10}$$

Integrating the given acoustic intensity over any surface of convenience results in the acoustic power formula

$$\Pi = \frac{1}{2}\mathrm{Re}\left(\int_S pu^* dS\right), \tag{A.11}$$

which is the same as Eq. (2.12).

The interested reader is referred to the first chapter of Fahy and Walker (1998) for this analysis and some other introductory topics.

APPENDIX B
SIMPLIFIED FAR-FIELD ACOUSTIC PRESSURE AND ACOUSTIC INTENSITY EXPRESSIONS FOR SIMPLY SUPPORTED RECTANGULAR PLATES

For even and odd values of m and n, the far-field pressure distribution given by Eq. (4.23) simplify further. These simplified forms are given as

for $(m,n)=(\text{even},\text{even})$:

$$p(R,\phi,\theta,t)=-i\frac{\rho\omega^2 W_0 A_p \exp\left[i(-\omega t+kR)\right]}{R} \times\frac{2\pi(m-1)(n-1)\cos(\psi_1 a/2)\cos(\psi_2 b/2)}{\left\{(\psi_1 a)^2-\left[\pi(m-1)\right]^2\right\}\left\{(\psi_2 b)^2-\left[\pi(n-1)\right]^2\right\}}, \tag{B.1}$$

for $(m,n)=(\text{even},\text{odd})$:

$$p(R,\phi,\theta,t)=\frac{\rho\omega^2 W_0 A_p \exp\left[i(-\omega t+kR)\right]}{R} \times\frac{2\pi(m-1)(n-1)\cos(\psi_1 a/2)\sin(\psi_2 b/2)}{\left\{(\psi_1 a)^2-\left[\pi(m-1)\right]^2\right\}\left\{(\psi_2 b)^2-\left[\pi(n-1)\right]^2\right\}}, \tag{B.2}$$

for $(m,n)=(\text{odd},\text{even})$:

$$p(R,\phi,\theta,t)=\frac{\rho\omega^2 W_0 A_p \exp\left[i(-\omega t+kR)\right]}{R} \times\frac{2\pi(m-1)(n-1)\sin(\psi_1 a/2)\cos(\psi_2 b/2)}{\left\{(\psi_1 a)^2-\left[\pi(m-1)\right]^2\right\}\left\{(\psi_2 b)^2-\left[\pi(n-1)\right]^2\right\}}, \tag{B.3}$$

and for $(m,n)=(\text{odd},\text{odd})$:

$$p(R,\phi,\theta,t)=i\frac{\rho\omega^2 W_0 A_p \exp\left[i(-\omega t+kR)\right]}{R} \times\frac{2\pi(m-1)(n-1)\sin(\psi_1 a/2)\sin(\psi_2 b/2)}{\left\{(\psi_1 a)^2-\left[\pi(m-1)\right]^2\right\}\left\{(\psi_2 b)^2-\left[\pi(n-1)\right]^2\right\}}. \tag{B.4}$$

Substituting the magnitudes of the given pressure expressions into Eq. (2.10), the acoustic intensity expressions can be obtained as

for $(m,n)=(\text{even},\text{even})$:

$$I(R,\phi,\theta)=\frac{2\rho\omega^4 W_0^{\,2} A_p^{\,2}}{R^2 c}\left\{\frac{\pi(m-1)(n-1)\cos(\psi_1 a/2)\cos(\psi_2 b/2)}{\left\{(\psi_1 a)^2-\left[\pi(m-1)\right]^2\right\}\left\{(\psi_2 b)^2-\left[\pi(n-1)\right]^2\right\}}\right\}^2, \quad \text{(B.5)}$$

for $(m,n)=(\text{even},\text{odd})$:

$$I(R,\phi,\theta)=\frac{2\rho\omega^4 W_0^{\,2} A_p^{\,2}}{R^2 c}\left\{\frac{\pi(m-1)(n-1)\cos(\psi_1 a/2)\sin(\psi_2 b/2)}{\left\{(\psi_1 a)^2-\left[\pi(m-1)\right]^2\right\}\left\{(\psi_2 b)^2-\left[\pi(n-1)\right]^2\right\}}\right\}^2, \quad \text{(B.6)}$$

for $(m,n)=(\text{odd},\text{even})$:

$$I(R,\phi,\theta)=\frac{2\rho\omega^4 W_0^{\,2} A_p^{\,2}}{R^2 c}\left\{\frac{\pi(m-1)(n-1)\sin(\psi_1 a/2)\cos(\psi_2 b/2)}{\left\{(\psi_1 a)^2-\left[\pi(m-1)\right]^2\right\}\left\{(\psi_2 b)^2-\left[\pi(n-1)\right]^2\right\}}\right\}^2, \quad \text{(B.7)}$$

and for $(m,n)=(\text{odd},\text{odd})$:

$$I(R,\phi,\theta)=\frac{2\rho\omega^4 W_0^{\,2} A_p^{\,2}}{R^2 c}\left\{\frac{\pi(m-1)(n-1)\sin(\psi_1 a/2)\sin(\psi_2 b/2)}{\left\{(\psi_1 a)^2-\left[\pi(m-1)\right]^2\right\}\left\{(\psi_2 b)^2-\left[\pi(n-1)\right]^2\right\}}\right\}^2. \quad \text{(B.8)}$$

In all of these equations, ψ_1 and ψ_2 are given by Eqs. (3.6) and (3.7), respectively.

APPENDIX C
SIMPLIFIED ACOUSTIC POWER EXPRESSIONS FOR SIMPLY SUPPORTED RECTANGULAR PLATES

The simplified acoustic power terms are

for $(m,n)=(\text{even},\text{even})$:

$$\Pi_0 = \frac{\rho\omega^4 W_0^{\,2} A_p^{\,2}}{4\pi c}\left\{\frac{16}{\pi^4(m-1)^2(n-1)^2}\right\}, \tag{C.1}$$

$$\Pi_1 = \frac{\rho\omega^4 W_0^{\,2} A_p^{\,2}}{4\pi c}\left\{-\frac{4\left\{1+R_a^{\,2}-\frac{8}{\pi^2}\left[\left(\frac{1}{m-1}\right)^2+\left(\frac{R_a}{n-1}\right)^2\right]\right\}}{3\pi^4(m-1)^2(n-1)^2}\right\}(ka)^2, \tag{C.2}$$

for $(m,n)=(\text{even},\text{odd})$:

$$\Pi_0 = 0, \tag{C.3}$$

$$\Pi_1 = \frac{\rho\omega^4 W_0^{\,2} A_p^{\,2}}{4\pi c}\left[-\frac{4R_a^{\,2}}{3\pi^4(m-1)^2(n-1)^2}\right](ka)^2, \tag{C.4}$$

for $(m,n)=(\text{odd},\text{even})$:

$$\Pi_0 = 0, \tag{C.5}$$

$$\Pi_1 = \frac{\rho\omega^4 W_0^{\,2} A_p^{\,2}}{4\pi c}\left[-\frac{4}{3\pi^4(m-1)^2(n-1)^2}\right](ka)^2, \tag{C.6}$$

and for $(m,n)=(\text{odd},\text{odd})$:

$$\Pi_0 = 0, \tag{C.7}$$

$$\Pi_1 = 0. \tag{C.8}$$

In these equations, R_a is the aspect ratio given by Eq. (4.7).

The total approximate acoustic power for each case can be obtained by adding Π_0 and Π_1 terms.

APPENDIX D
FAR-FIELD ACOUSTIC PRESSURE EXPRESSIONS FOR RECTANGULAR PLATES WITH TWO OPPOSING EDGES CLAMPED AND OTHER EDGES SIMPLY SUPPORTED

The far-field pressure expressions are

for $(m,n)=(\text{even},\text{even})$:

$$p(R,\phi,\theta,t)=i\frac{\rho\omega^2 W_0 A_p \exp\left[i(-\omega t+kR)\right]}{R}\frac{(n-1)\cos\left[(\psi_2 b)/2\right]}{\left\{(\psi_2 b)^2-\left[\pi(n-1)\right]^2\right\}}$$
$$\times\left\{\begin{array}{l}\dfrac{(\psi_1 a/2)\sin(\psi_1 a/2)\cos(\gamma/2)-(\gamma/2)\sin(\gamma/2)\cos(\psi_1 a/2)}{\left[(\psi_1 a/2)^2-(\gamma/2)^2\right]}\\ +K\dfrac{(\psi_1 a/2)\sin(\psi_1 a/2)\cosh(\gamma/2)+(\gamma/2)\sinh(\gamma/2)\cos(\psi_1 a/2)}{\left[(\psi_1 a/2)^2+(\gamma/2)^2\right]}\end{array}\right\}, \quad \text{(D.1)}$$

for $(m,n)=(\text{even},\text{odd})$:

$$p(R,\phi,\theta,t)=-\frac{\rho\omega^2 W_0 A_p \exp\left[i(-\omega t+kR)\right]}{R}\frac{(n-1)\sin\left[(\psi_2 b)/2\right]}{\left\{(\psi_2 b)^2-\left[\pi(n-1)\right]^2\right\}}$$
$$\times\left\{\begin{array}{l}\dfrac{(\psi_1 a/2)\sin(\psi_1 a/2)\cos(\gamma/2)-(\gamma/2)\sin(\gamma/2)\cos(\psi_1 a/2)}{\left[(\psi_1 a/2)^2-(\gamma/2)^2\right]}\\ +K\dfrac{(\psi_1 a/2)\sin(\psi_1 a/2)\cosh(\gamma/2)+(\gamma/2)\sinh(\gamma/2)\cos(\psi_1 a/2)}{\left[(\psi_1 a/2)^2+(\gamma/2)^2\right]}\end{array}\right\}, \quad \text{(D.2)}$$

for $(m,n)=(\text{odd},\text{even})$:

$$p(R,\phi,\theta,t)=-\frac{\rho\omega^2 W_0 A_p \exp\left[i(-\omega t+kR)\right]}{R}\frac{(n-1)\cos\left[(\psi_2 b)/2\right]}{\left\{(\psi_2 b)^2-\left[\pi(n-1)\right]^2\right\}}$$

$$\times\left\{\begin{array}{l}\dfrac{(\psi_1 a/2)\cos(\psi_1 a/2)\sin(\gamma'/2)-(\gamma'/2)\cos(\gamma'/2)\sin(\psi_1 a/2)}{\left[(\psi_1 a/2)^2-(\gamma'/2)^2\right]}\\ +K'\dfrac{-(\psi_1 a/2)\cos(\psi_1 a/2)\sinh(\gamma'/2)+(\gamma'/2)\cosh(\gamma'/2)\sin(\psi_1 a/2)}{\left[(\psi_1 a/2)^2+(\gamma'/2)^2\right]}\end{array}\right\}, \tag{D.3}$$

and for $(m,n)=(\text{odd},\text{odd})$:

$$p(R,\phi,\theta,t)=-i\frac{\rho\omega^2 W_0 A_p \exp\left[i(-\omega t+kR)\right]}{R}\frac{(n-1)\sin\left[(\psi_2 b)/2\right]}{\left\{(\psi_2 b)^2-\left[\pi(n-1)\right]^2\right\}}$$

$$\times\left\{\begin{array}{l}\dfrac{(\psi_1 a/2)\cos(\psi_1 a/2)\sin(\gamma'/2)-(\gamma'/2)\cos(\gamma'/2)\sin(\psi_1 a/2)}{\left[(\psi_1 a/2)^2-(\gamma'/2)^2\right]}\\ +K'\dfrac{-(\psi_1 a/2)\cos(\psi_1 a/2)\sinh(\gamma'/2)+(\gamma'/2)\cosh(\gamma'/2)\sin(\psi_1 a/2)}{\left[(\psi_1 a/2)^2+(\gamma'/2)^2\right]}\end{array}\right\}. \tag{D.4}$$

Again, ψ_1 and ψ_2 in these equations are given by Eqs. (3.6) and (3.7).

APPENDIX E

FAR-FIELD ACOUSTIC PRESSURE EXPRESSIONS FOR RECTANGULAR PLATES WITH TWO NEIGHBORING EDGES CLAMPED AND OTHER EDGES SIMPLY SUPPORTED

The far-field pressure expressions are given by

i. if the plate is rectangular, or, if it is square and $m = n$

$$p(R,\phi,\theta,t) = -i\frac{2\rho\omega^2 W_0 A_p \exp[i(-\omega t + kR)]}{\pi R}\frac{\exp[i(\psi_1 a + \psi_2 b)/2]}{\left[(2\psi_1 a)^4 - \gamma'^4\right]\left[(2\psi_2 b)^4 - \varepsilon'^4\right]}$$

$$\times\begin{Bmatrix} \gamma'\exp(-i\psi_1 a)\left[\gamma'^2(1-K') + (2\psi_1 a)^2(1+K')\right] \\ -K'\left[(2\psi_1 a)^2 - \gamma'^2\right]\left[\gamma'\cosh(\gamma'/2) - i(2\psi_1 a)\sinh(\gamma'/2)\right] \\ -\left[(2\psi_1 a)^2 + \gamma'^2\right]\left[\gamma'\cos(\gamma'/2) - i(2\psi_1 a)\sin(\gamma'/2)\right] \end{Bmatrix} \qquad \text{(E.1)}$$

$$\times\begin{Bmatrix} \varepsilon'\exp(-i\psi_2 b)\left[\varepsilon'^2(1-C') + (2\psi_2 b)^2(1+C')\right] \\ -C'\left[(2\psi_2 b)^2 - \varepsilon'^2\right]\left[\varepsilon'\cosh(\varepsilon'/2) - i(2\psi_2 b)\sinh(\varepsilon'/2)\right] \\ -\left[(2\psi_2 b)^2 + \varepsilon'^2\right]\left[\varepsilon'\cos(\varepsilon'/2) - i(2\psi_2 b)\sin(\varepsilon'/2)\right] \end{Bmatrix},$$

for a square plate with $m = n$, b in this expression can be replaced with a, because for a square plate they are the same;

ii. if it is square and $m \neq n$

$$
\begin{aligned}
p(R,\phi,\theta,t) = -i\frac{2\rho\omega^2 W_0 A_p \exp\left[i(-\omega t + kR)\right]}{\pi R}\frac{\exp\left[i(\psi_1+\psi_2)a/2\right]}{\left[(2\psi_1 a)^4 - \gamma'^4\right]\left[(2\psi_2 a)^4 - \varepsilon'^4\right]} \\
\times\begin{Bmatrix}
\gamma'\exp(-i\psi_1 a)\left[\gamma'^2(1-K') + (2\psi_1 a)^2(1+K')\right] \\
-K'\left[(2\psi_1 a)^2 - \gamma'^2\right]\left[\gamma'\cosh(\gamma'/2) - i(2\psi_1 a)\sinh(\gamma'/2)\right] \\
-\left[(2\psi_1 a)^2 + \gamma'^2\right]\left[\gamma'\cos(\gamma'/2) - i(2\psi_1 a)\sin(\gamma'/2)\right]
\end{Bmatrix} \\
\times\begin{Bmatrix}
\varepsilon'\exp(-i\psi_2 a)\left[\varepsilon'^2(1-C') + (2\psi_2 a)^2(1+C')\right] \\
-C'\left[(2\psi_2 a)^2 - \varepsilon'^2\right]\left[\varepsilon'\cosh(\varepsilon'/2) - i(2\psi_2 a)\sinh(\varepsilon'/2)\right] \\
-\left[(2\psi_2 a)^2 + \varepsilon'^2\right]\left[\varepsilon'\cos(\varepsilon'/2) - i(2\psi_2 a)\sin(\varepsilon'/2)\right]
\end{Bmatrix} \\
\pm i\frac{2\rho\omega^2 W_0 A_p \exp\left[i(-\omega t + kR)\right]}{\pi R}\frac{\exp\left[i(\psi_1+\psi_2)a/2\right]}{\left[(2\psi_1 a)^4 - \gamma'^4\right]\left[(2\psi_2 a)^4 - \varepsilon'^4\right]} \\
\times\begin{Bmatrix}
\varepsilon'\exp(-i\psi_1 a)\left[\varepsilon'^2(1-C') + (2\psi_1 a)^2(1+C')\right] \\
-C'\left[(2\psi_1 a)^2 - \varepsilon'^2\right]\left[\varepsilon'\cosh(\varepsilon'/2) - i(2\psi_1 a)\sinh(\varepsilon'/2)\right] \\
-\left[(2\psi_1 a)^2 + \varepsilon'^2\right]\left[\varepsilon'\cos(\varepsilon'/2) - i(2\psi_1 a)\sin(\varepsilon'/2)\right]
\end{Bmatrix} \\
\times\begin{Bmatrix}
\gamma'\exp(-i\psi_2 a)\left[\gamma'^2(1-K') + (2\psi_2 a)^2(1+K')\right] \\
-K'\left[(2\psi_2 a)^2 - \gamma'^2\right]\left[\gamma'\cosh(\gamma'/2) - i(2\psi_2 a)\sinh(\gamma'/2)\right] \\
-\left[(2\psi_2 a)^2 + \gamma'^2\right]\left[\gamma'\cos(\gamma'/2) - i(2\psi_2 a)\sin(\gamma'/2)\right]
\end{Bmatrix},
\end{aligned}
\tag{E.2}
$$

where ψ_1 and ψ_2 are given by Eqs. (3.6) and (3.7). Plus sign in the middle of Eq. (E.2) refers to the mode $m/n - n/m$ while minus sign refers to the mode $m/n + n/m$ of the plate.

APPENDIX F
FAR-FIELD ACOUSTIC PRESSURE EXPRESSIONS FOR RECTANGULAR PLATES WITH ONE SIMPLY SUPPORTED AND THREE CLAMPED EDGES

The far-field pressure expressions are

for even n:

$$p(R,\phi,\theta,t) = -i\frac{\rho\omega^2 W_0 A_p \exp\left[i(-\omega t + kR)\right]}{\pi R}\frac{\exp\left[i(\psi_1 a/2)\right]}{\left[(2\psi_1 a)^4 - \gamma'^4\right]}$$
$$\times\left\{\begin{array}{l}\gamma'\exp(-i\psi_1 a)\left[\gamma'^2(1-K')+(2\psi_1 a)^2(1+K')\right]\\ -K'\left[(2\psi_1 a)^2-\gamma'^2\right]\left[\gamma'\cosh(\gamma'/2)-i(2\psi_1 a)\sinh(\gamma'/2)\right]\\ -\left[(2\psi_1 a)^2+\gamma'^2\right]\left[\gamma'\cos(\gamma'/2)-i(2\psi_1 a)\sin(\gamma'/2)\right]\end{array}\right\} \qquad \text{(F.1)}$$
$$\times\left\{\begin{array}{l}\dfrac{(\psi_2 b/2)\sin(\psi_2 b/2)\cos(\varepsilon/2)-(\varepsilon/2)\sin(\varepsilon/2)\cos(\psi_2 b/2)}{\left[(\psi_2 b/2)^2-(\varepsilon/2)^2\right]}\\ +C\dfrac{(\psi_2 b/2)\sin(\psi_2 b/2)\cosh(\varepsilon/2)+(\varepsilon/2)\sinh(\varepsilon/2)\cos(\psi_2 b/2)}{\left[(\psi_2 b/2)^2+(\varepsilon/2)^2\right]}\end{array}\right\},$$

for odd n:

$$p(R,\phi,\theta,t) = \frac{\rho\omega^2 W_0 A_p \exp\left[i(-\omega t + kR)\right]}{\pi R}\frac{\exp\left[i(\psi_1 a/2)\right]}{\left[(2\psi_1 a)^4 - \gamma'^4\right]}$$
$$\times\left\{\begin{array}{l}\gamma'\exp(-i\psi_1 a)\left[\gamma'^2(1-K')+(2\psi_1 a)^2(1+K')\right]\\ -K'\left[(2\psi_1 a)^2-\gamma'^2\right]\left[\gamma'\cosh(\gamma'/2)-i(2\psi_1 a)\sinh(\gamma'/2)\right]\\ -\left[(2\psi_1 a)^2+\gamma'^2\right]\left[\gamma'\cos(\gamma'/2)-i(2\psi_1 a)\sin(\gamma'/2)\right]\end{array}\right\} \qquad \text{(F.2)}$$
$$\times\left\{\begin{array}{l}\dfrac{(\psi_2 b/2)\cos(\psi_2 b/2)\sin(\varepsilon'/2)-(\varepsilon'/2)\cos(\varepsilon'/2)\sin(\psi_2 b/2)}{\left[(\psi_2 b/2)^2-(\varepsilon'/2)^2\right]}\\ +C'\dfrac{-(\psi_2 b/2)\cos(\psi_2 b/2)\sinh(\varepsilon'/2)+(\varepsilon'/2)\cosh(\varepsilon'/2)\sin(\psi_2 b/2)}{\left[(\psi_2 b/2)^2+(\varepsilon'/2)^2\right]}\end{array}\right\}.$$

APPENDIX G

FAR-FIELD ACOUSTIC PRESSURE EXPRESSIONS FOR CLAMPED RECTANGULAR PLATES

The pressure expressions are

i. if the plate is rectangular, or, if it is square and $m-n \neq \pm 2,\ \pm 4,\ \pm 6,\ldots$

for $(m,n)=(\text{even},\text{even})$:

$$p(R,\phi,\theta,t)=-i\frac{\rho\omega^2 W_0 A_p \exp\left[i(-\omega t+kR)\right]}{2\pi R}$$
$$\times\left\{\begin{array}{l}\dfrac{(\psi_1 a/2)\sin(\psi_1 a/2)\cos(\gamma/2)-(\gamma/2)\sin(\gamma/2)\cos(\psi_1 a/2)}{\left[(\psi_1 a/2)^2-(\gamma/2)^2\right]}\\ +K\dfrac{(\psi_1 a/2)\sin(\psi_1 a/2)\cosh(\gamma/2)+(\gamma/2)\sinh(\gamma/2)\cos(\psi_1 a/2)}{\left[(\psi_1 a/2)^2+(\gamma/2)^2\right]}\end{array}\right\}$$
$$\times\left\{\begin{array}{l}\dfrac{(\psi_2 b/2)\sin(\psi_2 b/2)\cos(\varepsilon/2)-(\varepsilon/2)\sin(\varepsilon/2)\cos(\psi_2 b/2)}{\left[(\psi_2 b/2)^2-(\varepsilon/2)^2\right]}\\ +C\dfrac{(\psi_2 b/2)\sin(\psi_2 b/2)\cosh(\varepsilon/2)+(\varepsilon/2)\sinh(\varepsilon/2)\cos(\psi_2 b/2)}{\left[(\psi_2 b/2)^2+(\varepsilon/2)^2\right]}\end{array}\right\}, \qquad \text{(G.1)}$$

for $(m,n)=(\text{even},\text{odd})$:

$$p(R,\phi,\theta,t)=\frac{\rho\omega^2 W_0 A_p \exp\left[i(-\omega t+kR)\right]}{2\pi R}$$
$$\times\left\{\begin{array}{l}\dfrac{(\psi_1 a/2)\sin(\psi_1 a/2)\cos(\gamma/2)-(\gamma/2)\sin(\gamma/2)\cos(\psi_1 a/2)}{\left[(\psi_1 a/2)^2-(\gamma/2)^2\right]}\\ +K\dfrac{(\psi_1 a/2)\sin(\psi_1 a/2)\cosh(\gamma/2)+(\gamma/2)\sinh(\gamma/2)\cos(\psi_1 a/2)}{\left[(\psi_1 a/2)^2+(\gamma/2)^2\right]}\end{array}\right\}$$
$$\times\left\{\begin{array}{l}\dfrac{(\psi_2 b/2)\cos(\psi_2 b/2)\sin(\varepsilon'/2)-(\varepsilon'/2)\cos(\varepsilon'/2)\sin(\psi_2 b/2)}{\left[(\psi_2 b/2)^2-(\varepsilon'/2)^2\right]}\\ +C'\dfrac{-(\psi_2 b/2)\cos(\psi_2 b/2)\sinh(\varepsilon'/2)+(\varepsilon'/2)\cosh(\varepsilon'/2)\sin(\psi_2 b/2)}{\left[(\psi_2 b/2)^2+(\varepsilon'/2)^2\right]}\end{array}\right\}, \qquad \text{(G.2)}$$

for $(m,n)=(\text{odd},\text{even})$:

$$p(R,\phi,\theta,t)=\frac{\rho\omega^2 W_0 A_p \exp\left[i(-\omega t+kR)\right]}{2\pi R}$$
$$\times\left\{\begin{array}{l}\dfrac{(\psi_1 a/2)\cos(\psi_1 a/2)\sin(\gamma'/2)-(\gamma'/2)\cos(\gamma'/2)\sin(\psi_1 a/2)}{\left[(\psi_1 a/2)^2-(\gamma'/2)^2\right]}\\ +K'\dfrac{-(\psi_1 a/2)\cos(\psi_1 a/2)\sinh(\gamma'/2)+(\gamma'/2)\cosh(\gamma'/2)\sin(\psi_1 a/2)}{\left[(\psi_1 a/2)^2+(\gamma'/2)^2\right]}\end{array}\right\}$$
$$\times\left\{\begin{array}{l}\dfrac{(\psi_2 b/2)\sin(\psi_2 b/2)\cos(\varepsilon/2)-(\varepsilon/2)\sin(\varepsilon/2)\cos(\psi_2 b/2)}{\left[(\psi_2 b/2)^2-(\varepsilon/2)^2\right]}\\ +C\dfrac{(\psi_2 b/2)\sin(\psi_2 b/2)\cosh(\varepsilon/2)+(\varepsilon/2)\sinh(\varepsilon/2)\cos(\psi_2 b/2)}{\left[(\psi_2 b/2)^2+(\varepsilon/2)^2\right]}\end{array}\right\},\qquad\text{(G.3)}$$

for $(m,n)=(\text{odd},\text{odd})$:

$$p(R,\phi,\theta,t)=i\frac{\rho\omega^2 W_0 A_p \exp\left[i(-\omega t+kR)\right]}{2\pi R}$$
$$\times\left\{\begin{array}{l}\dfrac{(\psi_1 a/2)\cos(\psi_1 a/2)\sin(\gamma'/2)-(\gamma'/2)\cos(\gamma'/2)\sin(\psi_1 a/2)}{\left[(\psi_1 a/2)^2-(\gamma'/2)^2\right]}\\ +K'\dfrac{-(\psi_1 a/2)\cos(\psi_1 a/2)\sinh(\gamma'/2)+(\gamma'/2)\cosh(\gamma'/2)\sin(\psi_1 a/2)}{\left[(\psi_1 a/2)^2+(\gamma'/2)^2\right]}\end{array}\right\}$$
$$\times\left\{\begin{array}{l}\dfrac{(\psi_2 b/2)\cos(\psi_2 b/2)\sin(\varepsilon'/2)-(\varepsilon'/2)\cos(\varepsilon'/2)\sin(\psi_2 b/2)}{\left[(\psi_2 b/2)^2-(\varepsilon'/2)^2\right]}\\ +C'\dfrac{-(\psi_2 b/2)\cos(\psi_2 b/2)\sinh(\varepsilon'/2)+(\varepsilon'/2)\cosh(\varepsilon'/2)\sin(\psi_2 b/2)}{\left[(\psi_2 b/2)^2+(\varepsilon'/2)^2\right]}\end{array}\right\};\qquad\text{(G.4)}$$

ii. if it is square and $m-n=\pm 2,\ \pm 4,\ \pm 6,\ldots$

for $(m,n)=(\text{even},\text{even})$:

$$p(R,\phi,\theta,t)=-i\frac{\rho\omega^2 W_0 A_p \exp\left[i(-\omega t+kR)\right]}{2\pi R}$$

$$\times\left\{\begin{array}{l}\dfrac{(\psi_1 a/2)\sin(\psi_1 a/2)\cos(\gamma/2)-(\gamma/2)\sin(\gamma/2)\cos(\psi_1 a/2)}{\left[(\psi_1 a/2)^2-(\gamma/2)^2\right]}\\ +K\dfrac{(\psi_1 a/2)\sin(\psi_1 a/2)\cosh(\gamma/2)+(\gamma/2)\sinh(\gamma/2)\cos(\psi_1 a/2)}{\left[(\psi_1 a/2)^2+(\gamma/2)^2\right]}\end{array}\right\}$$

$$\times\left\{\begin{array}{l}\dfrac{(\psi_2 a/2)\sin(\psi_2 a/2)\cos(\varepsilon/2)-(\varepsilon/2)\sin(\varepsilon/2)\cos(\psi_2 a/2)}{\left[(\psi_2 a/2)^2-(\varepsilon/2)^2\right]}\\ +C\dfrac{(\psi_2 a/2)\sin(\psi_2 a/2)\cosh(\varepsilon/2)+(\varepsilon/2)\sinh(\varepsilon/2)\cos(\psi_2 a/2)}{\left[(\psi_2 a/2)^2+(\varepsilon/2)^2\right]}\end{array}\right\}$$

$$\pm i\frac{\rho\omega^2 W_0 A_p \exp\left[i(-\omega t+kR)\right]}{2\pi R}$$

$$\times\left\{\begin{array}{l}\dfrac{(\psi_1 a/2)\sin(\psi_1 a/2)\cos(\varepsilon/2)-(\varepsilon/2)\sin(\varepsilon/2)\cos(\psi_1 a/2)}{\left[(\psi_1 a/2)^2-(\varepsilon/2)^2\right]}\\ +C\dfrac{(\psi_1 a/2)\sin(\psi_1 a/2)\cosh(\varepsilon/2)+(\varepsilon/2)\sinh(\varepsilon/2)\cos(\psi_1 a/2)}{\left[(\psi_1 a/2)^2+(\varepsilon/2)^2\right]}\end{array}\right\}$$

$$\times\left\{\begin{array}{l}\dfrac{(\psi_2 a/2)\sin(\psi_2 a/2)\cos(\gamma/2)-(\gamma/2)\sin(\gamma/2)\cos(\psi_2 a/2)}{\left[(\psi_2 a/2)^2-(\gamma/2)^2\right]}\\ +K\dfrac{(\psi_2 a/2)\sin(\psi_2 a/2)\cosh(\gamma/2)+(\gamma/2)\sinh(\gamma/2)\cos(\psi_2 a/2)}{\left[(\psi_2 a/2)^2+(\gamma/2)^2\right]}\end{array}\right\}, \qquad \text{(G.5)}$$

where plus sign for the second part refers to the mode $m/n-n/m$ of the plate while minus sign refers to the mode $m/n+n/m$,

for $(m,n)=(\text{odd},\text{odd})$:

$$p(R,\phi,\theta,t)=i\frac{\rho\omega^2 W_0 A_p \exp[i(-\omega t+kR)]}{2\pi R}$$

$$\times\left\{\begin{array}{l}\dfrac{(\psi_1 a/2)\cos(\psi_1 a/2)\sin(\gamma'/2)-(\gamma'/2)\cos(\gamma'/2)\sin(\psi_1 a/2)}{\left[(\psi_1 a/2)^2-(\gamma'/2)^2\right]}\\ +K'\dfrac{-(\psi_1 a/2)\cos(\psi_1 a/2)\sinh(\gamma'/2)+(\gamma'/2)\cosh(\gamma'/2)\sin(\psi_1 a/2)}{\left[(\psi_1 a/2)^2+(\gamma'/2)^2\right]}\end{array}\right\}$$

$$\times\left\{\begin{array}{l}\dfrac{(\psi_2 a/2)\cos(\psi_2 a/2)\sin(\varepsilon'/2)-(\varepsilon'/2)\cos(\varepsilon'/2)\sin(\psi_2 a/2)}{\left[(\psi_2 a/2)^2-(\varepsilon'/2)^2\right]}\\ +C'\dfrac{-(\psi_2 a/2)\cos(\psi_2 a/2)\sinh(\varepsilon'/2)+(\varepsilon'/2)\cosh(\varepsilon'/2)\sin(\psi_2 a/2)}{\left[(\psi_2 a/2)^2+(\varepsilon'/2)^2\right]}\end{array}\right\} \quad \text{(G.6)}$$

$$\pm i\frac{\rho\omega^2 W_0 A_p \exp[i(-\omega t+kR)]}{2\pi R}$$

$$\times\left\{\begin{array}{l}\dfrac{(\psi_1 a/2)\cos(\psi_1 a/2)\sin(\varepsilon'/2)-(\varepsilon'/2)\cos(\varepsilon'/2)\sin(\psi_1 a/2)}{\left[(\psi_1 a/2)^2-(\varepsilon'/2)^2\right]}\\ +C'\dfrac{-(\psi_1 a/2)\cos(\psi_1 a/2)\sinh(\varepsilon'/2)+(\varepsilon'/2)\cosh(\varepsilon'/2)\sin(\psi_1 a/2)}{\left[(\psi_1 a/2)^2+(\varepsilon'/2)^2\right]}\end{array}\right\}$$

$$\times\left\{\begin{array}{l}\dfrac{(\psi_2 a/2)\cos(\psi_2 a/2)\sin(\gamma'/2)-(\gamma'/2)\cos(\gamma'/2)\sin(\psi_2 a/2)}{\left[(\psi_2 a/2)^2-(\gamma'/2)^2\right]}\\ +K'\dfrac{-(\psi_2 a/2)\cos(\psi_2 a/2)\sinh(\gamma'/2)+(\gamma'/2)\cosh(\gamma'/2)\sin(\psi_2 a/2)}{\left[(\psi_2 a/2)^2+(\gamma'/2)^2\right]}\end{array}\right\},$$

where plus sign for the second part refers to the mode $m/n+n/m$ of the plate while minus sign refers to the mode $m/n-n/m$.

In all of the above equations, ψ_1 and ψ_2 are given by Eqs. (3.6) and (3.7).

APPENDIX H
SECONDARY ACOUSTIC POWER EXPRESSIONS FOR CIRCULAR PLATES

The second terms of the acoustic power radiation for circular plates (both clamped and simply supported) are given by

for the free vibration:

$$\Pi_1 = \frac{\rho\omega^4 A^2 {A_p}^2}{4\pi c}\left\{-\frac{4}{3(\bar{\lambda}r_0)^3}\left[J_1(\bar{\lambda}r_0)-\frac{J_0(\bar{\lambda}r_0)I_1(\bar{\lambda}r_0)}{I_0(\bar{\lambda}r_0)}\right]\right\} \times\left\{(\bar{\lambda}r_0)J_1(\bar{\lambda}r_0)-2J_2(\bar{\lambda}r_0)-\frac{J_0(\bar{\lambda}r_0)}{I_0(\bar{\lambda}r_0)}\sum_{s=0}^{\infty}\frac{(\bar{\lambda}r_0)^{2(s+1)}}{2^{2s+1}(s+2)(s!)^2}\right\}(kr_0)^2, \tag{H.1}$$

and for the forced vibration:

$$\Pi_1 = \frac{\rho\Omega^4 {A_p}^2}{4\pi c}\left\{-\frac{2}{3}\left\{\frac{2\left[AJ_1(\mu r_0)+CI_1(\mu r_0)\right]}{(\mu r_0)}-\frac{F_0}{\rho_p\Omega^2}\right\}\right\} \times\left\{\frac{A\left[(\mu r_0)J_1(\mu r_0)-2J_2(\mu r_0)\right]}{(\mu r_0)^2}+C\sum_{s=0}^{\infty}\frac{(\mu r_0)^{2s}}{2^{2s+1}(s+2)(s!)^2}-\frac{F_0}{4\rho_p\Omega^2}\right\}(kr_0)^2. \tag{H.2}$$

In Eq. (H.2), the constant A is given by Eq. (5.43) for a clamped circular plate while it is given by Eq. (5.63) for a simply supported circular plate. The constant C in the same equation can be calculated by using Eq. (5.42) together with both plates' corresponding A values.

PERMISSION TO COPY

In presenting this thesis in partial fulfillment of the requirements for a master's degree at Texas Tech University or Texas Tech University Health Sciences Center, I agree that the Library and my major department shall make it freely available for research purposes. Permission to copy this thesis for scholarly purposes may be granted by the Director of the Library or my major professor. It is understood that any copying or publication of this thesis for financial gain shall not be allowed without my further written permission and that any user may be liable for copyright infringement.

Agree (Permission is granted.)

Disagree (Permission is not granted.)

_____ _____

Student's Signature Date